공학박사학위논문

SYNTHESIS AND APPLICATION OF ANTIMICROBIAL POLY(VINYL ALCOHOL) ELECTROSPUN NANOFIBERS FOR WATER FILTRATION

항미생물 폴리비닐 알코올계 전기방사
나노파이버 제조 및 수처리 여과 적용

2015 년 8 월

서울대학교 대학원

생태조경·지역시스템공학부

지역시스템공학전공

박 정 안

SYNTHESIS AND APPLICATION OF ANTIMICROBIAL POLY(VINYL ALCOHOL) ELECTROSPUN NANOFIBERS FOR WATER FILTRATION

A DISSERTATION

SUBMITTED TO THE DEPARTMENT OF LANDSCAPE ARCHITECTURE AND RURAL SYSTEMS ENGINEERING AND THE COMMITTEE ON GRADUATE STUDIES OF SEOUL NATIONAL UNIVERSITY

IN PARTIAL FULFILLMENT OF THE REQUIREMENTS FOR THE DEGREE OF

DOCTOR OF PHILOSOPHY

By

JEONG-ANN PARK

AUGUST, 2015

SYNTHESIS AND APPLICATION OF ANTIMICROBIAL POLY(VINYL ALCOHOL) ELECTROSPUN NANOFIBERS FOR WATER FILTRATION

항미생물 폴리비닐 알코올계 전기방사 나노파이버 제조 및 수처리 여과 적용

지도교수 김 성 배

이 논문을 공학박사 학위논문으로 제출함

2015 년 5 월

서울대학교 대학원
생태조경·지역시스템공학부 지역시스템공학전공

박 정 안

박정안의 공학박사 학위논문을 인준함

2015 년 6 월

위 원 장 李寅馥 (인)

부위원장 金成培 (인)

위 원 [illegible] (인)

위 원 崔在佑 (인)

위 원 朴成直 (인)

I certify that I have read this dissertation and that in my opinion it is fully adequate, in scope and quality, as dissertation for the degree of Doctor of Philosophy.

Chairman

I certify that I have read this dissertation and that in my opinion it is fully adequate, in scope and quality, as dissertation for the degree of Doctor of Philosophy.

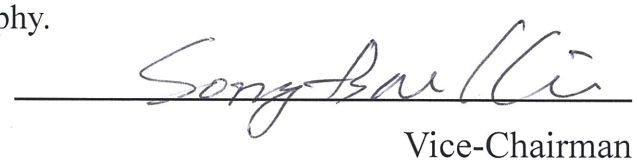

Vice-Chairman

I certify that I have read this dissertation and that in my opinion it is fully adequate, in scope and quality, as dissertation for the degree of Doctor of Philosophy.

I certify that I have read this dissertation and that in my opinion it is fully adequate, in scope and quality, as dissertation for the degree of Doctor of Philosophy.

I certify that I have read this dissertation and that in my opinion it is fully adequate, in scope and quality, as dissertation for the degree of Doctor of Philosophy.

Seong-Jik Park

ABSTRACT

This thesis deals with the fabrication, characterization, and evaluation antimicrobial and anti-biofouling activity of electrospun poly (vinyl alcohol) (PVA) nanofibers with quaternary ammonium compound (QAC) and PVA/poly acrylic acid (PAA) nanofibers with protease for applying in water filtration. BTEAC-PVA electrospun nanofibers was fabricated via co-electrospinning, and PVA/PAA-Cu(II) containing α-chymotrypsin was synthesized with soaking treatment after electrospinning. The synthesized nanofibers were characterized by various analytical techniques such as SEM, EDS, DSC, TGA, FTIR, and CFP.

BTEAC-PVA nanofibers containing 2.6% BTEAC were fabricated to test the antibacterial and antiviral activities. For the BTEAC-PVA nanofibers, the bacterial reduction ratio increased with increasing contact time, demonstrating that BTEAC-PVA nanofibers successfully inhibited the growth of bacteria. In addition, the antiviral tests against viruses (bacteriophages MS2 and PhiX174) showed that the BTEAC-PVA nanofibers inactivated both MS2 and PhiX174. BTEAC-PVA deposited on GF membrane (BTEAC-PVA/GF ENMs) for increasing mechanical strength. BTEAC-PVA/GF ENMs were also examined water stability, flux, pore size, leaching, and *D.magna* toxicity that they are good candidate for environmental friendly micro-filter as water filter. After 10 ml filtration, 4.88 LRV (*E. coli*) and 5.75 LRV (*S. aureus*) was achieved using

BTEAC-PVA/GF ENMs. Finally, 2.26 LRV (*E. coli*) and 3.29 LRV (*S. aureus*) was obtained after 500 ml filtrate volume with BTEAC-PVA/GF ENMs. The antibacterial water filtration test for river water were also performed that 67 CFU/mL (Total coliforms) in river water was removed all by BTEAC-PVA/GF ENMs during the filtration test. For anti-biofouling activity, deposited BTEAC-PVA on PC membrane (BTEAC-PVA/PC ENMs) could enhance the flux due to protect from biofouling of PC membrane with microorganism (*K. pneumonia*) solutions. Anti-biofouling effect was due to contact-dependent killing of sessile cells rather than reduction in the number of planktonic cells through biofouling resistance test. Antimicrobial mechanism of BTEAC-PVA nanofibers is damaging bacterial membrane observed by fluorescence microscopy and field emission scanning electron microscopy (FESEM) images. BTEAC-PVA/PC ENMs generally showed retaining antimicrobial activity over 6 cycles in regeneration study with bacteria, and mixed bacteria strain solution.

PVA/PAA nanofibers were successfully coordinated/chelated with Cu(II), then immobilization of α-chymotrypsin. The α-chymotrypsin is a proteas that could inhibit 53.50% of *P. aeruginosa* and 35.53% of *S. aureus* biofilm formation and reduce 58.2 % of *P. aeruginosa* biofilm and 43.5% of *S. aureus* biofilm with a microtiter assay. The Cu(II) adsorption capacity of PVA/PAA nanofibers is 44.85 mg/g (initial Cu(II) concentration = 500 mg/L, reaction time = 24 h) then immobilized amount of α-chymotrypsin on PVA/PAA-Cu(II)

nanofibers is 25.56 ± 2.72 mg/g. PVA/PAA-Cu(II) nanofibers containing α-chymotrypsin have a good performance of anti-biofouling by reducing sessile cells via degrade EPS, especially protein.

The functionalized PVA nanofibers were applied as a water filter, and showed antibacterial and anti-biofouling performance with various tests including contact test, dynamic test, dead-end filtration test, and incubation test. In addition, this dissertation provides the possibility of eco-friendly approaches for the preparation of PVA based nanofibers containing QAC and protease, and their potential applications in water filtration.

Keywords: Electrospun nanofiber, Poly (vinyl alcohol), Antimicrobial, Quaternary ammonium compound, Protease, Water filtration

***Student Number*: 2011-30344**

CONTENTS

LIST OF TABLES

LIST OF FIGURES

Chapter 1 Introduction

1.1 Background

1.1.1 Electrospun nanofibers for water filtration

Electrospinning is one of famous methods for preparation nanofibers with dissolved polymers. It was firstly patterned by Anton Formhals in 1934 for fabrication yarn (Table 1.1) (Huang et al., 2003). In mid-1990s, nanofibers were formed using electrospinning (Ranakrishna et al., 2010; Bhattarai et al., 2014). Electrospinning is simple, inexpensive and effective method to produce non-woven nanofibers with nanometer range diameter (Qin et al., 2012). Many parameters of electrospinning procedures affect to morphology of nanofibers (Table 1.2). In the electrospinning process, straight jet ejected from taylor cone could overcome the surface tension when the applied electric field strength (Figure 1.1). The jet remains straight for some distance and then it flies to collector following looping path. Finally, the jet solidified and deposits on the collector as a nonwoven fiber (Liu et al., 2012a).

Nanofibers are defined as fibers with diameter generally between 50~1000 nm and aspect ratio above 1000. Although, there is no regular diameter range of nanofibers in water filter application, however, it is good for filter media with diameter under 500 nm, and, recently, ultrafine nanofibers (diameter below 200 nm) have been paid attention due to their promising applications. The nanofibers have a quite large surface area, flexibility, multiple surface

functionalities, and high permeability with many small pores (Qin et al., 2012). Owing to the small fiber diameter and pore size, nanofibers have high filtration efficiency even easily trapping particles (< 0.5 μm) without reducing flow resistantce (Du Plessis, 2011). There has been an increase in publication of research papers in the field of nanofibers (Figure 1.2) because of these interesting properties. Briefly, nanofibers have a great attention for various application mainly in biomedical materials (48.64 %) and water/air filtration (25.82 %) followed by electrode or battery (12.28 %), liquid crystal device (6.53 %), clothing (2.00 %), and so on (4.72 %). The ratio of water filtration in water/air filtration field is about 17.27 %, however, application of electrospun nanofiber in water filtration is rising issues due to great potential of leading new direction of water technology since 2006 (Figure 1.2). The published research papers about water filtration has been grown steadily so far. Numerous articles have defined electrospun nanofibers for water treatment as "Electrospun nanofibrous membranes (ENMs)" (Nasreen et al., 2013). The use of ENMs for water filtration is classified majorly removal of microbes (42.56 %), and removal of heavy metals (22.06 %). About a half of researches have been studied antimicrobial electrospun nanofibers due to problem in membrane filtration of water, biofouling. Antimicrobial ENMs could enhance anti-biofouling activity during water filtration. Antimicrobial electrospun nanofibers appeared to be an attractive anti-biofouling method because of

immobilizing antimicrobial agent by embedding or achieving covalent bond in nanofibers that antimicrobial agents have advantages of chemically stable, environmentally safe, and prolonging lifetime without leaching.

1.1.2 Anti-biofouling activity using antimicrobial ENMs

Membrane biofouling is a major problem encountered in membrane filtration processes that biofouling is one of significant obstacle for ENMs, either. Many conventional physical (mechanical cleaning) and chemical (biocides and disinfectant) methods have been performed to control biofilm through killing bacteria and remove biofilms from surface, however, both still have some problems such as increasing retaining cost and producing toxic by-product (Stewart et al., 2000).

The two major strategies for anti-biofouling on ENMs are based on adhesion inhibition and killing bacteria (Banerjee et al., 2011). One way to enhance the adhesion inhibition is weakening hydrophobic interaction between biofoulant (microorganism, extracellular polymeric substances and proteins) and ENMs surface through increasing hydrophilicity of surface (Nisola et al., 2012; Mei et al., 2012). Many of hydrophobic ENMs have been used due to their superior mechanical, chemical and thermal stability, however, it is necessary to improve surface hydrophilicity for application in water filtration/purification and

biofouling resistance (Wang et al., 2006; Sun et al., 2010; Botes & Cloete, 2010). Therefore, many attempts to improve the surface hydrophillicity have been performed through surface grafting (Hu et al., 2005, Zuwei et al., 2006; Ramakrishana et al., 2005), adding inorganic particles (Pant et al., 2011), blending polymers (Li et al., 2010), adding materials for quorum sensing inhibiting (Gule et al., 2013), and depositing hydrophilic layers (Na et al., 2000; Wang et al., 2012). Adhesion inhibition strategy have a great effect to hinder the biofilm growth, however, microorganisms are not be killed. The more active approach of anti-biofouling ENMs is killing bacteria with antimicrobial agent such as guanidine compound, metal or metal oxide nanoparticles (Ag, TiO_2, CuO, ZnO), phosphonium salts, carboneous nanomaterials (CNTs, Graphene), and quaternary ammonium compound (QAC). Recently, the studies of metal or metal oxide nanoparticles, and carbonaceous nanomaterials as an antimicrobial agent have been performed, however, potential eco-toxicity and environmental health effects are still concerning issues.

1.1.3 Quaternary ammonium compound as antimicrobial agent

QAC are known as having a broad spectrum of antimicrobial activity. General structure of QAC is as followed that four of the substituents (R_1-R_4) are alkyl or heterocyclic groups and the X^- is chloride, iodide or bromide

(Bshena, 2012) (Figure 1.3). Quaternary ammonium salt containing at least one alkyl substitute are good candidates for killing microorganisms including bacteria, algae, and fungi (Nurdin et al., 1993). Quaternary ammonium compounds are polycationic non-oxidising biocide and widely used in many fields, such as filters, paints, and packaging materials, as an antimicrobial agent to hinder bacterial growth on the surfaces. The antimicrobial mechanism was summarized that electrostatic interaction and adsorption occurred between positively charged ammonium ion on QAC and negatively charged bacteria at the beginning (Figure 1.4). Then, the log lipophilic chain diffuses through the cell wall and leads to disrupt cytoplasmic membrane that K^+ ion and other cytoplasmic constituents are released. In the end, cells are dead followed by precipitation of cell contents (Kawabata & Nishiguchi, 1988; Nurdin et al., 1993). In the case of virus, electrostatic and hydrophobic ineteraction is dominated that inactivation is caused by the disruption of the viral envelope and release nucleocapsid (Tsao et al., 1989).

1.1.4 Enzymes as anti-biofouling agent

Many antimicrobial agent have a difficulties to effectively kill the bacterial cells because they are encased in a matrix of extracellular polymeric substances (EPS) in biofilm, protecting cells within (Donlan & Costerton, 2002; Molobela

et al., 2010). Therefore, there is an urgent needs for alternative anti-biofouling strategy with destroying biofilm such as using hydrolytic enzymes.

The use of enzyme is good biofilm control agents because of rapid degradability, commercially availability and nontoxic to environment (Olsen et al., 2007; Leroy et al., 2008). The most popular targets for biofilm control using enzymes are degrading proteins and polysaccharides because of major components of biofilm (Kristensen et al., 2008). Enzymes remove biofilms by destroying physical integrity of the EPS through weakening the structure of proteins, carbohydrate and lipid through degradation process (Xavier et al., 2005). Especially, protease is important not only degrading protein structure but also preventing attachment of cells to the surface. Also, regulating quorum sensing (QS) enzymes have been used for reducing EPS because QS rules gene expression when reaching the cell density threshold (Kim et al., 2013). Signal molecules such as acyl homoserine lactones (AHLs) are produced and contributed to the microbial attachment on the surface during QS system. Therefore, the studies for protease and QS signal molecule hydrolases have been needed for biofilm reduction. Enzyme immobilization on electrospun nanofibers have great potential to overcome the limitation because nanofibers have a large surface to volume ratio to high enzymes loading, and easily functionalized with chemical/physical treatment to benefit enzyme activity (Wang et al., 2009).

1.1.5 Poly (vinyl alcohol) (PVA) polymer

Two types of polymers have been used for the synthesis of antimicrobial nanofibers. The first is related to solvent-soluble polymers such as polyamide (Daels et al., 2011; De Vriez et al., 2011), polyacrylonitrile (Mahapatra et al., 2012; Zhang et al., 2011, Rujitanaroj et al., 2010; Ren et al., 2009; Du Plessis, 2011), polyurethane (Yousef et al., 2012), poly(methyl methacrylate) (Kong et al., 2008), poly(vinylidene) fluoride (Peng et al., 2007), polycarbonate (Kim et al., 2007), poly(vinyl phenol) (Kenawy & Abdel-Fattah, 2002), and cellulose acetate (Anitha et al., 2012). The second includes water-soluble polymers such as polyethylene oxide (An et al., 2009; El-Newehy et al., 2012), poly(acrylic acid) (Li & Hsieh, 2005; Kim et al., 2005), poly(vinylpyrrolidone) (Peng et al., 2007; Srisitthiratkul et al., 2011) and poly(vinyl alcohol) (PVA) (Nirmala et al., 2011; Su et al., 2012; Alipour et al., 2009; Ignatova et al., 2006; Supaphol et al., 2008).

Recently, without toxic organic solvent for environmental friendships, water soluble polymers were useful for electrospinning. PVA is one of the most promising hydrophilic polymer with excellent chemical and thermal stability (Huang et al., 2009; Gule et al., 2012). PVA is soluble in water without solvent (highly hydrophilic), nontoxic (environmentally friendly), biocompatible material, good resistance (chemical, thermal, ultra-violet, oil, organic solvent and infra-red) (Gule et al., 2012), and inexpensiveness. Also, PVA nanofibers

have a quite large surface area to mass which means a higher sorption capacity of contaminants in water, possibility for surface functionalization with many hydroxyl group (Liu et al., 2012), and relatively low cell (or protein) adhesion property due to hydrophilic property (Burczak et al., 1996; Wei et al., 2012; Qi et al., 2013). For this reason, PVA nanofibers have been widely used and excellent candidates for water filtration (Gule et al., 2013).

However, it is essential to crosslink the polymer chains in PVA nanofibers for application due to easily soluble in water. Chemical crosslinking is common method to improve the water resistance using glutaraldehyde, acetaldehyde, or formaldehyde. However, it could be toxic to use nanofibers as water filter. Hence, heat and methanol treatment is an alternative environmental friendly method for increasing stability of PVA nanofibers. In addition, hybrid with other non-toxic hydrophilic polymers could be another way to crosslink PVA such as poly(acrylic acid) (PAA) and poly(vinyl pyrrolidone). PAA used as crosslinking reagent that strong crosslinking by ester linkage is formed between the hydroxyl group of PVA and the carboxyl group of PAA with simple heat treatment (Figure 1.5) (Kumeta et al., 2003; Li & Hsieh, 2005).

1.2 Objective

This thesis concerned with the synthesis antimicrobial PVA based electrospun nanofibers through electrospinning and their application in water filtration. The specific objectives of the dissertation are:

1. To manufacture non-woven nanofibers with PVA using electrospinning method and optimize the electrospinning conditions.

2. To improve water stability of PVA nanofibers using environmental friendly crosslinking methods.

3. To synthesize antimicrobial PVA nanofibers containing QAC and characterize them.

4. To evaluate antimicrobial activity of nanofibers containing QAC against different gram-positive and gram-negative bacteria using various methods including contact test, batch experiments, and filtration test.

5. To examine anti-biofouling activity of nanofibers containing QAC by contact killing through filtration test and preventing biofouling through incubation test.

6. To synthesize anti-biofouling PVA/PAA hybrid nanofibers immobilized hydrolytic enzymes and characterize them.

7. To examine the potential of water filtration application without biofouling with QAC and hydrolytic enzyme.

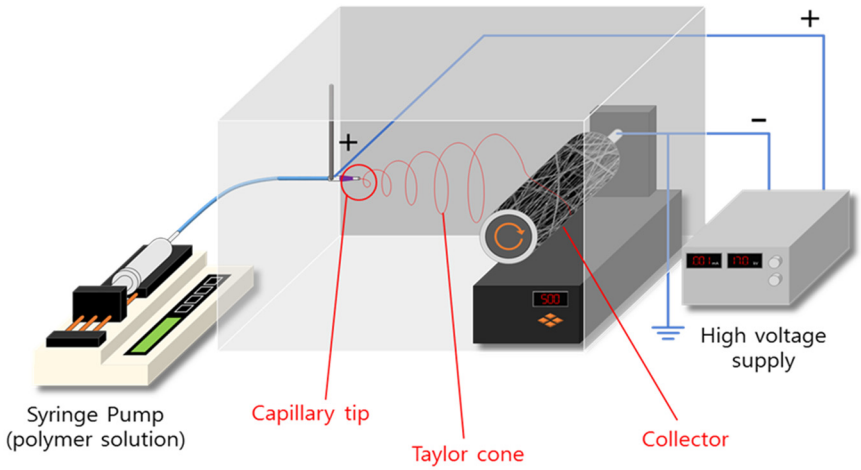

Figure 1.1 Electrospinning set up

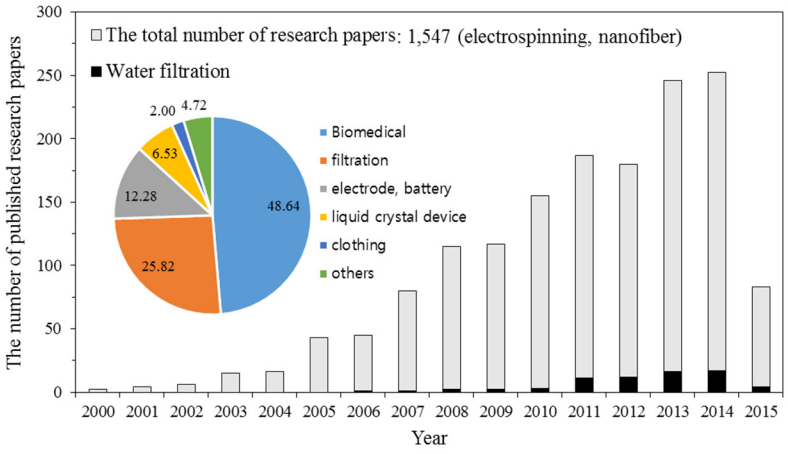

Figure 1.2 The number of published research papers about nanofiber and electrospinning in each year

Table 1.1 Electrospinning timeline

Year	History
1934	Anton Formhals: first patent filed on yarn fabrication using Electrospinning. (1934-1944)
1936	Norton: patent filed for melt electrospinning.
1952	Vonnegut & Newbauer: invented simple apparatus for electrical atomization and produced streams of highly electrified uniform roplets of about 0.1 mm in diameter.
1955	Drozin: investigated dispersion of series of liquids into aerosols under high electric potential.
1966	Simon: patent filed of an apparatus for the production of non-woven fabrics that were ultrathin and very light in weight with different patterns using electrical spinning.
1971	Baumgarten: made an apparatus to electrospin acrylic fibers with diameter in the range of 0.05 – 1 μm.
1976 - 1987	• Dispersal of fine particles on electrospinning het
	• Electrospun fibers as tissue scaffold
	• Tubular scaffolds for vascular grafts
	• Mass production of electrospun fibers for filtration
1990 - 2000	• Parameters studies of electrospinning to form nanofibers
	• Electrospun fibers as composite reinforcement
	• Electrospun fibers as template
	• Electrospinning modelling

Ref. Huang et al., 2003; Ranakrishna et al., 2010; Bhattarai et al., 2014

Table 1.2 Processing parameters in eletrospinning

Solution properties	Viscosity
	Polymer concentration
	Molecular weight of polymer
	Electrical conductivity
	Elasticity
	Surface tension
Processing condition	Applied voltage
	Distance from needle to collector
	Volume feed rate
	Needle diameter
Ambient conditions	Temperature
	Humidity
	Atmospheric pressure

Ref. Tan et al., 2005

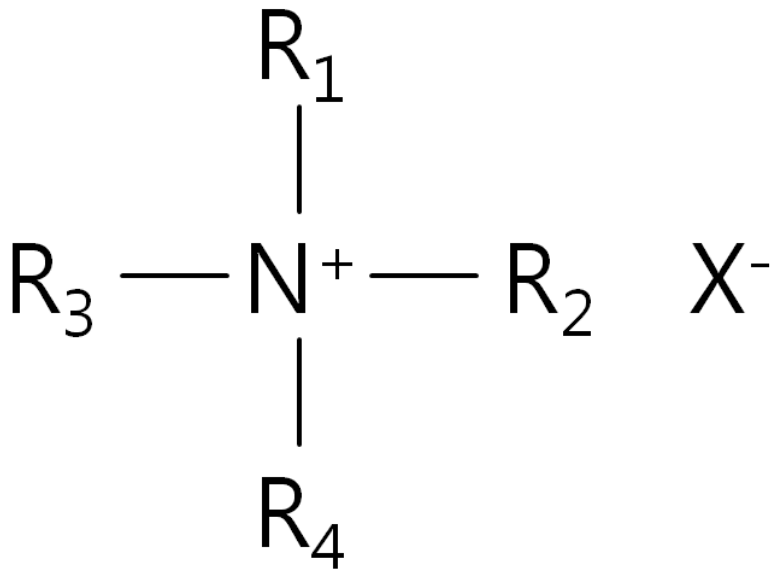

Figure 1.3 General structure of QAS
(Bshena, 2012)

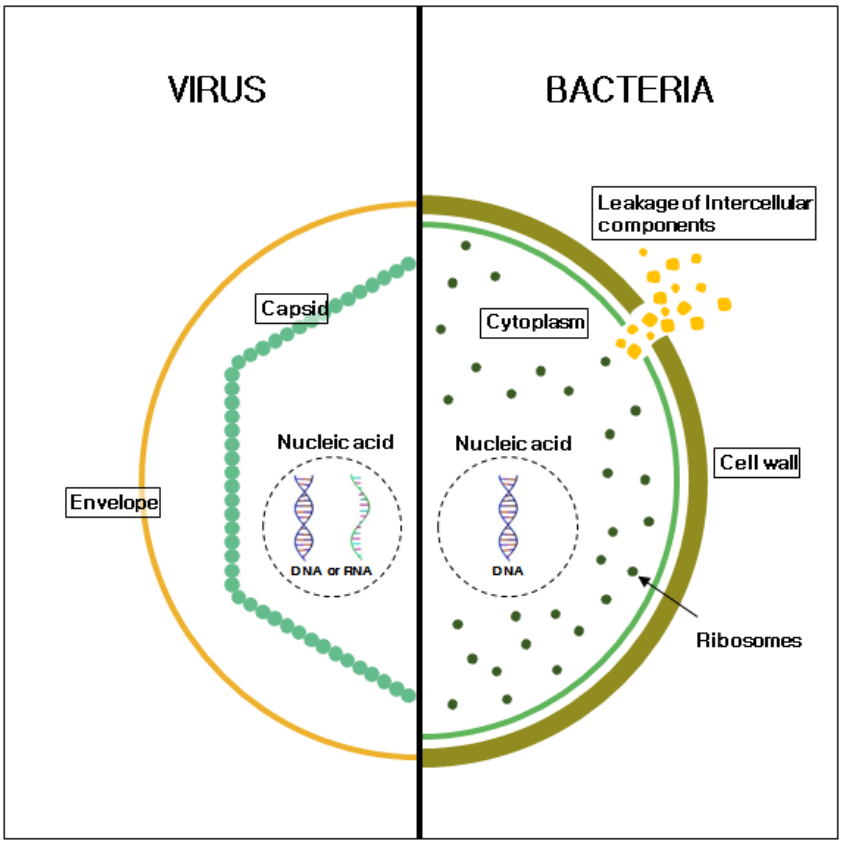

Figure 1.4 Antimicrobial mechanisms of QAC

(Ref. Kawabata & Nishiguchi, 1988; Nurdin et al., 1993; Tsao et al., 1989)

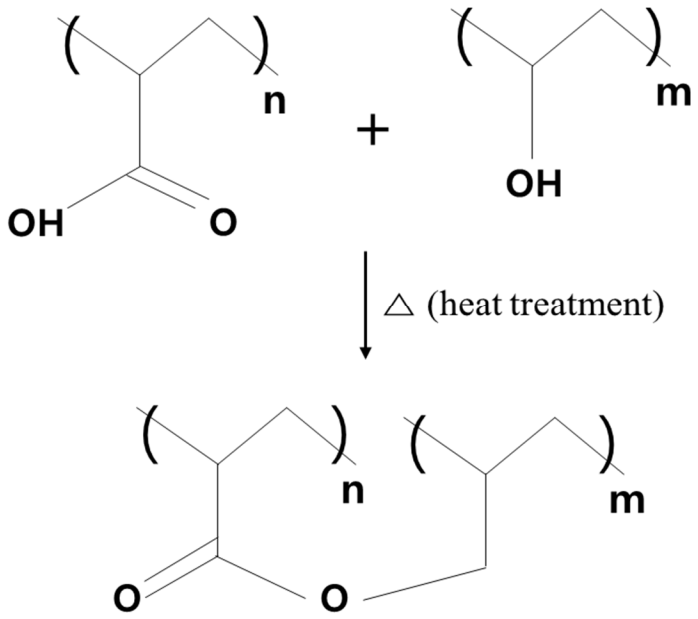

Figure 1.5 Thermal cross-linking mechanism between PVA and PAA through esterification reaction
(Kumeta et al., 2003)

Chapter 2 Literature Review

2.1 Electrospun condition of PVA nanofiber

Many researchers have investigated various parameters of electrospinning condition such as PVA concentration (Supaphol & Chuangchote, 2008), applied voltage (Supaphol & Chuangchote, 2008; Zhang et al., 2005; affandi et al., 2010), solution viscosity (Liu et al., 2012), solution conductivity (Arumugam et al., 2009), solution pH (Son et al., 2005), degree of hydrolysis (Park et al., 2010), surface tension (Jia & Qin, 2013), tip-to-distance (TCD) (Zhang et al., 2005; Supaphol & Chuangchote, 2008), and molecular weight (Koski et al., 2004) affecting to produce electrospun fibers for past a few years.

Supaphol & Chuangchote (2008) conducted experiments to understand the effect of solution properties (concentration, viscosity) and process condition (applied voltage, TCD). The viscosity of solution depends on PVA concentration that critical solution viscosity is needed to be formation of stable charged jet (higher than molecular entanglements and lower than discrete droplets). The diameters of PVA fibers were generally increased from 85 nm to 647 nm with increasing PVA concentration (6 - 14 wt%). The average diameters of PVA fibers were slightly decreased with the initially increase applied electrical potential (12.5 – 17.5 kv), and increased with further higher applied voltage (17.5 – 25 kv). This trends would be significant only in the higher PVA concentration (12, 14 wt%). The PVA fibers (6 - 10 wt%) were not statistically significant. Zhang et al (2005) found that there was a slightly increase in

average fiber diameter with increasing applied electric field (5-13 kv), however, above 10 kv, ultrafine fibers (Dia <150 nm) were observed because of obtaining broad distribution in the fiber diameter. TCD (8-15 cm) had no significant effect on electrospun fibers with full hydrolyzed PVA. In the case of concentration of PVA (6 - 8 wt%) molphology of fiber was changed from beaded fiber to uniform fiber with increasing diameter gradually. Above 8.3 wt%, PVA solutions could not form fibers but big droplets. Affandi et al. (2010) also insisted that slightly increasing diameter between 15 and 20 kv increasing voltage, however, did not significantly affect PVA-fiber diameter. The increased applied electrical potential induced increasing both coulombic repulsion and electrostatic forces with carrying many number of charges in a jet segment. The increased coulombic repulsion force could cause thinner fiber (with smaller elongated beads), due to increasing stretching forces, while the increased electrostatic forces could lead to increase fiber diameter due to occur bending instability of the jet with increasing speed of the jet segment and mass flow rate. For TCD, the increasing TCD would trigger to decrease the diameter of PVA fiber, however, below 15 cm was suggested that the jet was too dry and strong to stretch further above 15 cm. Jia & Qin (2013) showed that adding surfactant(less than 1%) could reduce the surface tension and fiber diameter of PVA was remarkably deceased from 405 to 100 nm. Park et al. (2010) examined the effects of PVA with various degree of hydrolysis (DH= 88, 96, and 99.9 %)

to produce electrospun fibers. The results indicated that the average diameter of the electrospun PVA fibers (conc. ~ 8 wt%) increased with increasing DH.

Son et al. (2005) investigated the effect of pH (2.0 – 12.9) with 7 wt% PVA solutions that PVA fibers became straighter and finer with increasing pH (basic condition), while PVA fibers with beads-on-stiring structures were manufactured under acidic condition because of the protonation of PVA. Liu et al (2012) fabricated uniform ultrafine PVA fiber (< 200nm) by adding hydrazine monochloride (HMC), reducing 60 % of viscosity. On the other hand, a beaded morphology was found when the viscosity was too low. Arumugam et al. (2009) compared the effect of adding small amount of three different types salts HMIMCl (room temperature ionic liquid), BTEAC (a quaternary ammonium salt), KCl (inorganic chloride salt) in PVA solution to understand the impact of conductivity on electrospun fibers. Adding salts could cause not only increasing conductivity but also variating surface tension that PVA fibers with electrospinning salted solution were greater than pristine PVA without two exeptions. This phenomenon was explained by collision mechanism that fibers would be combined with aggregation and fusion (self-bundling). Koski et al (2004) studied the effect of average molecular weight of PVA polymer (Mw) that the fiber diameter generally increases with Mw.

2.2 QAC functionalized electrospun nanofibers for antimicrobial and anti-fouling activity in aqueous solution

Many kinds of QAC were used as an antimicrobial agent in electrospun nanofibers (Table 2.1), and the most famous QAC is 3-(trimethoxysilyl)-propyldimethyloctadecyl ammonium chloride (Voigt, 2009; Park et al., 2013). Another QAC, such as benzyl triethylammonium chloride (BTEAC), poly[(dimethylimino)(2-hydroxy-1,3-propanedily)chloride] (WSCP), N,N, n,n,-didecyl-N, N-dimethylammonium chloride (DDAC), have been studies for antimicrobial activity on electrospun nanofibers (Kim et al., 2007; Bjorge et al., 2010; Daels et al., 2011; De Vrieze et al., 2011; Gliscinska et al., 2012). Kim et al (2007) found that BTEAC was efficient antimicrobial agent for the first time and electrospun well with Polyamide (PA) polymer. Bjorge et al. (2010), Daels et al. (2011) and De Vrieze et al. (2011) synthesized PA nanofibers containing WSCP and evaluated antimicrobial activity in hospital waste water. Gliscinska et al. (2012) fabricated polyacrylonitrile (PAN) nanofibers modified with DDAC.

QAC is simply incorporated by adding QAC into PVA solution during electrospinning and have great effect to antimicrobial activity. Voight (2009) successfully synthesized antimicrobial functionalisation PVA nanofibers with 3-(trimethoxysilyl)-propyl-dimethyloctadecyl ammonium chloride that mostly

inhibited the *B. subtilis*, while nearly no effect on *E. coli* with contact and shaking method. Park (2013) fabricated PVA electrospun nanofibers containing 3-(trimethoxysilyl)-propyl-dimethyloctadecyl ammonium chloride. They were performed antibacterial property to both gram-negative bacteria (*E. coli*) and Gram-positive bacteria (*S. aureus*) by charge-charge interaction. Also, the mat killed bacteria more than 99 % of its population during 5 times recycling.

2.3 Enzyme immobilized on electrospun nanofibers for anti-biofouling

Some researchers have been studied anti-biofouling effect on using enzymes (Leroy et al., 2008; Molobela et al., 2010; Kim et al., 2013). Leroy et al. (2008) evaluated antifouling potential of commercial proteases, glucosidases and lipase that Savinase was the most effective enzyme in both the prevention of bacterial adhesion and the removal of adhered bacteria. Molobela et al. (2010) determined the effect of commercial proteases (savinase, everlase, and polarzyme) and amylases (amyloglucosidase and bacterial amylase novo) on biofilms and extracted EPS formed by *p. fluorescens* that proteases, especially, savinase and everlase were the most effective enzyme on removing biofilms and degrading the EPS. Kim et al. (2013) investigated the reduction of biofouling on RO membrane with enzyme (acylase I and proteinase K) caused by incubation *P. aeruginosa* for 4 days. Acylase I (5 μg/ml), proteinase K (100

μg/ml), and combination both enzymes removed 9.0, 56.6 and 33.7 % of bacteria on RO membrane, respectively. Proteinase K removed EPS concentration, while, acylase I reduced bacteria numbers not EPS concentration. However, applications of enzymes are limited due to instability, difficulty of recovery and non-reusability in aqueous solutions (Brady & Jordaan, 2009; Wang et al., 2009).

Enzyme immobilization on electrospun nanofibers have great potential to overcome the limitation because nanofibers have a large surface to volume ratio to high enzymes loading, and easily functionalized with chemical/physical treatment to benefit enzyme activity (Wang et al., 2009). Du Plessis et al. (2012) observed anti-biofilm activity in water filtration system with immobilized Savinase, Alcalase, and BAN on PAN electrospun nanofibers. Park et al (2013) electrospun chitosan/PVA nanofibers then aggregate lysozyme on the surface with glutaraldehyde for antibacterial.

PVA nanofibers have been studied for enzyme immobilization electrospun nanofibers (Xia & Hsieh, 2003; Wu et al., 2005; Ren et al., 2006; Sakai et al., 2008; Wang & Hsieh, 2008; Moradzadegan et al., 2010, Feng et al.,2014) (Table 2.2). Mostly, enzymes were mixed with PVA solutions then electrospun for immobilization enzyme on PVA nanofibers, however, Feng et al. (2014) successfully developed electrospun PVA/PA6-Cu(II) nanofibrous membrane for immobilization of catalase.

2.4 Electrospun PVA nanofibers for water treatment

Although many conventional methods are widely used for water purification, the new generation of nanofiltration system is the rising issue (Mahanta & Valiyaveettilm, 2013). Application of electrospun nanofibers in water treatment are mainly divided in the two aspects, one is heavy metal removal and another is microbial removal. However, a few studies have been performed related in water treatment.

Removal of heavy metals using PVA electrospun nanofibers was mostly conducted via batch experiment. Wu et al (2010a, b) synthesized thiol-functionalized mesoporous PVA/SiO_2 composite nanofibers (Dia 300- 500 nm) by electrospinning and examined heavy metal ions (Cu^{2+}) adsorption capacity in aqueous solution using batch test. The largest adsorption capacity was 489.12 mg/g at 303 K and maintained through six recycling processes. PVA/SiO_2 composite was also studied as an adsorbent for indigo carmine dye (Teng et al., 2011). Mahanta & Valiyaveettilm (2013) investigated functionalized poly (vinyl alcohol) based nanofibers for the removal of arsenic from water. PVA nanofibers adding Fe^{3+} ions were prepared and arsenic removal capacity was found to be 67 mg/g (As(III)), and 36 mg/g (As(V)), each from bath experiments. Arsenic ions were adsorbed on the sorbent surface according to FTIR and XPS results. Wang & Ge (2013) prepared chitosan/poly (vinyl alcohol) fiber mat containing Cerium (III) to remove chromium (VI) from

aqueous solution with batch test. Based on the best fit Langmuir model, maximum adsorption capacity is 52.88 mg/g. The removal mechanisms of Cr(VI) by fibrous mat can be explained by two aspects that the electrostatic force attraction and chemisorptions. Abbasizadeh et al. (2013) manufactured PVA/TiO_2 nanofiber adsorbent modified with mercapto groups to remove radioactive waste, such as uranium (VI) and thorium (IV), from aqueous solution. The influence of TiO_2 (and mercapto) contents, adsorbent dose, pH, contact time, temperature, initial concentration of uranium (VI) and thorium (IV) were examined in batch experiments. The maximum sorption capacities of uranium (VI) and thorium (IV) by langmuir isotherm model were calculated to be 196.1 and 238.1 mg/g at 45 ℃ with pH 4.5 and 5.0, respectively.

For removal of microbes, several studies have been started to evaluate PVA electrospun nanofibers application in water treatment (Gule et al., 2012; Gule et al., 2013; Mi et al., 2014; Dobrowsky et al., 2015) (Table 2.3). Gule et al (2012) fabricated PVA nanofibers containing biocide Aquaqure that antimicrobial tests show nanofibers achieved up to 5 LRV of various bacteria. Gule et al (2013) produces furanone-containing PVA (PVA/DMHF) nanofibers supported on 0.22 μm sized filter that antimicrobial activity was determined using dead-end filtration system with desired contact time. PVA/DMHF nanofibers reduced 3.5 log in population of *P. aeruginosa* Xen 5, *E. coli* Xen 14, and about 2.2 log in population of *S. aureus* Xen 36, *S. typhimurium* Xen

26, *K. pneumonia* Xen 39 after 30 min contact followed by filtration. Mi et al (2014) synthesized quaternized chitosan in to PVA electrospun nanofibers for virus removal that 3.3 LRV for PPV and 4.2 LRV for sindbis. Dobrowsky et al (2015) used PVA nanofiber membrane/activated carbon column for treatment harvested rain water for removal of bacteria and virus.

Table 2.1 Previous studies for QAC containing electrospun nanofibers for antimicrobial activity in aqueous solution.

Author (Year)	Polymer	Types of QAC
Park (2013)	Poly(vinyl alcohol)	3-(trimethoxysilyl)-propyldimethyloctadecyl ammonium chloride
Gliscinska et al. (2012)	polyacrylonitrile	N,N, n,n,-didecyl-N, N-dimethylammonium chloride
De Vrieze et al. (2011)	polyamide	poly[(dimethylimino)(2-hydroxy-1,3-propanedily)chloride]
Daels et al. (2011)	polyamide	poly[(dimethylimino)(2-hydroxy-1,3-propanedily)chloride]
Bjorge et al. (2010)	polyamide	poly[(dimethylimino)(2-hydroxy-1,3-propanedily)chloride]
Voigt (2009)	Poly(vinyl alcohol)	3-(trimethoxysilyl)-propyldimethyloctadecyl ammonium chloride
Kim et al. (2007)	Poly carbonate	benzyl triethylammonium chloride

Table 2.2 Previous studies for immobilization enzymes on PVA based electrospun nanofibers

Author (Year)	Types of Enzymes	Application	Immobilization method
Feng et al. (2014)	Bovine liver catalase	Biocatalysist	Metal chelation
Moreno et al. (2011)	Lactate dehydrogenase	Drug delivery	Co-electrospinning
Moradzadegan et al. (2010)	Acetylcholinesterase (AChE)	Catalyst	Co-electrospinning
Wang & Hsieh (2008)	Lipase form C.rugosa	Catalyst	Co-electrospinning
Sakai et al. (2008)	Lipase	-	Co-electrospinning
Ren et al. (2006)	Glucose oxidase	Biosensor	Co-electrospinning
Wu et al. (2005)	Cellulase	-	Co-electrospinning
Xie & Hsieh (2003)	Casein lipase	-	Co-electrospinning

Table 2.3 Previous studies for removal microbes from aqueous solution using PVA electrospun nanofibers.

Author (year)	Experimental types	Antimicrobial/ anti-biofouling agent	Microorganism	Efficiency
Dobrowsky et al. (2015)	Filtration	SMI-Q-10, activated carbon	Bacteria & virus from surface and river water	Above 2 LRV for bacteria, 0.12 LRV for virus
Mi et al. (2014)	Batch	Quaternized chitosan (N-[(2-hydroxyl-3-trimethylammonium) propyl] chitosan)	Virus (PPV, Sindbis,)	3.3 LRV for PPV, 4.2 LRV for Sindbis
Gule et al. (2013)	Filtration	Furanone	Bacteira (*P. aeruginosa*, *E. coli, S. aureus S. typhimurium*, *K. pneumonia)*	2.2 -3.5 LRV
Gule et al. (2012)	Filtration	AquaQure	Bacteria (*E. coli, S. aureus. S.tryphimurium, P. aeruginosa, K. pneumoniae*)	5 LRV

Chapter 3

Preparation and Characterization of Antimicrobial Electrospun Poly(vinyl alcohol) Nanofibers Containing Benzyl Triethylammonium chloride

Published. Park, JA; Kim, SB. 2015.

Reactive and Functional Polymers.

3.1 Materials and methods

3.1.1 Electrospinning of PVA nanofibers

PVA (M.W. = 85,000–124,000, 99 % hydrolyzed) were purchased from Sigma Aldrich. A PVA solution (8 wt%) was prepared by dissolving PVA powder in deionized water at 80 ^{o}C for 16 h and then cooling the solution at room temperature. Electrospinning of the PVA nanofibers was performed at room temperature using an electrospinning system (ESP200/ESP100, NanoNC, Seoul, Korea). The as-prepared PVA solution was placed in a 25 mL syringe with a metal needle (inner diameter = 0.51 mm), which was connected to the positive terminal of a high-voltage power supply. The electrospun PVA nanofibers were collected on a rotating cylinder (diameter = 9 cm; speed = 1000 rpm) on a negative terminal wrapped with aluminum foil. The PVA nanofibers were then dried at 65 ^{o}C for 18 h.

In order to examine the effects of applied voltage and flow rate on the synthesis of PVA nanofibers, voltage was varied from 15 to 20 kV, whereas the flow rate of the spinning solution was changed from 0.5 to 2.0 mL h^{-1} using a syringe pump (KDS 100, NanoNC, Seoul, Korea). Note that the tip-to-collector distance (TCD) was fixed at 15 cm during electrospinning. Prior to use in the antimicrobial tests, the PVA nanofibers were heat-treated for 20 min at 150 ^{o}C.

3.1.2 Electrospinning of BTEAC-PVA nanofibers

Prior to the electrospinning of the BTEAC-PVA nanofibers, minimum inhibitory concentration (MIC) tests were performed to determine the amount of BTEAC to be added to the PVA solutions (8 wt%). Three bacteria, *S. aureus* (ATCC 6538), *K. pneumonia* (ATCC 4352), and *E. coli* (ATCC 11105), were used in the MIC tests. In order to determine the suitable BTEAC concentration for bacterial growth inhibition, the BTEAC concentration was varied from 1.0 to 4.0 %. In the MIC tests, 5 mL of sterilized Luria-Bertani (LB) media solution containing BTEAC were inoculated with bacteria (0.1 mL) and then incubated for 24 h at 37 ^{o}C. Inhibition of bacterial growth was determined using a UV-vis spectrophotometer (Thermo Scientific, Waltham, MA, USA) at a wavelength of 600 nm.

After determining the suitable BTEAC concentration, the BTEAC-PVA nanofibers were manufactured using the pre-functionalized method. Prior to the electrospinning of BTEAC-PVA nanofibers, BTEAC was added to the PVA solution in order to impregnate BTEAC into the PVA nanofibers during the electrospinning process. The electrospinning conditions for BTEAC-PVA nanofibers were as follows: applied voltage of 15 kV, flow rate of 1.0 mL h^{-1} and TCD of 15 cm. Prior to use in antimicrobial tests, the BTEAC-PVA nanofibers were heat-treated for 20 min at 150 ^{o}C.

3.1.3 Characterization of PVA and BTEAC-PVA nanofibers

The properties of the BTEAC-PVA solution were determined using various methods. The solution conductivity was measured by a conductivity meter (HC3010, Trans Instruments, Singapore). The viscosity was estimated using a Brookfield digital viscometer (Model DV-E, Brookfield Engineering Laboratories, Inc., Stoughton, MA, USA). The surface tension was determined by a Sigma Model 702 surface tension meter (KSV Instruments Ltd., Helsinki, Finland). The pH was measured with a pH probe (9107BN, Thermo Scientific, Waltham, MA, USA).

The characteristics of the electrospun nanofibers were determined by various techniques. The morphology of the nanofibers was examined by a field emission scanning electron microscope (FESEM, SUPRA 55VP, Carl Zeiss, Oberkochen, Germany). The average diameter of the nanofibers was determined by measuring fibers (n = 30) in each SEM image using ImageJ 1.43u software (National Institutes of Health, Bethesda, MD, USA). The energy dispersive X-ray spectrometry (EDS) analysis was also performed using the FESEM. Infrared spectra were obtained using a Nicolet 6700 (Thermo Scientific, Waltham, MA, USA) Fourier-transform infrared (FTIR) spectrometer at the range of 400–4000 cm^{-1}. Thermogravimetric analysis (TGA) was conducted on a TGA Q5000 IR (TA Instruments, New Castle, DE, USA) in a N_2 atmosphere (flow rate = 100 mL min^{-1}) under a heating rate of 10 ^oC

min^{-1} to measure the thermal stability of nanofibers. Weight loss (%) was recorded over the temperature range of 0 to 600 ^{o}C.

3.1.4 Antibacterial tests

Antibacterial properties of electrospun nanofibers were evaluated by three established methods (agar diffusion method, intimate contact method, dynamic contact method) (Gao et al., 2014). In the first test (agar diffusion method), the circular PVA and BTEAC-PVA nanofibers (diameter = 5 mm) were arranged on the agar plates containing 1 mL (~10^7 colony forming unit (CFU)) of each bacteria (*E. coli, S. aureus, K. pneumonia*) inoculums. The plates were incubated at 37 ^{o}C for 24 h.

Antibacterial properties of the BTEAC-PVA nanofibers were also examined against *S. aureus* and *K. pneumonia* using other two test methods. In the second test (intimate contact method), a modified version of the American Association of Textile Chemists and Colorists (AATCC) test method 100-2012 (AATCC, 2012) was used for the antibacterial test for PVA and BTEAC-PVA nanofibers. Aluminum foil was used as a control. The circular foil sample and nanofibers (diameter = 2.5 cm) were placed on a petri dish and sterilized under an ultraviolet radiation lamp for 30 min. A 0.25 mL volume of the test organisms (~ 10^5 CFU mL^{-1}) was dropped onto the surface of the foil or nanofibers. The

contact times were varied from 0, 30, 60, and 120 min in order to assess the effect of contact time on antibacterial activity. After inoculation, the foil and nanofibers were placed into 25 mL neutralizing water in a conical tube. The mixture was vigorously shaken on a vortex (Vortex–2 Genie, Scientific Industries, New York, USA) for 1 min, and then 100 μL of the bacterial suspension was removed from the conical tube and diluted 10^1-, 10^2-, or 10^3-fold. Finally, 100 μL each of the bacterial suspension and the diluted solutions were placed on a nutrient agar plate and incubated at 37 °C for 24 h. The following equation was used to calculate the bacterial reduction rate (R) and log reduction:

$$R\ (\%) = (B - A/B) \times 100;\ \text{Log reduction} = -\log_{10}(1 - \frac{R}{100}) \quad (1)$$

where A is the number of bacteria recovered from the foil or nanofibers after incubation at the desired contact time, and B is the number of bacteria recovered at contact time zero.

In the third test (dynamic contact method), the foil, PVA nanofibers, and BTEAC-PVA nanofibers (diameter = 2.5 cm) were added to conical tubes containing 25 mL of bacteria (~10^5 CFU mL^{-1}). The mixture was shaken at 100 rpm with a shaking incubator (IS-971R, Jeio Tech., Gimpo, Korea) for a contact time of 60, 120, and 300 min. Then, the number of bacteria present in the solution in the conical tube after the desired contact time (D) was determined

using the same procedures (serial dilution and spread plate method) used in the first test. In addition, the foil and nanofibers were removed from the conical tube after the desired contact time and immersed into another conical tube containing a phosphate buffer solution in order to detach bacteria on the surfaces of the foil and nanofibers. The mixture was vigorously vortexed for 1 min, and the number of bacteria detached from the foil and nanofibers (E) was determined following the same procedures described in the first test. The following equation was used to calculate the bacterial reduction rate (*R*):

$$R\ (\%) = [(C - D + E)/C] \times 100 \qquad (2)$$

where *C* is the number of bacteria initially present in the conical tube before addition of the foil, PVA nanofibers, and BTEAC-PVA nanofibers.

3.1.5 Antiviral tests

Bacteriophages MS2 (ATCC 15597-B1) and PhiX174 (ATCC 13706-B1), obtained from the American Type Culture Collection, were used as an indicator of the human enteric virus (Leclerc et al., 2000). MS2 is an F-specific and unenveloped single-stranded RNA phage, whereas PhiX174 is a somatic and single-stranded DNA phage (Adams, 1959). MS2 and PhiX174 were grown on *Escherichia coli* (ATCC 15597) and *Escherichia coli C* (ATCC 13706), respectively, using the double agar overlay method (Zhang et al., 2005).

The antiviral properties of the BTEAC-PVA nanofibers were examined against MS2 and PhiX174 by following the same procedures as used in dynamic contact method of the antibacterial test. In the test, the foil, PVA nanofibers, and BTEAC-PVA nanofibers (diameter = 2.5 cm) were added to conical tubes containing 25 mL of bacteriophages (~10^5 plaque forming unit (PFU) mL^{-1}) in a 10 mM NaCl solution. The bacteriophages were enumerated using the plaque assay method with the aforementioned hosts. The host culture (0.2 mL) and 0.1 mL of the diluted virus sample with 5 mL of soft agar were added to the tubes, and then the mixture was poured onto trypticase soy agar (TSA) plates to solidify. After solidifying, the plates were incubated at 37°C for 18 h. The reduction rate (R) of the bacteriophage was calculated using Equation (2).

3.2 Results and discussion

3.2.1 Electrospun PVA nanofibers

FESEM images of PVA nanofibers prepared at various electrospinning conditions (voltage and flow rate) are shown in Fig. 3.1. The optimal voltage and flow rate for electrospinning were 15 kV and 1.0 mL h^{-1}, respectively. At a voltage of 15 kV, beaded nanofibers appeared at flow rates of 0.5 (Fig. 3.1a) and 1.5 mL h^{-1} (Fig. 3.1c), whereas beaded nanofibers were rarely observed at 1.0 mL h^{-1} (Fig. 3.1b). At higher voltages of 17.5 and 20 kV (Figs. 3.1d-3.1j), many beaded nanofibers appeared, regardless of the applied flow rate. At a low flow rate, beaded nanofibers occurred because the polymer solution could not overcome the surface tension. At a high flow rate, beaded nanofibers appeared because the polymer solution exceeded the fixed electric field. The diameter ranges of the PVA nanofiber prepared at a voltage of 15 kV and flow rate of 1.0 mL h^{-1} are shown in Fig. 3.2a. At this optimal electrospinning condition, the average diameter of the PVA nanofibers was 181.0 ± 48.8 nm. The PVA nanofibers had diameters ranging from 100 to 350 nm, with the highest percent (50 %) having a diameter of 150–200 nm. Approximately 77 % of the PVA nanofibers had diameters less than 200 nm (Fig. 3.2a).

The average diameters of PVA nanofibers prepared at various electrospinning conditions (voltage and flow rate) are presented in Fig. 3.3. Our

results show that the average diameters of the nanofibers generally decreased with increasing applied voltage. The applied voltage is an important factor in electrospinning for controlling the surface charge on electrospinning solution (Sajeev et al., 2008). Some researchers reported that a high-voltage application increased electrostatic repulsion at the solution jet, resulting in formation of thinner nanofibers (Sajeev et al., 2008). Atabey et al. (2012) reported that the average diameter of PVA nanofibers decreased from 284 nm to 164 nm with increasing voltage from 20 to 25 kV. Lee et al. (2004) also observed that PVA nanofibers became thinner with increasing voltage from 10 to 25 kV. However, Supaphol & Chuangchote (2008) reported that the average diameter of PVA fibers decreased slightly with increasing applied voltage from 12.5 to 17.5 kV but increased at higher applied voltages of 17.5–25 kV.

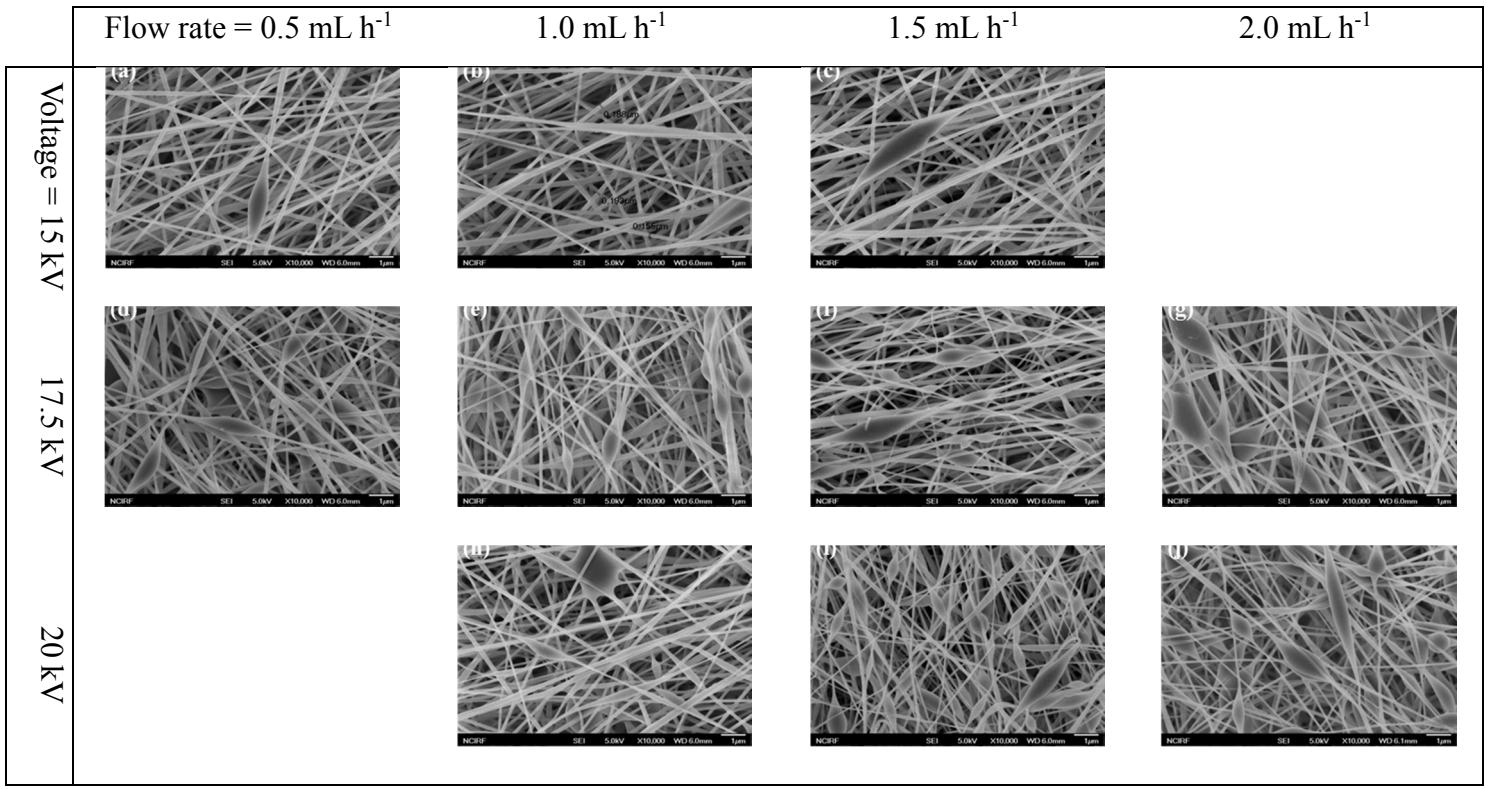

Figure 3.1. FESEM images of PVA nanofibers prepared at various electrospinning conditions (voltage and flow rate).

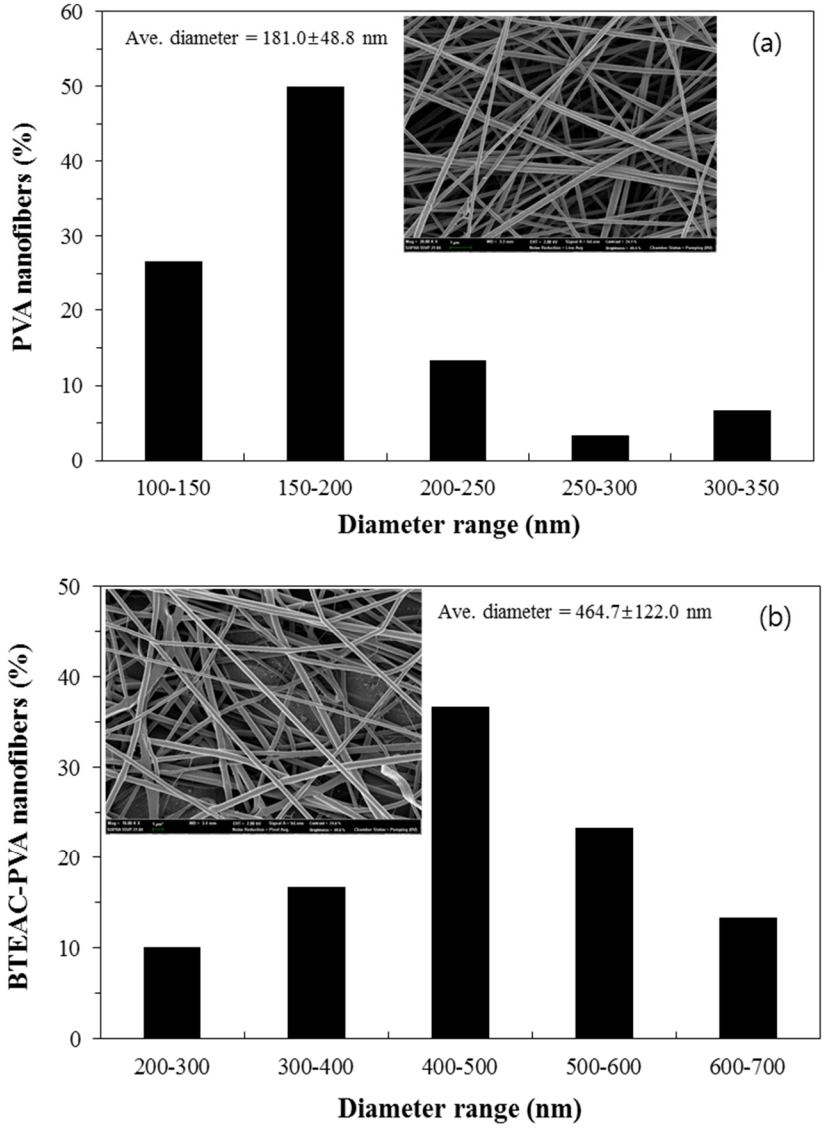

Figure 3.2 Diameter ranges of nanofibers prepared at a voltage of 15 kV and flow rate of 1.0 mL h^{-1} (inset = FESEM image of nanofibers): (a) PVA nanofibers; (b) 2.6 % BTEAC-PVA nanofibers.

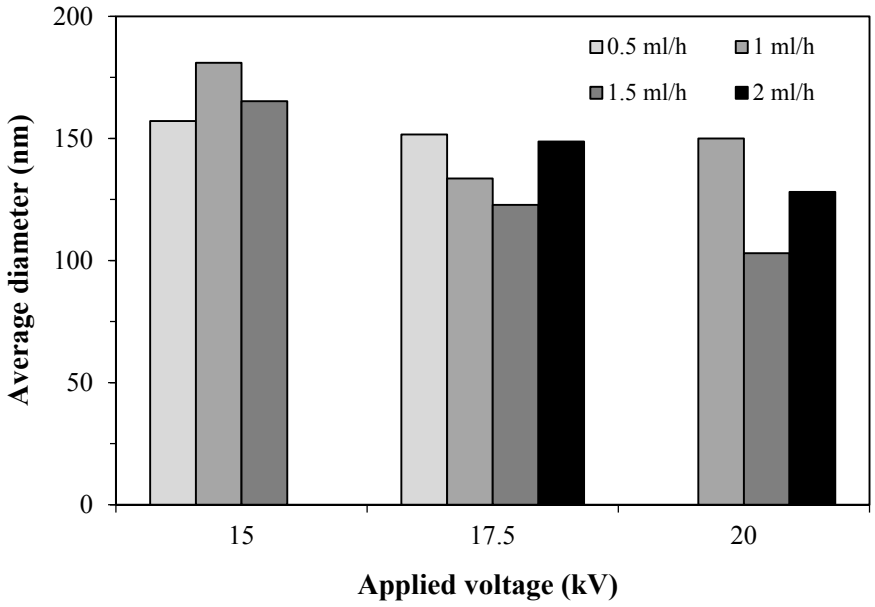

Figure 3.3 Average diameters of PVA nanofibers prepared at various electrospinning conditions (voltage and flow rate).

3.2.2 Electrospun BTEAC-PVA nanofibers

The results of the MIC tests under various concentrations of BTEAC are presented in Table 3.1. The growth of *K. pneumonia* was completely inhibited at the 1.8 % BTEAC concentration. In addition, the growth of *E. coli* was completely inhibited at 2.4 %, whereas the growth of *S. aureus* was inhibited at 2.6 %. Even though *S. aureus* was more resistant to BTEAC than *K. pneumonia* and *E. coli*, all bacteria were completely inhibited at ≥ 2.6 % of BTEAC. Therefore, antimicrobial BTEAC-PVA nanofibers were fabricated by adding 2.6 % BTEAC to the PVA solution. The diameter ranges of the 2.6 % BTEAC-PVA nanofibers are shown in Fig. 3.2b, along with the FESEM image of the BTEAC-PVA nanofibers. The average diameter of the BTEAC-PVA nanofibers was 464.7 ± 122.0 nm. The BTEAC-PVA nanofibers had diameters ranging from 200 to 700 nm, with the highest percentage (37 %) at 400–500 nm (Fig. 3.2b).

The electrospinning of nanofibers is closely related to the electrical conductivity, viscosity and surface tension of electrospinning solutions (Tan et al., 2005). In order to understand the effect of BTEAC-PVA solution characteristics on the diameter of the BTEAC-PVA nanofibers, the measured values of electrical conductivity, viscosity, surface tension, and pH of the BTEAC-added solutions, along with the diameter of the BTEAC-PVA

nanofibers, are compared in Table 3.2. The electrical conductivity of the BTEAC-added solutions increased from 1355 to 7270 μS cm^{-1} with increasing BTEAC concentration from 0 to 2.6 %. The surface tension remained relatively constant between 65.8 and 69.0 mN m^{-1}, whereas the viscosity fluctuated between 524 and 680 cp. The pH of the BTEAC-added solutions decreased slightly from 5.9 to 5.6 with increasing BTEAC concentration from 0 to 2.6 %. The average diameter of the BTEAC-PVA nanofibers increased from 181.0 to 464.7 nm with increasing BTEAC concentration from 0 to 2.6 %. Our results showed that the average diameter of the BTEAC-PVA nanofibers was closely related to the electrical conductivity; the diameter of the BTEAC-PVA nanofibers increased with increasing electrical conductivity of the BTEAC-PVA solution.

Researchers reported that the electrical conductivity is an important factor affecting the diameter of electrospun nanofibers (Wang et al., 2008; Arumugam et al., 2009). In highly conductive solutions, a fiber collision phenomenon can occur, resulting in the formation of aggregated and fused fibers. The collision phenomenon also occurred in our electrospinning process for the BTEAC-PVA nanofibers (Fig. 3.4). A single fiber intersected four other fibers (Fig. 3.4a), and two or three single fibers agglomerated into a single thicker fiber (Fig. 3.4b). Arumugam et al. (2009) prepared BTEAC-PVA fibers, reporting that the addition of BTEAC to the PVA solution caused an increase in solution

conductivity. The diameter of the BTEAC-PVA fibers was greater than that of the PVA fibers due to fiber aggregation and fusion. Wang et al. (2008) also reported that the degree of fiber aggregation (self-bundling) was enhanced with increasing conductivity of the polymer solutions. Lundin et al. (2014) prepared antimicrobial Nylon and polycarbonate electrospun fibers using QACs (CTAB and C16EO1) as antimicrobial agents, reporting that the diameter of QAC-Nylon fibers was larger than that of the Nylon fibers, whereas the diameter of QAC-polycarbonate fibers was smaller than that of the polycarbonate fibers. They stated that the diameter of the electrospun fibers was dependent on polymer type and QAC concentration.

Table 3.1 Results of MIC tests using various concentrations of BTEAC

BTEAC concentration (%)	*K. pneumonia*	*E. coli*	*S. aureus*
1.0	+	+	+
1.2	+	+	+
1.4	+	+	+
1.6	+	+	+
1.8	–	+	+
2.0	–	+	+
2.2	–	+	+
2.4	–	–	+
2.6	–	–	–
2.8	–	–	–
3.0	–	–	–
4.0	–	–	–

Table 3.2 Properties of BTEAC-PVA solutions and average diameters of the BTEAC-PVA nanofibers

BTEAC concentration in PVA solution (%)	Electrical conductivity ($\mu s\ cm^{-1}$)	Viscosity (cp)	Surface tension ($mN\ m^{-1}$)	pH	Average diameter of nanofibers (nm)
0	1355	654	69.0	5.9	181.0 ± 48.8
0.2	2050	524	66.2	5.9	196.6 ± 31.7
0.3	2170	535	67.1	5.9	299.7 ± 90.8
0.4	2420	678	67.1	5.8	173.7 ± 31.4
0.5	2730	680	66.4	5.8	187.9 ± 35.4
1.0	3840	671	67.1	5.8	281.7 ± 103.8
1.2	4670	666	65.8	5.7	440.1 ± 82.2
2.6	7270	676	66.3	5.6	464.7 ± 122.0

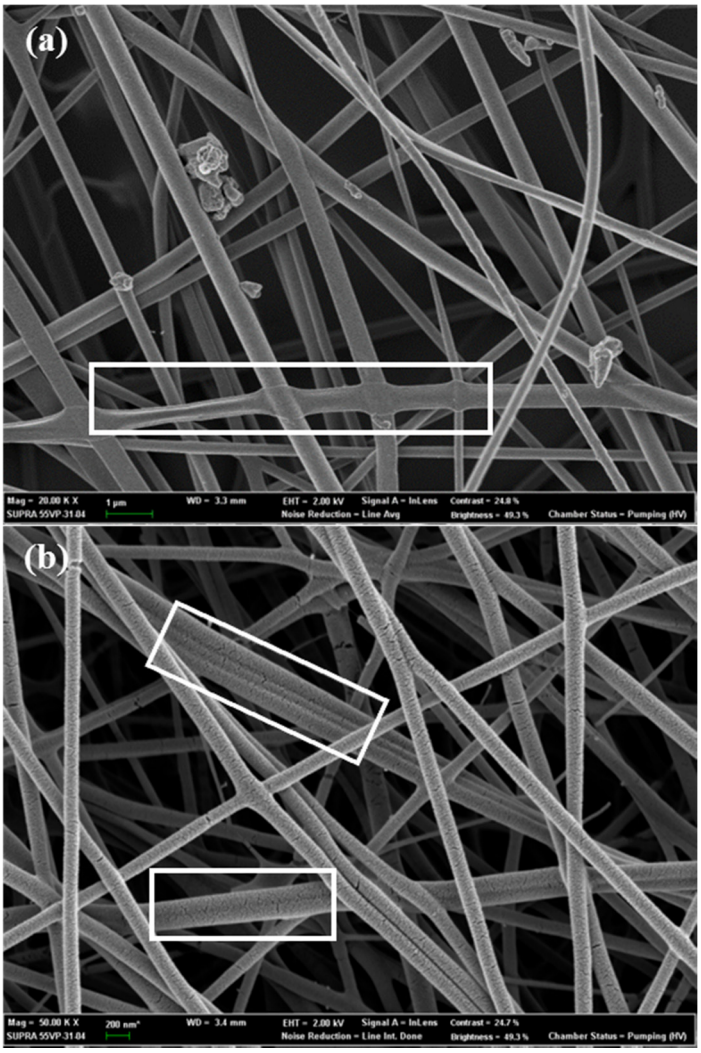

Figure 3.4 FESEM images: (a) branched nanofibers; (b) fused nanofibers.

3.2.3 FT-IR, TGA and EDS analyses

The FT-IR spectra and TGA thermograms of PVA and BTEAC-PVA nanofibers are compared in Fig. 3.6. In the FT-IR spectra of PVA nanofibers (Fig. 3.6a), the broad band at 3315 cm^{-1} corresponded to the stretching vibration of the O-H groups. The peaks at 1654 cm^{-1} and 917 cm^{-1} also corresponded to the O-H vibration. The peak at 2940 cm^{-1} was attributed to C-H stretching, whereas the bands at 1420 cm^{-1} and 1329 cm^{-1} corresponded to C-H bending (Gule et al., 2012; Linh et al., 2010). In addition, the peaks at 849, 1095 and 1143 cm^{-1} were assigned to C-C-O, C-O and C-C-C stretching, respectively. The peak at 1236 cm^{-1} was attributed to C-C stretching (Sui et al., 2005; Li et al., 2013; Siriwatcharapiboon et al., 2013). The FT-IR spectra of BTEAC-PVA nanofibers (Fig. 3.5a) showed the same major bands observed in PVA nanofibers. In addition, peaks at 756 and 707 cm^{-1} corresponding to the C-H bond in the aromatic mono-substituted benzene ring of BTEAC were observed (Larkin et al., 2011), indicating that BTEAC was successfully trapped in the PVA polymer.

The TGA thermograms of PVA and BTEAC-PVA nanofibers (Fig. 3.5b) showed that the thermal decomposition of PVA and BTEAC-PVA nanofibers occurred in two similar steps. In the first step (30–100 ^{o}C), a small weight loss in PVA and BTEAC-PVA nanofibers occurred due to the evaporation of water.

In the second step (220–360 ^{o}C), a major weight loss occurred due to thermal degradation of PVA. The TGA thermograms indicate that the thermal stability of PVA nanofibers does not change greatly in the presence of BTEAC.

The EDS pattern of BTEAC-PVA nanofibers (Fig. 3.5c) indicated that nitrogen (N) and chlorine (Cl) were appeared due to incorporation of BTEAC into PVA nanofibers, with the weight percents of N and Cl being 3.20 and 3.74%, respectively. In the EDS pattern, N was evident at the peak position of 0.392 keV as the K alpha X-ray signal, whereas Cl was evident at the peak positions of 2.622 and 2.815 keV as the K alpha and K beta X-ray signals, respectively.

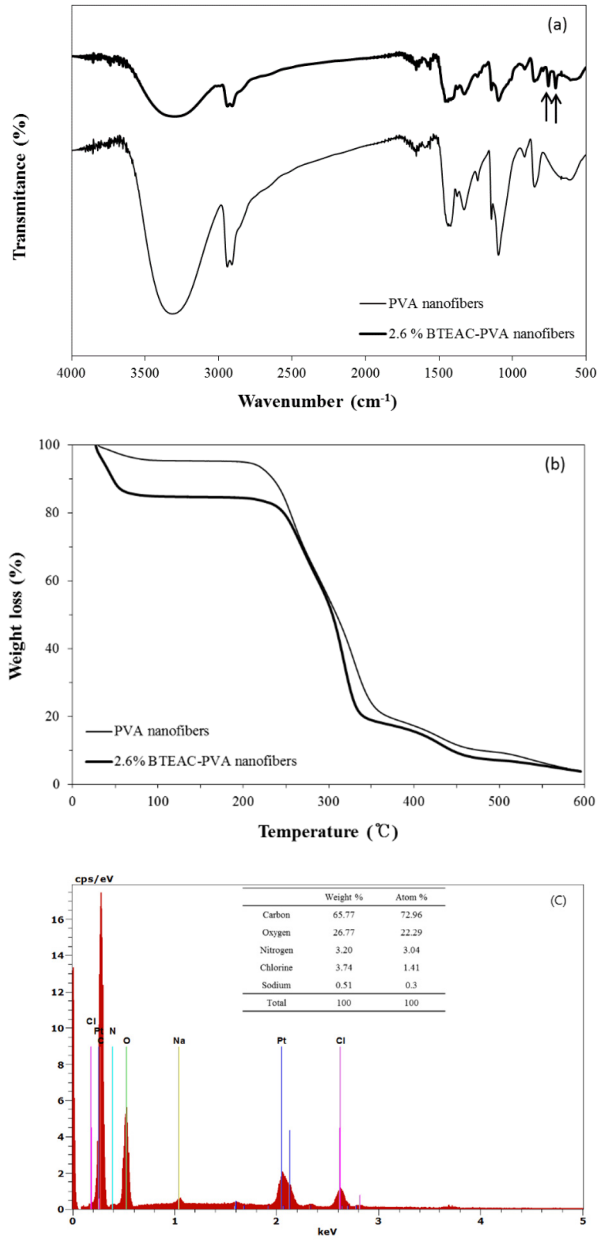

Figure 3.5 Characteristics of nanofibers: (a) FT-IR spectra; (b) TGA thermograms; (c) EDS pattern.

3.2.4 Antibacterial tests

The test results of the agar diffusion method using PVA and BTEAC-PVA nanofibers are summarized in Table 3.3. The zone of inhibition was not seen around both PVA and BTEAC-PVA nanofibers with all three bacteria. All bacteria even grew under the PVA nanofibers, whereas no growth of bacteria was observed in the zone of agar medium, which was in contact with BTEAC-PVA nanofibers. The results demonstrated that the BTEAC-PVA nanofibers could inhibit the growth of bacteria, and the antimicrobial agent BTEAC could not diffuse and release into agar because it was successfully embedded in the nanofibers. Endo et al. (1987) performed the agar diffusion test to examine the release of antimicrobial substance (tertiary amine) in polystyrene fiber, reporting that the zone of inhibition was not found because tertiary amine was covalently bonded to a polystyrene fiber.

The antibacterial test results of the 2.6 % BTEAC-PVA nanofibers using intimate contact method are presented in Fig. 6. In the case of *S. aureus* (Fig. 3.6a), the bacteria were reduced by 0.65 log after a 30 min incubation in BTEAC-PVA nanofibers, whereas the bacteria were not reduced in the control or PVA nanofibers. After a 60 min incubation, the bacteria were reduced by 0.90 log in the BTEAC-PVA nanofibers, whereas the bacteria reductions in the control and PVA nanofibers were 0.11 and 0.07 log, respectively. In addition,

the bacteria reduction in the BTEAC-PVA nanofibers was 1.23 log after a 120 min incubation, whereas those in the control and PVA nanofibers were 0.25 and 0.37 log, respectively.

In the case of *K. pneumonia* (Fig. 3.6b), the bacteria were reduced by 0.08 log after a 30 min incubation in BTEAC-PVA nanofibers, whereas the bacteria were not reduced in the control or PVA nanofibers. After a 60 min incubation, the bacteria reduction in the BTEAC-PVA nanofibers was 0.90 log, whereas that in the control and PVA nanofibers was 0.06 and 0.10 log, respectively. In addition, the bacteria reduction in the BTEAC-PVA nanofibers was 4 log after a 120 min incubation, whereas the bacteria reductions in the control and PVA nanofibers were 1.03 and 0.90 log, respectively.

The results demonstrated that the bacterial reduction in PVA nanofibers was similar to the control value, indicating that PVA had a minimal effect on bacterial death. In the case of BTEAC-PVA nanofibers, the bacterial reduction ratio increased with increasing contact time, demonstrating that BTEAC-PVA nanofibers successfully inhibited the growth of both bacteria. Similar findings were reported by Kim et al. (2007), who prepared PC nanofibers containing 2 wt% BTEAC. They reported that the reduction ratio of bacteria (*S. aureus*, *K. pneumonia, E. coli*) in the BTEAC-PC nanofibers was > 90 % after 18 h incubation, which was far greater those in the PC nanofibers (12.5–41.2 %).

QACs, including BTEAC, are membrane-active agents (McDonnell et al., 1999). The target sites for antibacterial activity of QACs are primarily at the cytoplasmic membrane of bacteria. QACs can disrupt the cytoplasmic membrane, leading to the release of K^+ ions and other cytoplasmic constituents (Kawabata et al., 1988; Kenawy et al., 2003)

The antibacterial test results of 2.6 % BTEAC-PVA nanofibers in the dynamic contact test are provided in Fig. 7. After a 60 min incubation, *S. aureus* was reduced by 0.07 log in BTEAC-PVA nanofibers, whereas there was no bacteria reduction in the control or PVA nanofibers. After a 120 min incubation, the *S. aureus* reduction in the BTEAC-PVA nanofibers was 0.25 log, whereas the bacteria were not reduced in the control or PVA nanofibers. In addition, the *S. aureus* reduction in the BTEAC-PVA nanofibers was 0.43 log after a 300 min incubation, whereas the *S. aureus* reductions in the control and PVA nanofibers were 0 and 0.08 log, respectively (Fig. 3.7a).

K. pneumonia was reduced by 0.13 log after a 60 min incubation in the BTEAC-PVA nanofibers, whereas the *K. pneumonia* reductions in control and PVA nanofibers were 0.003 and 0.04 log, respectively. After a 120 min incubation, the *K. pneumonia* reduction in the BTEAC-PVA nanofibers was 0.34 log, whereas the *K. pneumonia* reductions in the control and PVA nanofibers were 0.05 and 0.14 log, respectively. In addition, the *K. pneumonia*

reduction in BTEAC-PVA nanofibers was 0.35 log after a 300 min incubation, whereas the *K. pneumonia* reductions in control and PVA nanofibers were 0.09 and 0.17 log, respectively (Fig. 3.7b). The results demonstrated that the bacterial reduction by BTEAC-PVA nanofibers in the dynamic contact method was less than that in the intimate contact test. This result could be attributed to the larger volume of bacteria used in the dynamic contact method than the intimate contact method.

Table 3.3 Results of agar diffusion method using PVA and BTEAC-PVA nanofibers

Sample	Bacteria	Growth assessment	
		Zone of Inhibition (mm)	Growth under nanofibers
PVA nanofiber	*K. pneumonia*	0.0	average growth
	E. coli	0.0	average growth
	S. aureus	0.0	average growth
BTEAC-PVA nanofiber	*K. pneumonia*	0.0	no growth
	E. coli	0.0	no growth
	S. aureus	0.0	no growth

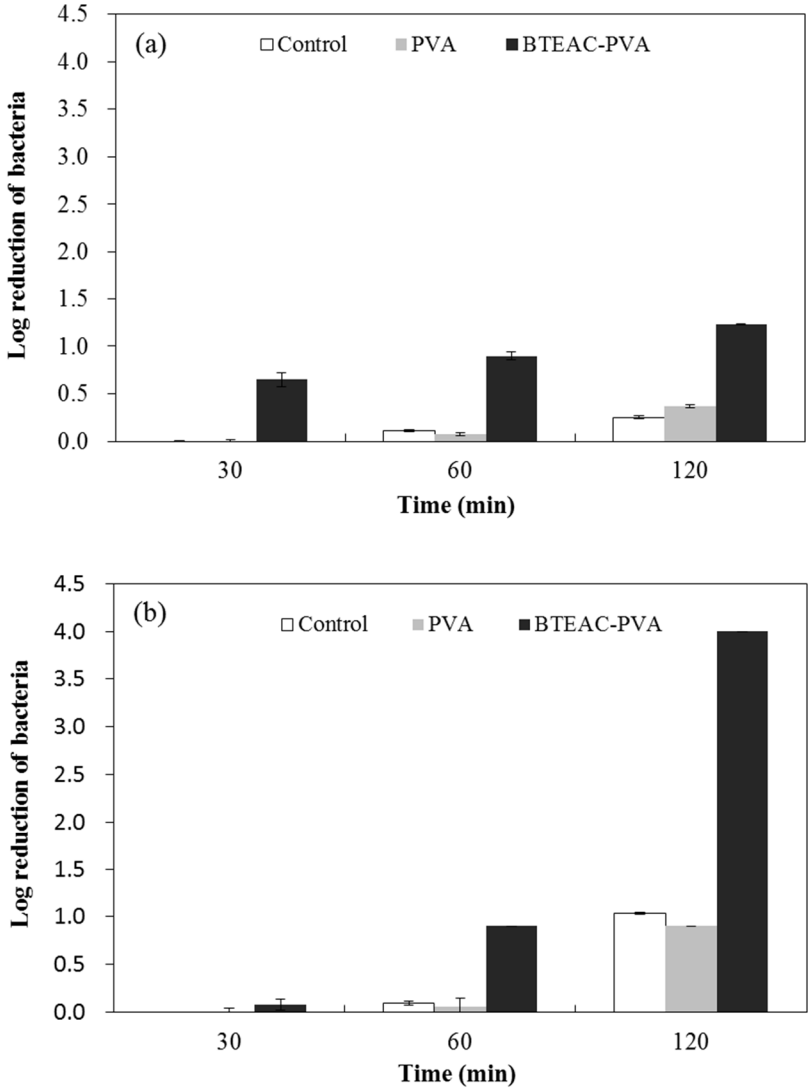

Figure 3.6 Antibacterial test results of 2.6 % BTEAC-PVA nanofibers (intimate contact method): (a) *S. aureus*; (b) *K. pneumonia.*

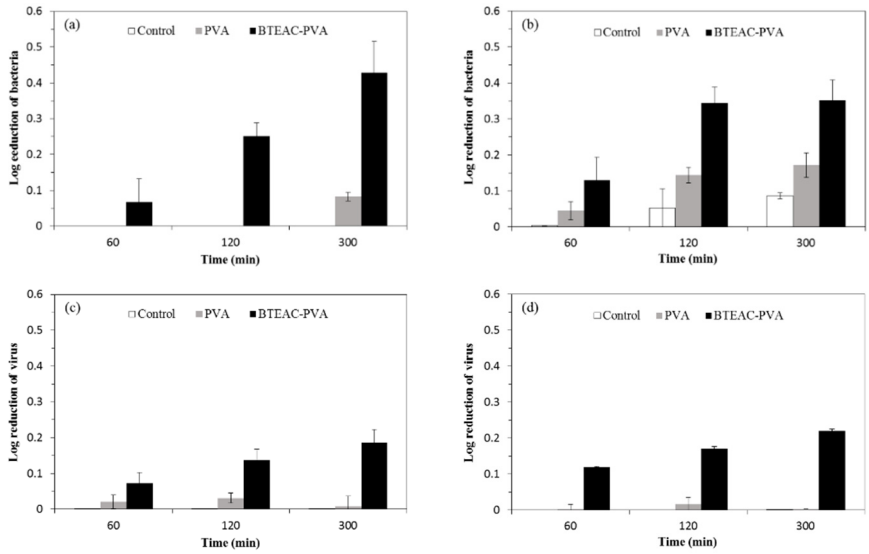

Figure 3.7 Antibacterial test results of 2.6 % BTEAC-PVA nanofibers (dynamic contact method): (a) *S. aureus*; (b) *K. pneumonia*; (C) PhiX174; (d) MS2

3.2.5 Antiviral tests

The antiviral test results of 2.6 % BTEAC-PVA nanofibers in the dynamic contact method are presented in Fig. 7. In the case of PhiX174 (Fig. 3.7c), the bacteriophage was reduced by 0.12 log after a 60 min incubation in BTEAC-PVA nanofibers, whereas the bacteriophage was not reduced in the control or PVA nanofibers. After a 120 min incubation, the bacteriophage reduction in the BTEAC-PVA nanofibers was 0.17 log, whereas the bacteriophage reductions in the control and PVA nanofibers were 0.0 and 0.01 log, respectively. In addition, the bacteriophage reduction in BTEAC-PVA nanofibers was 0.22 log after a 300 min incubation, whereas the bacteriophage reductions in the control and PVA nanofibers were both 0 log, respectively.

In the case of MS2 (Fig. 3.7d), the bacteriophage reduction was 0.07 log after a 60 min incubation in BTEAC-PVA nanofibers, whereas the bacteriophage reductions in the control and PVA nanofibers were 0 and 0.02 log, respectively. After a 120 min incubation, the bacteriophage reduction in the BTEAC-PVA nanofibers was 0.14 log, whereas the bacteriophage reductions in control and PVA nanofibers were 0 and 0.03 log, respectively. In addition, the bacteriophage reduction in the BTEAC-PVA nanofibers was 0.19 log after a 300 min incubation, whereas the bacteriophage reductions in the control and PVA nanofibers were 0 and 0.01 log, respectively.

The results showed that bacteriophage reduction in PVA nanofibers was similar to the control value, indicating that PVA had a minimal effect on bacteriophage reduction. BTEAC-PVA nanofibers inactivated both MS2 and PhiX174. The bacteriophage reduction ratio in the BTEAC-PVA nanofibers increased with increasing contact time. Previous studies have reported that the removal of enveloped virus by QACs was greater than that of unenveloped virus (Mi et al., 2014; Park et al., 2013), presumably due to the higher affinity of enveloped virus to QAC-treated surfaces through hydrophobic interactions (Tsao et al., 1989). QACs can disrupt the viral envelope, which is a lipid layer around the nucleocapsid (nucleic acid + capsid), resulting in the release of the nucleocapsid (Tsao et al., 1989). However, the inactivation mechanisms of the unenveloped virus by QACs are not clear but are presumably related to denaturation of the capsid (Hegstad et al., 2010). Note that MS2 is an unenveloped virus, composed of single-stranded RNA (nucleic acid) encapsulated within a capsid (protein coat), whereas Phix174 is an unenveloped virus, comprised of single-stranded DNA encapsulated within a capsid (Madigan et al., 2009).

Chapter 4

Functionalization of Poly(vinyl alcohol) Electrospun Nanofibrous Membranes with Benzyl Triethylammonium Chloride for Antimicrobial Water Filtration

4.1 Materials and methods

4.1.1 Fabrication of ENMs

Electrospinning of the PVA/GF ENMs was performed at room temperature using an electrospinning system (ESP200/ESP100, NanoNC, Seoul, Korea). The as-prepared PVA solution (8 wt%) was placed in a 25-mL syringe with a metal needle (inner diameter = 0.51 mm) that was connected to the positive terminal of a high-voltage power supply. The PVA nanofibers were deposited on a commercial glass microfiber filter (GF, Whatman 1822-047) fixed to a rotating cylinder (diameter = 9 cm; speed = 1000 rpm) on a negative terminal.

The BTEAC-PVA/GF ENMs were synthesized using the pre-functionalized method. Prior to the electrospinning of BTEAC-PVA/GF nanofibers, 2.6% BTEAC was added to the PVA solution (8 wt%) to impregnate BTEAC into the PVA nanofibers during the electrospinning process. The BTEAC-PVA nanofibers were also deposited on a commercial glass microfiber filter (GF, Whatman 1822 047, Maidstone, UK) fixed to a rotating cylinder. The electrospinning conditions for both PVA/GF ENMs and BTEAC-PVA/GF ENMs were as follows: applied voltage of 15 kV, flow rate of 1.0 mL h^{-1} and tip-to-collector distance of 15 cm. Prior to use in the antimicrobial filtration tests, both PVA/GF ENMs and BTEAC-PVA/GF ENMs were prepared by heat-methanol treatment (heat treatment for 20 min at 150 ^{o}C and followed by

methanol treatment for 24 h) to improve the water stability of the ENMs by crosslinking the polymer chains.

4.1.2 Characterization of ENMs

The characteristics of the ENMs excluding the support layer (GF) were determined by various techniques. The morphology was examined by a field emission scanning electron microscope (FESEM, SUPRA 55VP, Carl Zeiss, Oberkochen, Germany). The average diameter was determined by measuring the fibers (n = 30) in each SEM image using ImageJ 1.43u software (National Institutes of Health, Bethesda, MD, USA). The porosity (n) was obtained by the following relationship (Ma et al., 2005):

$$n\ (\%) = \left(1 - \frac{a_n}{b_n}\right) \times 100 \qquad (1)$$

where a_n is the apparent density of the nanofibers, and b_n is the bulk density of the polymer solution. For the calculation of a_n, the thickness of the electrospun nanofibers was determined from a FESEM image. The water contact angle was measured by the sessile drop method using a contact angle analyzer (Phoenix 300, Surface Electro Optics Co. Ltd, Seoul, Korea). Thermal properties, such as the melting point (T_m) and heat (enthalpy) of fusion (ΔH_f), were determined using differential scanning calorimetry (DSC-Q1000, TA instrument, New

Castle, DE, USA) with heating from 30 to 450 °C at 10 °C min^{-1}. The degree of crystallinity (X_c) was calculated by the following equation (Peppas & Merrill, 1976; Kong & Hay, 2002):

$$X_c = \frac{\Delta H_f(T_m)}{\Delta H_f{}^0(T_m{}^0)} \quad (2)$$

where $\Delta H_f(T_m)$ is the heat of fusion measured at the melting point, and $\Delta H_f{}^0(T_m{}^0)$ is the heat of fusion for a 100% crystalline polymer measured at the equilibrium melting point (100% crystalline PVA = 138.6 J g^{-1}) (Yao et al., 2003).

The filter characteristics of the ENMs were also determined. The filter thickness was determined using the cross-sectional FESEM images. The pore size distribution was examined by capillary flow porometry (CFP-1500AE, Porous Materials Inc., Ithaca, NY, USA). The water permeability was determined at room temperature using a dead-end filtration system; the pressure across the filter (transmembrane pressure, TMP) was 0.6 bar (= 60 kPa). The pure water flux (J) was calculated by the following equation:

$$J = \frac{V}{S \times t} \quad (3)$$

where V is the total permeation volume (= 100 mL), S is the total permeation area (= 1.1×10^{-3} m^2), and t is the total permeation time (min).

Destructive tests were also observed by filtering water using a dead-end filtration system until the ENMs were damaged.

4.1.3 Immersion, leaching, and toxicity tests for BTEAC

Immersion tests were performed for BTEAC-PVA ENMs with no treatment, heat treatment, and heat-methanol treatment to evaluate the water stability of the ENMs and to quantify the amount of BTEAC in the immersed ENMs. The BTEAC-PVA ENMs were immersed in water (25 ^{o}C) for various times (4, 24, and 48 h), and their web structures were examined by FESEM (SUPRA 55VP, Carl Zeiss, Oberkochen, Germany). In addition, the nitrogen content of BTEAC-PVA ENMs was determined to indirectly quantify the amount of BTEAC in the immersed ENMs by energy-dispersive X-ray spectrometry (EDS, XFlash 4000, Bruker AXS, Berlin, Germany), combined with an electron microscope at an accelerating voltage of 15 kV.

Leaching tests were conducted to quantify the amount of BTEAC that leached from BTEAC-PVA ENMs with heat-methanol treatment. Starting from 10 mL, various volumes of deionized water were filtered serially through a dead-end filtration system (total volume of water = 500 mL). The leached BTEAC concentration in the filtrate water was monitored by UV-Visible

spectrophotometry (Helios, Thermo Scientific, Waltham, MA, USA) at a wavelength of 208 nm.

Acute toxicity tests for BTEAC to *D. magna* neonates (age, < 24 h) were performed with DAPHTOXKIIT F *magna* (MicroBioTests Inc., Mariakerke-Gent, Belgium) following the procedures described in the test manual. Five neonates were placed in a 10 mL solution containing 10 different types of BTEAC concentrations ranging from 0.1 to 1000 mg/L (4 replicates for each) at 20 ± 1 ^{o}C in the dark. The numbers of mobile and immobile neonates were observed 24 and 48 h after contact with BTEAC solutions. A median effective concentration (EC_{50}) and associated 95% confidence interval (CI) were calculated from dose-response curves using a USEPA Trimmed Spearman-Karber program (USEPA, 1999).

4.1.4 Antimicrobial water filtration tests

Antibacterial water filtration tests were performed for BTEAC-PVA/GF ENMs, PVA/GF ENMs, and GF. Two bacteria, *E. coli* (ATCC 11105) and *S. aureus* (ATCC 6538), were used in the tests. A bacterial solution was prepared by adding ~10^5 colony forming units (CFU)/mL of each bacterium to autoclaved deionized water (total volume of bacteria solution = 500 mL). Starting from 10 mL, various volumes of bacterial solution were filtered serially

through a dead-end filtration system (TMP = 0.6 bar). The number of bacteria that were collected in the filtrate water was enumerated by inoculating on a nutrient agar plate, which was incubated at 37 ^{o}C for 24 h. The log reduction value (LRV) was calculated by the following relationship:

$$\mathrm{LRV} = -\log_{10}\left(\frac{C_f}{C_0}\right) \quad (4)$$

where C_0 is the initial concentration of bacteria, and C_f is the concentration of bacteria in the filtrate water.

Additional antibacterial water filtration tests were conducted for BTEAC-PVA/GF ENMs using river water samples collected from the Han River in Seoul, Korea. The river water samples had the following characteristics: biochemical oxygen demand (BOD) = 1.4 mg/L, dissolved oxygen (DO) = 7.2 mg/L, turbidity = 4.53 NTU, suspended solid (SS) = 8.93 mg/L, pH = 7.51, and electrical conductivity (EC) = 219 μs/cm. Starting from 50 mL, various volumes of river water were filtered serially through a dead-end filtration system (total volume of river water = 500 mL; TMP = 0.6 bar). From filtrate water, the total coliform, heterotrophic plate count (HPC), and turbidity were determined using the following methods: 3M Petrifim^{TM} *E. coli*/coliform count plates (3M Microbiology Products, St. Paul, MN, USA) for total coliform, R2A agar (Difco Laboratories, Detroit, MI, USA) for HPC, and portable turbidimeter (2100Q, Hach Company, Mississauga, Ontario, Canada) for turbidity.

Antiviral water filtration tests were performed for BTEAC-PVA/GF ENMs, PVA/GF ENMs, GF, and a commercial polycarbonate filter (PC, Whatman, 111106, Maidstone, UK). Bacteriophages MS2 (ATCC 15597-B1) and PhiX174 (ATCC 13706-B1), obtained from the American Type Culture Collection, were used as indicators of the human enteric virus (Leclerc et al., 2000). MS2 is an F-specific and unenveloped single-stranded RNA phage, whereas PhiX174 is a somatic and single-stranded DNA phage (Adams, 1959). MS2 and PhiX174 were grown on *Escherichia coli* (ATCC 15597) and *Escherichia coli C* (ATCC 13706), respectively, using the double agar overlay method (Zhang et al., 2005). A virus solution was prepared by adding 1.3×10^5 plaque forming units (PFU)/mL to a 10 mM NaCl solution (total volume of virus solution = 300 mL). Starting from 10 mL, various volumes of virus solution were filtered serially through a dead-end filtration system (TMP = 0.6 bar). The number of viruses collected in the filtrate water was enumerated by the plaque assay method with the aforementioned hosts. The host culture (0.2 mL) and 0.1 mL of the diluted virus sample with 5 mL of soft agar were added to the tubes, and the mixture was then poured onto trypticase soy agar (TSA) plates to solidify. After solidifying, the plates were incubated at 37°C for 18 h.

4.2 Results and discussion

4.2.1 Characteristics of BTEAC-PVA ENMs

FESEM images and diameter ranges of BTEAC-PVA ENMs and PVA ENMs prepared by heat-methanol treatment are shown in Fig. 4.1. The FESEM images (Fig. 4.1a and 4.1c) showed that both BTEAC-PVA ENMs and PVA ENMs were well fabricated through electrospinning. The characteristics of BTEAC-PVA ENMs and PVA ENMs, excluding the support layer (GF), are presented in Table 1. BTEAC-PVA ENMs had diameters ranging from 100 to 450 nm, with the highest percent (36.7%) at 150–200 nm (Fig. 1b). The diameter of BTEAC-PVA ENMs was 216.6 ± 50.9 nm (Table 1). PVA ENMs had diameters ranging from 80 to 220 nm, with the highest percent (30%) having a diameter of 160–180 nm. Approximately 97% of the PVA nanofibers had diameters of less than 200 nm (Fig. 1d). The diameter of PVA ENMs was 154.6 ± 27.7 nm (Table 4.1). These results demonstrate that the diameter of BTEAC-PVA ENMs became larger than that of PVA ENMs due to the impregnation of BTEAC. The porosities of BTEAC-PVA ENMs and PVA ENMs were 79.0 and 80.4%, respectively, which were larger than the value of the supporting layer of GF (48.6%).

The water contact angle of BTEAC-PVA ENMs with the heat-methanol treatment was 29.0 ± 1.6^{o}, which was lower than that (54.7 ± 6.4^{o}) of PVA

ENMs with the heat-methanol treatment (Table 4.1). These results indicate that BTEAC-PVA ENMs were more hydrophilic than PVA ENMs due to the incorporation of BTEAC, which has hydrophilic characteristics (Tagle et al., 1998). Similar findings were reported by Liu et al. (2010) who prepared the chitosan/cellulose acetate (CS/CA) blend membrane and modified the CS/CA blend membrane with QAC. These authors reported that the QAC-modified CS/CA blend membrane was more hydrophilic than CS/CA blend membrane. The water contact angle of the QAC-modified CS/CA blend membrane was 39.8^{o}, which was lower than that (69.6^{o}) of the CS/CA blend membrane. Zhang et al. (2014) also reported that the water contact angles (28 – 43^{o}) of the QAC-modified aromatic polyamide thin film (APA-TFC) membrane were smaller than those (54 – 61^{o}) of the APA-TFC membrane. These authors attributed this phenomenon to the fact that QAC provided the APA-TFC membrane with high hydrophilicity. It should be noted that hydrophilic surfaces are desirable for water filtration/purification application because they can increase the water permeability of the membrane (Ma et al., 2011; Reisner et al., 2014). In addition, hydrophilic surfaces can supply instant contact with bacteria in an aqueous medium, resulting in the rapid death of bacteria (Sun et al., 2002).

The melting point and heat of fusion of BTEAC-PVA ENMs and PVA ENMs are presented in Table 4.1, demonstrating that BTEAC-PVA ENMs had a better thermal property than did PVA ENMs. The melting point and heat of fusion of

BTEAC-PVA ENMs with the heat-methanol treatment were 424.6 ^{o}C and 314.4 J/g, respectively, which were greater than the values (229.6 ^{o}C and 66.6 J/g) of PVA ENMs with the heat-methanol treatment (Table 4.1). In addition, the melting point and heat of fusion of BTEAC-PVA ENMs with the heat-methanol treatment were greater than the values (259.3 ^{o}C and 241.5 J/g) of BTEAC-PVA ENMs with no treatment. These results indicate that the thermal property and crystallinity of BTEAC-PVA ENMs were improved through the heat-methanol treatment. The same trend was found for PVA ENMs. The melting point and heat of fusion of PVA ENMs prepared by the heat-methanol treatment were larger than the values (227.8 ^{o}C and 54.6 J/g) of BTEAC-PVA ENMs with no treatment. The degree of crystallinity of PVA ENMs prepared by heat-methanol treatment was 48.1%, which was larger than that (39.4%) of PVA ENMs that were prepared with no treatment. Similar findings were reported by Yao et al. (2003), who prepared electrospun PVA fibers. These authors reported that the degree of crystallinity of PVA was enhanced through methanol treatment; the melting point and heat of fusion of methanol-treated PVA fibers were greater than the values of PVA fibers without methanol treatment. They attributed this phenomenon to the residual water removal within PVA fibers by methanol treatment, resulting in the replacement of PVA-water hydrogen bonding by intermolecular polymer hydrogen bonding.

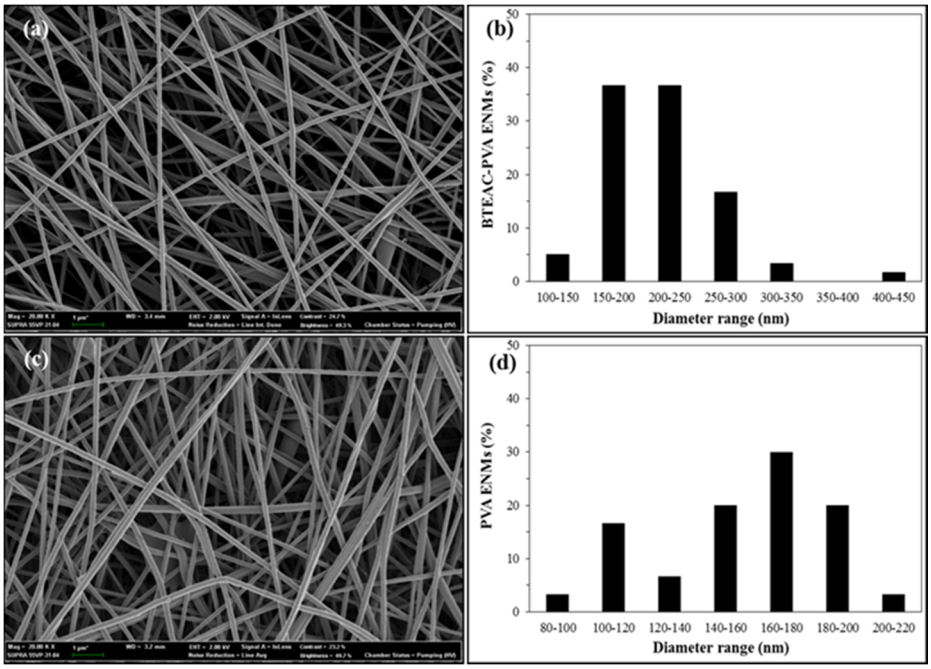

Figure 4.1 Characteristics of electrospun nanofiber membranes (ENMs) that were prepared with the heat-methanol treatment: (a) SEM image of BTEAC-PVA ENMs (bar = 1 um); (b) diameter range of BTEAC-PVA ENMs; (c) SEM image of PVA ENMs (bar = 1 um); (d) diameter range of PVA ENMs.

Table 4.1 Characteristics of BTEAC-PVA ENMs and PVA ENMs excluding the support layer (GF)

Type of ENMs	Diameter of nanofiber (nm)	Porosity (%)	Water contact angle (^{o})	Melting point (^{o}C)	Heat of fusion (J/g)
BTEAC-PVA ENMs	216.6 ± 50.9	79.0	29.0 ± 1.6	424.6	314.4
PVA ENMs	154.6 ± 27.7	80.4	54.7 ± 6.4	229.6	66.6

4.2.2 BTEAC leaching and toxicity

The nitrogen contents of BTEAC-PVA ENMs with the heat-methanol treatment obtained from the immersion tests are presented as a function of immersion time in Fig. 4.2. The nitrogen contents of BTEAC-PVA ENMs with no treatment and with heat treatment are also presented for the comparison. According to the EDS analysis, the nitrogen content (3.80%) of BTEAC-PVA ENMs with the heat-methanol treatment at a water immersion of 0 h was slightly lower than that (4.74 and 5.43%) of BTEAC-PVA ENMs with no treatment and with heat treatment. This result could be attributed to BTEAC loss occurring during the preparation of BTEAC-PVA ENMs using the heat-methanol treatment, especially during methanol soaking. After the heat-methanol treatment, however, the nitrogen content of BTEAC-PVA ENMs remained relatively constant at 3.80 ± 0.26% after water immersion for 0 – 48 h, indicating that BTEAC release was minimal for BTEAC-PVA ENMs with the heat-methanol treatment. The FESEM images (inset in Fig. 4.2) demonstrate that BTEAC-PVA ENMs with the heat-methanol treatment had good water stability. The web structure was preserved after water immersion at 24 and 48 h even though slight swelling was observed. Meanwhile, after the heat treatment, the nitrogen content of BTEAC-PVA ENMs became 0% at 24 h of immersion time due to the release of all of the BTEAC into the water. The FESEM image (inset in Fig. 4.2) shows that the web structure of BTEAC-PVA

ENMs with the heat treatment was still preserved at 24 h of immersion time, even though swelling was observed. In the case of BTEAC-PVA ENMs with no treatment, which are readily soluble in water, nitrogen content became 0% at 4 h of immersion time because BTEAC-PVA ENMs dissolved in water.

The leached BTEAC concentrations from BTEAC-PVA ENMs with heat-methanol treatment obtained from the leaching tests are presented in Fig. 4.3 as a function of the filtrate water volume. The leached BTEAC concentration curve demonstrated that the BTEAC concentration from BTEAC-PVA ENMs after 10 mL of water filtration was 0.72 mg/L and decreased to 0.38 mg/L after 20 mL of water filtration. The BTEAC concentration decreased further to 0.075 mg/L after 100 mL of water filtration and arrived at 0 mg/L after 150 mL of water filtration. The accumulative BTEAC curve showed that the amount of BTEAC released from BTEAC-PVA ENMs was 0.0072 mg after 10 mL of water filtration, reached 0.0076 mg after 20 mL of water filtration, and equilibrated thereafter during 500 mL of water filtration. These results indicate that a minimal amount of BTEAC was leached mostly at the beginning of water filtration.

Our results indicate that the heat-methanol treatment has an advantage over the heat treatment in maintaining the BTEAC content in BTEAC-PVA ENMs during water filtration. Previous studied have reported that electrospun PVA

nanofibers could be stabilized against water through the crosslinking of the polymer chain. Hong et al (2006) used both heat treatment (155 ^{o}C, 3 min) and methanol treatment (12 h) to crosslink PVA/$AgNO_3$ nanofibers and compared their water stability after immersion at 37 ^{o}C water for 5 h. These authors reported that heat-treated PVA/$AgNO_3$ nanofibers were more stable against water than methanol-treated nanofibers. Voigt (2009) used heat treatment to crosslink PVA nanofibers (150 ^{o}C, 10 min) and PVA/Ag nanofibers (150 ^{o}C, 25 min). The author reported that heat-treated PVA nanofibers had water stability up to an immersion time of 24 h, whereas heat-treated PVA/Ag nanofibers showed water stability after immersion for 1 h, swelling after 4 h, and agglutination after 24 h.

The acute toxicity test results for BTEAC to *D. magna* are presented in Fig. 4.4, along with the calculated EC_{50} values. The concentration-response curves demonstrated that in the 24 h acute toxicity test, *D. magna* was not affected by BTEAC concentration ranging from 0.1 to 25 mg/L (immobilization = 0%). As the BTEAC concentration increased from 50 to 200 mg/L, the immobilization of *D. magna* increased sharply from 5 to 95%. At a BTEAC concentration of 1000 mg/L, all *D. magna* were immobilized. The 24-h EC_{50} of BTEAC to *D. magna* was 112.61 mg/L with a confidence limit (CI, 95% probability) of 97.05 – 130.66 mg/L, which was higher than the value (0.72 mg/L) of 3-(trimethoxysilyl)-propyldimethyl octadecyl ammonium chloride (TPOAC) to

D. magna as reported in the literature (Geiger et al., 1988). These results indicate that BTEAC is far less toxic than TPOAC, which has been used as QAC for antimicrobial water filtration (Voigt, 2009; Abbaszadegan et al., 2006). In 48 h test, *D. magna* was not affected by BTEAC concentration ranging from 0.1 to 5 mg/L. The immobilization of *D. magna* increased rapidly from 5 to 75% with an increase in the BTEAC concentration from 10 to 100 mg/L. All of the *D. magna* were immobilized at BTEAC concentrations of 150–1000 mg/L. It should be noted that the highest BTEAC concentration that leached from BTEAC-PVA ENMs during water filtration was 0.72 mg/L, which was far below the BTEAC concentration affecting the immobilization of *D. magna* (5 mg/L). The 48-h EC_{50} of BTEAC to *D. magna* was 89.54 mg/L with a CI of 75.43 – 106.28 mg/L. Note that the 96-h LC_{50} (median lethal concentration) of BTEAC to *Pimephales promelas* (fathead minnow) was reported as 161 mg/L in the literature (Geiger et al., 1988).

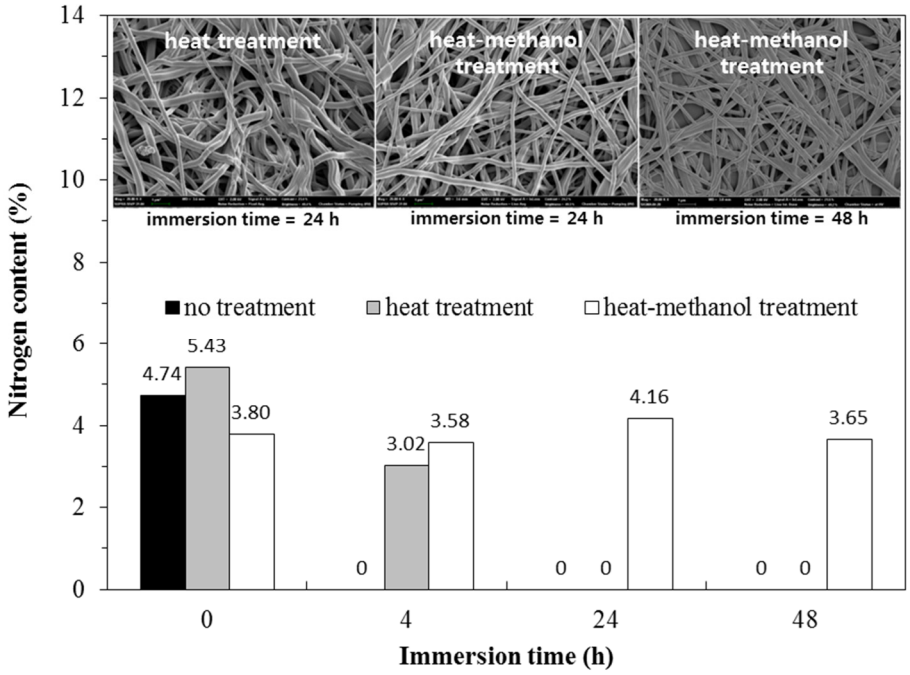

Figure 4.2 Nitrogen contents of BTEAC-PVA ENMs under various immersion times (inset = FESEM images of immersed BTEAC-PVA ENMs).

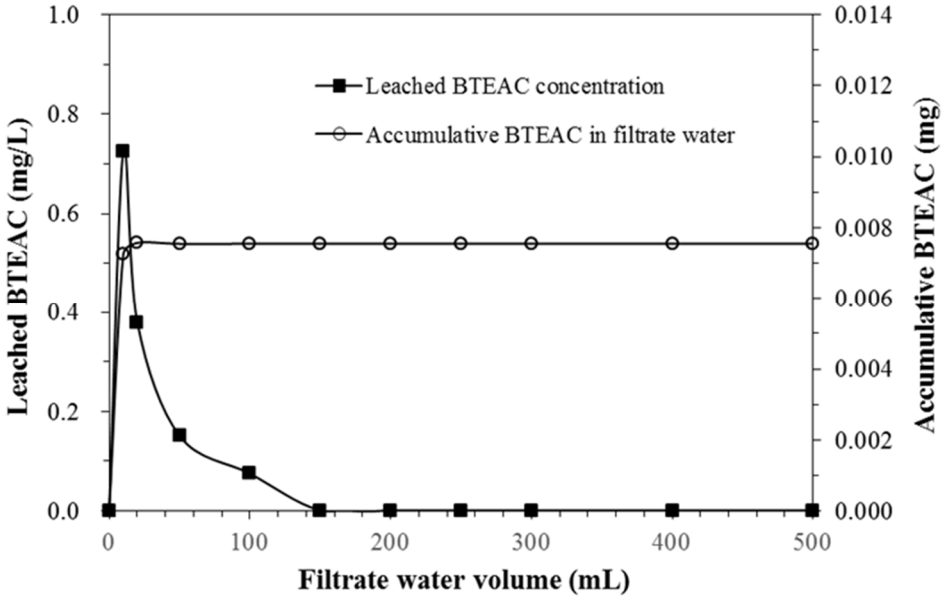

Figure 4.3 BTEAC leached from BTEAC-PVA ENMs during water filtration.

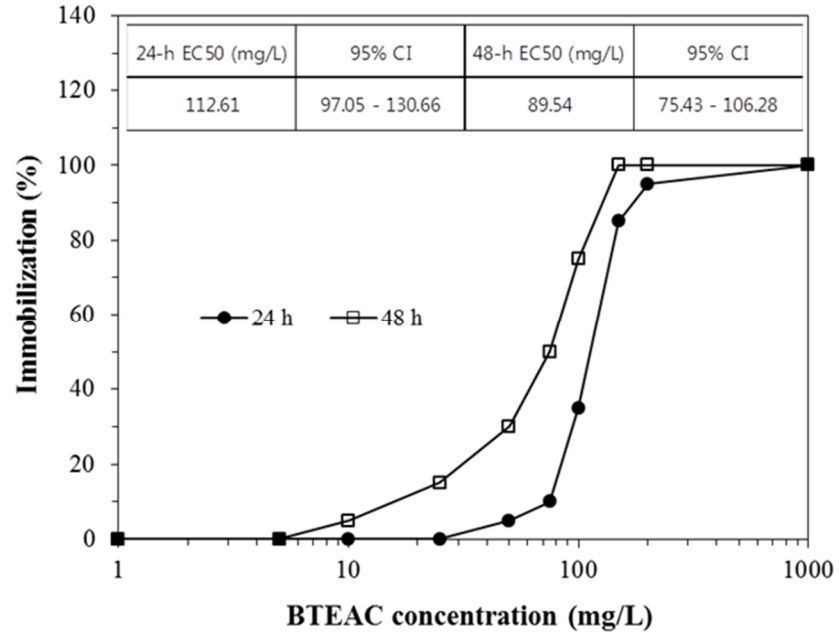

Figure 4.4 Immobilization of D. magna as a function of BTEAC concentrations (inset = 24-h and 48-h EC50 values along with 95% confidence intervals).

4.2.3 Antibacterial assessment with filtration test

The bacteria log removals (LRV) by BTEAC-PVA/GF ENMs, PVA/GF ENMs, and GF obtained from the antibacterial water filtration tests are compared in Fig. 4.5 as a function of the filtrate water volume. In the BTEAC-PVA/GF ENMs, the LRV for *E. coli* was 4.88 after 10 mL of water filtration and decreased to 2.81 after 100 mL of water filtration. A LRV for *E. coli* decreased further to 2.25 after 500 mL of water filtration. For PVA/GF ENMs, the LRV for *E. coli* decreased from 3.43 to 1.13 with an increase in the water filtrate volume from 10 to 500 mL, whereas it changed from 2.41 to 0.81 for GF. A similar trend was found for *S. aureus*. In the case of BTEAC-PVA/GF ENMs, the LRV decreased from 5.75 to 3.29 with an increase in the water filtrate volume from 10 to 500 mL. The LRV decreased from 3.80 to 2.46 for PVA/GF ENMs in the same range of water filtrate volume, whereas it changed from 3.53 to 1.89 for GF.

Our results indicate that the bacterial removal efficiency was on the order of BTEAC-PVA/GF ENMs > PVA/GF ENMs > GF. This trend could be attributed to the fact that both sieving and contact killing could contribute to the removal of bacteria for BTEAC-PVA/GF ENMs, whereas sieving is the main removal mechanism for PVA/GF ENMs and GF. PVA/GF ENMs were more effective in the removal of bacteria than GF. This result could be related to the mean pore

sizes of PVA/GF ENMs and GF. The mean pore size of PVA /GF ENMs was 0.78 ± 0.47 μm, which was smaller than that (1.10 ± 0.73 μm) of GF (Table 4.2). The pore size distributions of the filters are shown in Fig. 4.6, demonstrating that the maximum and minimum pore sizes of PVA /GF ENMs were smaller than GF. The filter depths of PVA/GF ENMs and GF were 296.3 ± 3.2 and 250.0 ± 5.0 μm, respectively. The pure water flux of PVA/GF ENMS was 294.0 L/m^2/min at 0.6 bar, which was 5.8 times smaller than that (1701.3 L/m^2/min) of GF. In the case of BTEAC-PVA/GF ENMs, the filter depth and mean pore size were 299.6 ± 1.8 and 0.94 ± 0.56 μm, respectively. The pure water flux of BTEAC-PVA/GF ENMs was 448.0 L/m^2/min at 0.6 bar, which was 1.7 times larger than that of PVA/GF ENMS. This result could be attributed to the fact that the incorporation of BTEAC into PVA ENMs increases the mean pore size and improves the hydrophilicity of the ENMs, resulting in an enhancement of the pure water flux. The commercial membrane flux for microfiltration is over 500 L/m2/hr/atm that is much lower than the flux of BTEAC-PVA/GF ENMs (48,161 L/m2/hr/atm). For microfiltration, the pore size of the filter varies from 0.05 to10 μm, and the trans-membrane pressure ranges from 0.1 to 1.0 bar (Mulder et al., 1996). From destructive test, BTEAC-PVA/GF ENMs could filter water up to 6.45 L without damaging of ENMs. Considering the pore size, porosity, and pure water flux, BTEAC-PVA ENMs are good candidates for microfiltration.

The antibacterial water filtration test results for river water are presented in Table 4.3 as a function of the filtrate water volume. In the case of total coliforms, 67 CFU/mL in river water was removed all by BTEAC-PVA/GF ENMs during the filtration test. HPC was initially present at 9500 CFU/mL in the river water and decreased to 645 CFU/mL after 50 mL of water filtration. As the water filtrate volume increased from 100 to 500 mL, HPC increased from 832 to 1436 CFU/mL. The LRV for HPC changed from 1.12 to 0.82 with an increase in the water filtrate volume from 50 to 500 mL. For turbidity, the initial 4.53 NTU decreased to 0.78 NTU after 50 mL of water filtration. As the water filtrate volume increased to 500 mL, the turbidity decreased to 0.23 NTU. Simply, ENMs (0.0011 m^2) can treat 500 ml of water that over 22.7 – 40.9 tons of water can be treated considering area of membranes module is around 50 -90 m^2 in water treatment plant.

Limited studies have been performed for antibacterial water filtration by QAC-functionalized ENMs. Daels et al. (2011) synthesized polyamide ENMs that were functionalized with poly[(dimethylimino)(2-hydroxy-1,3-propanedily)chloride] for water disinfection. These authors demonstrated that bacteria could be removed effectively from water that was inoculated with *S. aureus* and *E. coli*. QACs can effectively kill both Gram-positive and Gram-negative bacteria (Li et al., 2006). As membrane-active agents, QACs can adsorb onto the bacterial cell surface and disrupt the cytoplasmic membrane of

bacteria, leading to the release of K^+ ions and other cytoplasmic constituents (Kawabata & Nishiguchi. 1988).

Table 4.2 Filter characteristics of the BTEAC-PVA/GF ENMs, PVA/GF ENMs, GF, and PC used in the antimicrobial filtration tests

Type of filter	Filter thickness (μm)	Mean pore size (μm)	Maximum pore size (μm)	Minimum pore size (μm)	Pure water flux ($L/m^2/min$)
BTEAC-PVA/GF ENMs	299.6 ± 1.8	0.94 ± 0.56	2.16	0.38	488.0
PVA ENMs/GF ENMs	296.3 ± 3.2	0.78 ± 0.47	1.80	0.28	294.0
GF	250.0 ± 5.0	1.10 ± 0.73	3.52	0.95	1701.3
PC	8.9 ± 0.5	0.14 ± 0.02	0.18	0.11	45.3

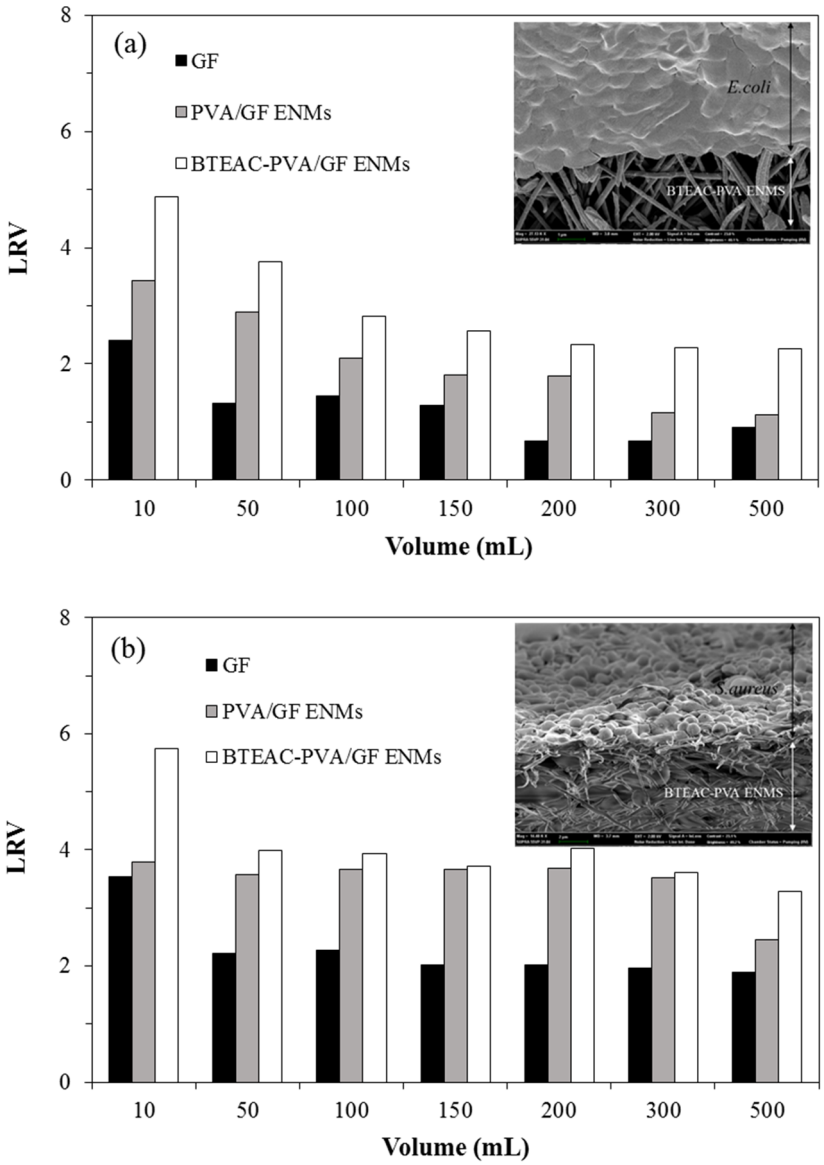

Figure 4.5 Bacteria log removal (LRV) by BTEAC-PVA/GF ENMs, PVA/GF ENMs, and GF: (a) *E. coli*; (b) *S. aureus*. Inset = FESEM image of bacteria-deposited BTEAC-PVA ENMs (cross-sectional view).

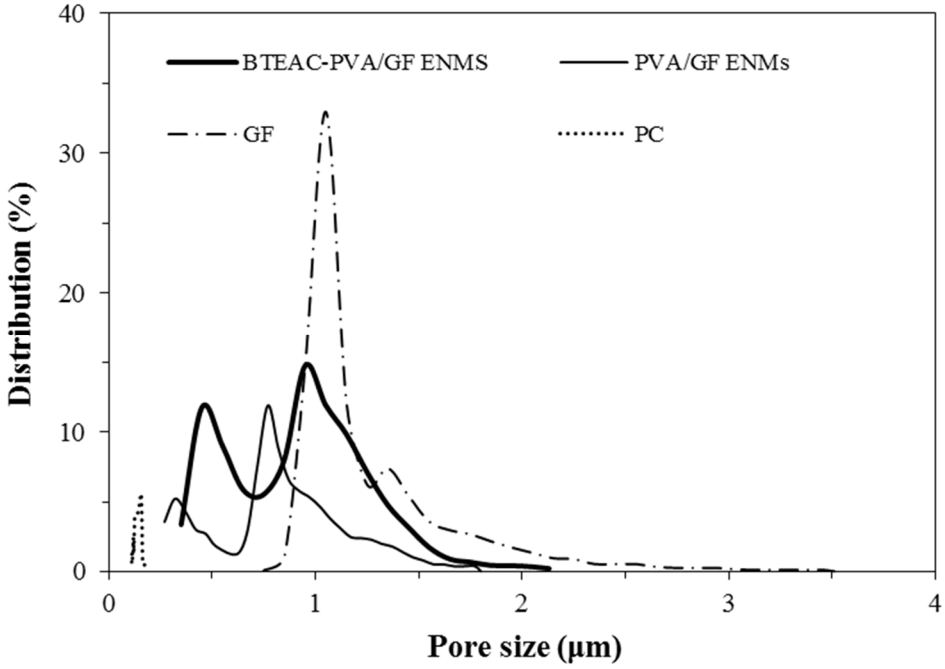

Figure 4.6 Pore size distribution of the BTEAC-PVA/GF ENMs, PVA/GF ENMs, GF, and PC used in the antimicrobial filtration tests.

Table 4.3 Antibacterial water filtration test results for river water collected from the Han River, Seoul, Korea

Bacteria	River water	Filtrate water (mL)					
		50	100	200	300	400	500
Total coliforms (CFU/100mL)	67	0	0	0	0	0	0
HPC (CFU/mL)	9500	645 (1.12)	832 (1.06)	1178 (0.91)	1381 (0.84)	1380 (0.84)	1436 (0.82)
Turbidity (NTU)	4.53	0.78	0.37	0.24	0.25	0.27	0.23

4.2.4 Antiviral water filtration tests

The virus log removals (LRV) obtained from the antiviral water filtration tests are presented in Fig. 4.7 as a function of the filtrate water volume. In addition to BTEAC-PVA/GF ENMs, PVA/GF ENMs, GF, and PC was used in the antiviral tests because the mean pore size of PC was smaller than that of GF, which was used for the antibacterial tests. Note that the filter depth and mean pore size of PC were 8.9 ± 0.5 and 0.14 ± 0.02 μm, respectively. In addition, the pure water flux of PC was 45.3 L/m^2/min at 0.6 bar (Table 4.2). In MS2, the LRV values of BTEAC-PVA/GF ENMs changed from 0.06 to 0.12 at water filtrate volumes of 10–300 mL, whereas the LRV values of PVA/GF ENMs changed from 0.03 to 0.1 in the same range. Meanwhile, the LRV values of PC and GF were below 0.03 and 0.02, respectively. For PhiX174, LRV values of BTEAC-PVA/GF ENMs changed from 0.23 to 0.32, whereas LRV values of PVA/GF ENMs changed from 0.19 to 0.24. In addition, the LRV values of PC were less than 0.16.

Our results indicate that BTEAC-PVA/GF ENMs were more effective in the removal of bacteriophage than PVA/GF ENMs and PC. This result could be attributed to the inactivation of MS2 and PhiX174 by BTEAC. MS2 and PhiX174 are unenveloped viruses; MS2 is composed of single-stranded RNA that is encapsulated within a capsid (protein coat), whereas Phix174 is

comprised of single-stranded DNA that is encapsulated within a capsid (Madigan et al., 2009). The inactivation mechanisms of the unenveloped virus by QACs are not clear but are presumably related to the denaturation of the capsid (Hegstad et al., 2010). For the enveloped virus, which has a lipid layer around the nucleocapsid (nucleic acid + capsid), the inactivation mechanism is the release of the nucleocapsid due to the disruption of the viral envelope by QACs (Tsao et al., 1989). Limited studies have been conducted for antiviral water filtration by QAC-functionalized ENMs. Dobrowsky et al. (2015) synthesized antimicrobial SMI-Q10 nanofibers containing QACs to test virus removal from river water and harvested rainwater using dead-end filtration. These authors reported that the SMI-Q10 nanofiber membrane could not remove adenovirus present in water samples.

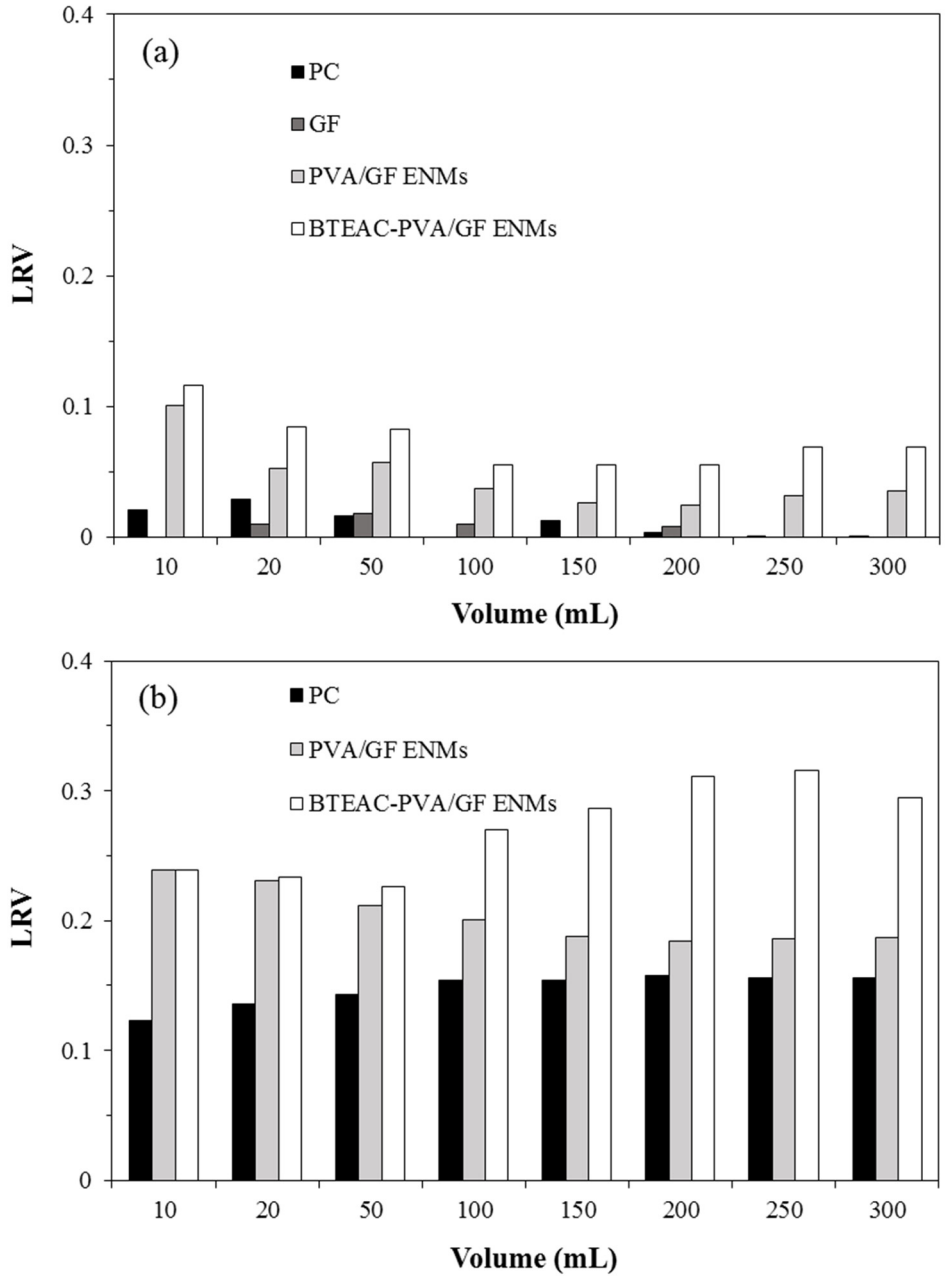

Figure 4.7 Bacteriophage log removal (LRV) by BTEAC-PVA/GF ENMs, PVA/GF ENMs, PC, and GF: (a) MS2; (b) PhiX174.

Chapter 5

Anti-biofouling Activity of Poly(vinyl alcohol) Electrospun Nanofibrous Membranes with Benzyl Triethylammonium Chloride

5.1 Materials and methods

5.1.1 Electrospun BTEAC-PVA ENMs

Poly (vinyl alcohol) (PVA) (Mw 85,000 - 124,000, 99 % hydrolyzed), and Benzyltriethylammonium chloride (BTEAC, $C_6H_5CH_2N(Cl)(C_2H_5)_3$) were purchased from Sigma Aldrich. PVA solution (8 wt%) was prepared by dissolving PVA powder in distilled water at 80 ℃, incubating for, 16 h, and cooling at room temperature. To determine the antimicrobial property, 2.6% BTEAC was added to the PVA solution (8 wt%). The electrospinning system was carried out using NanoNC (ESP200/ESP100, Korea). The as-prepared polymer solution was placed in a 25 mL syringe with a 0.51 mm ID (inner diameter) metal needle, and the needle was connected to a high voltage power supply at the positive terminal. The PVA or BTEAC-PVA electrospun nanofibers were collected on a commercial PC membrane (0.22 μm, Whatman) on a rotating cylinder (Dia: 9 cm, speed: 1000 rpm) at the negative terminal. The applied voltage was 15 kV, the flow rate of spinning solution was 1 ml/h, and the tip-to-distance (TCD) was fixed at 15 cm. All of the experiments were performed at room temperature. PVA/PC or BTEAC-PVA/PC ENMs were heated at 150 ℃ for 20 min and then methanol treated for crosslinking.

5.1.2 Characterization of BTEAC-PVA ENMs

The morphology and average diameter of BTEAC-PVA ENMs were determined by field emission scanning electron microscopy (FESEM) (Supra 55VP, Carl Zeiss, Germany) in our previous Chapter 4. The thickness of BTEAC-PVA ENMs was measured by a cross section view through SEM images.

For the water content and BTEAC remaining tests, 0.01 g of PVA and BTEAC-PVA ENMs was immersed 10 ml of distilled water at room temperature for 4, 24, and 48 h. Then these nanofibers were blotted dry with tissue paper to determine the water content. The difference in mass between nanofibers was calculated and viewed under the SEM to observe the morphology. The water content (W) was calculated as follows (1):

$$W\ (\%) = \left(\left(m_{wet} - m_{dry}\right) \times 100\right) m_{dry} \quad (1)$$

where, m_{wet} and m_{dry} are the masses of the immersed and dried nanofibers, respectively. In addition, the concentration of BTEAC in the water was monitored for 48 h by UV-Vis spectrophotometry (Helios, Thermo Scientific, Waltham, MA, USA) at a wavelength of 208 nm.

A capillary flow porometer (CFP-1500AE, PMI, USA) was used to determine the maximum pore size and mean pore size of the PC membrane,

PVA/PC ENMs and BTEAC-PVA/PC ENMs. The permeation flux of PC membrane, PVA/PC ENMs and BTEAC-PVA/PC ENMs was determined by pure water at room temperature with dead-end filtration. In addition, bacterial (*K. pneumonia,* ATCC 4352) solutions as biofoulants were used to estimate the flux. The pressure across the nanofibers was 0.7 bar. The permeation flux (J) was calculated by (2):

$$J = V/(S \times t) \quad (2)$$

where, V is the total permeation volume (L), S is the total permeation area (m^2), and t is the total permeation time (h).

5.1.3 Anti-biofouling activity of BTEAC-PVA ENMs

The anti-fouling activity was evaluated using two strategies: contact killing through filtration and preventing biofilm formation through incubation.

5.1.3.1 Anti-fouling activity by contact killing

Autoclaved distilled water contained with *S. aureus* (ATCC 10537)*, E. coli* (ATCC 11105)*,* and *K. pneumonia* (~10^5 cfu/ml) was used for contact killing test. These tests were performed using a dead-end-filtration system (0.7 bar) in which 100 ml of water spiked with each bacterium was filtered through PVA/PC, and BTEAC-PVA/PC ENMs (11.34 cm^2), allowing us to evaluate the

effect of killing bacteria with contact on surfaces of PVA, and BTEAC-PVA ENMs. In addition, the PC membrane was used as a control test. After the desired contact time (0 - 60 min), BTEAC-PVA/PC ENMs, PVA/PC ENMs and PC membrane were vigorously rinsed with sterile PBS. The viability of the cells remaining on the ENMs and PC membrane was determined by counting the number of cells that were recovered from each membrane. To study the effect of the number of bacteria, 200 and, 500 ml of bacteria solution was filtered, and allowed 30 min of contact time. The bacterial reduction was estimated by the spread plate procedure. Serial dilutions were conducted, plated onto selective agar plates, and then incubated for 18h at 37℃. The log reduction was calculated by the following equation:

$$\log reduction = -\log_{10}(\frac{C_f}{C_0}) \quad (3)$$

where, C_f is the concentration of recovered bacteria after the filtration test, and C_0 is the initial concentration of bacteria. In addition, the cell viability after contact with BTEAC-PVA/PC ENMs and PVA/PC ENMs was investigated by fluorescence staining using the Live/Dead BacLight™ Bacterial Viability Kit (L13152, Invitrogen Inc., Eugene, USA), and then observed under a Super-resolution Confocal Microscope (SP8 X STED, Leica, German). The surface analysis of PVA and BTEAC-PVA ENMs after filtration was carried out using FESEM.

Reusability is an important factor in water filtration systems in terms of maintaining antifouling efficiency. A total of 100 ml of water with each bacterium (*S. aureus*, *E. coli*, *K. pneumonia*) was filtered through BTEAC-PVA/PC ENMs for each cycle. In addition, Han River water from South Korea (BOD=0.2 mg/L, DO= 8.3 mg/L, Turbidity=1.03 NTU, pH=7.03, EC=303 μs/cm, initial bacteria conc. =8.35×10^3 CFU/ml) was used to evaluate the antimicrobial efficiency with mixed bacteria species. Culturable bacteria were enumerated using R2A (Difco, USA) at 20℃ for 7 days. The used BTEAC-PVA/PC ENMs were washed after filtration testing more than 3 times in sterile distilled water and then irradiated with ultra violet light. These reused ENMs were filtered through spiked water or river water as prepared, and the antibacterial efficiency was measured over 6 cycles.

5.1.3.2 Anti-fouling activity by preventing biofilm formation

Single-species biofilms of *S. aureus* and *P. aeruginosa* (ATCC 15442) were used in biofilm-forming bacteria (Pitt et al., 2003; Mei et al., 2014). The method of biofilm formation on the membrane surface is described by Prijck et al. (2007), and Zodrow et al. (2009). Simply, stationary-phase cultures of bacteria were diluted to 10^5 cell/ml in 5 mL media, and then incubated at 37℃ with 0.01 g of sterile BTEAC-PVA ENMs, and PVA ENMs for 24, 48, and 72 h. Both the planktonic cells in the supernatant and the sessile cells in the biofilm were

counted by the spread plate procedure. To enumerate the sessile cells, the ENMs were removed from the medium and rinsed gently in sterile DI water. Then, the ENMs were soaked in 1 ml of NaCl (0.85 %) solution, vortexed (Vortex Genie 2, VWR Scientific, USA) on the highest setting for 30 s, and sonicated for 30 s. This procedure was performed twice to disrupt the biofilm (sessile cells) on the ENMs surface.

5.2 Results and discussion

5.2.1 Characteristics of BTEAC-PVA/PC ENMs

5.2.1.1 Morphology

The average diameter of BTEAC-PVA nanofibers was 216.58 ± 50.88 nm, and PVA ENMs had a diameter of 154.59 ± 27.66 nm after crosslinking treatment (Chapter 4). The depth of the BTEAC-PVA/PC ENMs was composed of 34.88 ± 1.95 μm of BTEAC-PVA nanofibers and PC membrane (8.94 ± 0.51 μm) (Fig. 5.1). Both PVA ENMs (54.1 °) and BTEAC-PVA ENMs (29.0 °) had a lower water contact angle than did the PC membrane (60.0 °), indicating that PVA or BTEAC-PVA deposition on the PC membrane improved the hydrophilic property of the surface (Schöller et al., 2014). Having more hydrophilic surfaces increases the flux and reduces fouling, by reducing hydrophobic interactions (Nasreen et al., 2014; Ma et al., 2011).

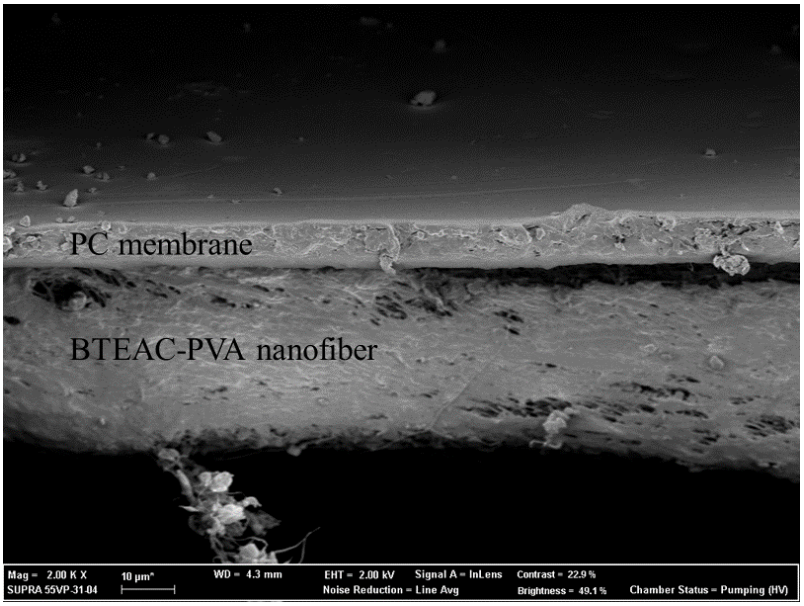

Figure 5.1 SEM image of BTEAC-PVA/PC ENMs.

5.2.1.2 Swelling property of BTEAC-PVA nanofibers

The swelling of BTEAC-PVA nanofibers was investigated by the water content. Both BTEAC-PVA and PVA nanofibers absorbed more water with increasing immersion time from 0 to 48 h (Table 5.1). The water contents of BTEAC-PVA nanofibers increased from 33.33% to 61.54% by increasing immersion the time from 4 to 48 h. On the other hand, the water contents of PVA nanofibers (85.71 - 100%) were much higher than those of BTEAC-PVA nanofibers. The BTEAC-PVA nanofibers slightly swelled after exposure in water, however, the morphology was retained well even after 48 h of immersion (Fig. 5.2). However, some of the PVA nanofibers were disintegrated, became gelatinous and rolled up after 48 h of immersion, indicating that PVA nanofibers itself were not sufficient for water filter media. In contrast, BTEAC-PVA nanofibers have a higher water stability than PVA nanofibers by adding BTEAC.

Table 5.1 Properties of PVA and BTEAC-PVA nanofibers after water immersion

ENMs	Immersion time	Dry mass (g)	Wet mass (g)	Water content (%)
PVA	4	0.014	0.026	85.71
	24	0.011	0.021	90.91
	48	0.013	0.026	100
BTEAC-PVA	4	0.012	0.016	33.33
	24	0.013	0.020	53.85
	48	0.013	0.021	61.54

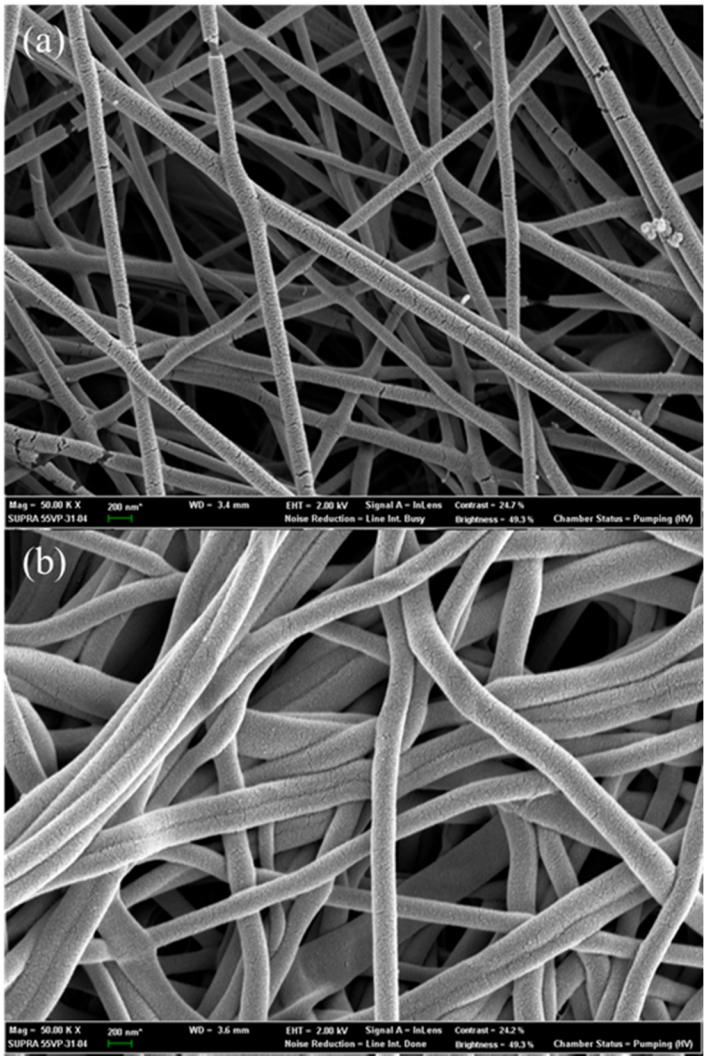

Figure 5.2 SEM images of BTEAC-PVA nanofibers: (a) no water immersion; (b) after water immersion for 48 h.

5.2.1.3 Water permeability evaluation

The maximum pore size of BTEAC-PVA/PC ENMs was 0.80 ± 0.11 μm, and the mean flow pore diameter was 0.30 ± 0.17 μm. PVA/PC ENMs had a smaller maximum pore size (0.17 μm) and mean flow pore diameter (0.16 ± 0.04 μm) than did BTEAC-PVA/PC ENMs due to thinner diameters of nanofibers. The PC membrane has a maximum pore size of 0.18 μm, and a mean flow pore diameter of 0.14 ± 0.02 μm.

The average permeation flux after filtration with 500 ml of pure water was 2815.32 $L/m^2/h$ with BTEAC-PVA/PC ENMs, similar to the flux of the PC membrane (2866.97 $L/m^2/h$) (Table 5.2). The flux of both PVA/PC (2220.25 $L/m^2/h$) and BTEAC-PVA/PC ENMs with pure water was slightly lower than that of the PC membrane due to the depth of nanofibers. The depth of the nanofiber itself was approximately 3.7 times thicker than that of the PC membrane. The permeation flux decreased when the filtration solutions included the bacterium *K. pneumonia* (Fig. 5.3). The normalized flux of the PC membrane decreased to 0.5 with *K. pneumonia*. The normalized flux of PVA/PC ENMs was estimated to be higher than that of the PC membrane, while, it was decreased by *K. pneumonia* (Normalized flux = 0.84) presence. On the other hand, the permeation flux of BTEAC-PVA/PC ENMs was retained even when filtering the *K. pneumonia* solution. Generally, compared to conventional

polymers and ceramic membranes, ENMs possess higher porosity, a large surface area, and interconnected pore structures that enhance the flux performance (Wang et al., 2012). Furthermore, embedded antimicrobial agents improved the flux performance with bacteria containing water. Thus, loaded BTEAC-PVA ENMs on the PC membrane enhance the flux due to protection from biofouling of the PC membrane with bacterial solutions, indicating that BTEAC-PVA/PC ENMs are good materials for anti-biofouling.

Table 5.2 Average water flux after filtration testing (500 ml)

	Distilled water ($L/m^2/h$)	MS2 solution ($L/m^2/h$)	*K. pneumonia* solution ($L/m^2/h$)
BTEAC-PVA/PC ENMs	2815.32	2783.47	2669.37
PVA/PC ENMs	2220.25	1602.98	1393.55
PC membrane	2866.97	1700.24	1497.20

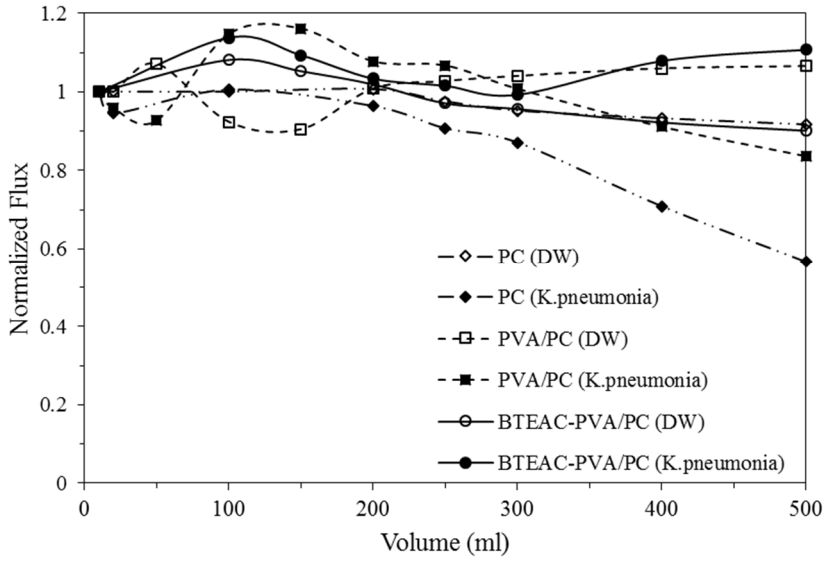

Figure 5.3 The normalized flux of BTEAC-PVA/PC ENMs, PVA/PC ENMs, and PC membrane with distilled water (DW), and DW with K. pneumonia.

5.2.1.4 Retaining BTEAC from BTEAC-PVA nanofibers

The content of BTEAC slightly decreased when BTEAC-PVA nanofibers were immersed in water for 48 h (Fig. 5.4). The initial content of BTEAC is 20.85 mg per gram of BTEAC-PVA nanofibers after the heat and methanol treatments. A total of 20.62 mg/g of BTEAC remained within 1 h, and slightly decreased over time. Finally, 20.54 mg/g of BTEAC was maintained after immersion for 48 h, which is less than 1.27% of the initial content. Therefore, PVA is a good polymer for immobilizing the BTEAC.

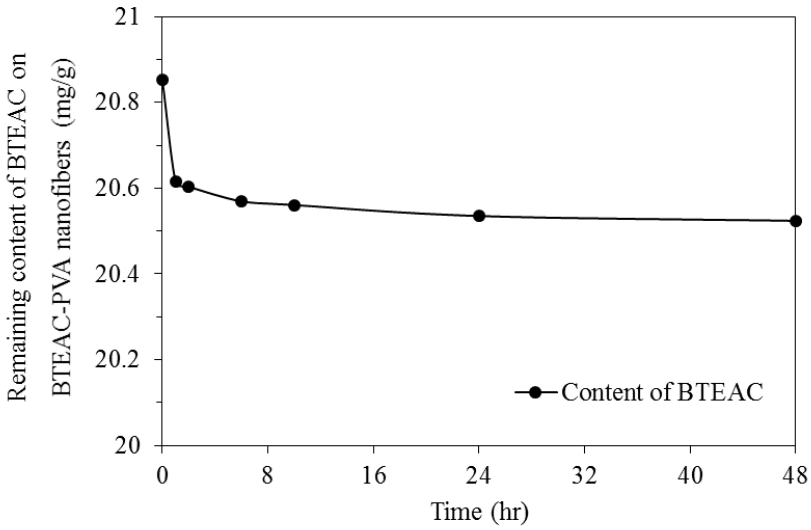

Figure 5.4 The remaining content of BTEAC on BTEAC-PVA nanofibers after immersion testing.

5.2.2 Evaluation of BTEAC-PVA ENMs anti-biofouling

5.2.2.1 The effect of contact time for contact killing

The total log removal of *S. aureus, E. coli,* and *K. pneumoniae* was observed with various contact periods from 5-60 min (Fig. 5.5). The LRV of all bacteria by BTEAC-PVA/PC ENMs increased with increasing contact time. The LRV of *S. aureus* was 0.56-0.79 (BTEAC-PVA/PC ENMs), and 0.48-0.77 (PVA/PC ENMs) had similar trend until 30 min, while the LRV of *S. aureus* increased up to 3.05 ± 0.00 after 60 min of contact. *S. aureus* was inactivated on the control PC membrane as 0.42 ± 0.01, and PVA/PC ENMs as 0.78 ± 0.01 within 60 min. The removal of Gram negative bacteria (*E. coli, K. pneumoniae)* was more distinguished BTEAC-PVA/PC ENMs from PVA/PC ENMs. In the case of *K.pneumoniae,* the LRV with BTEAC-PVA/PC ENMs was 0.71 ± 0.00 within 5 min, 1.22 ± 0.00 within 30 min, and 1.23 ± 0.01 within 60 min. The LRV of *K.pneumoniae* with PVA/PC nanofibers was 0.71 ± 0.02, and that of the PC membrane was 0.58 ± 0.00 within 60 min. Likewise, the LRV of *E. coli* was 0.83 ± 0.01 within 5 min and 1.04 ± 0.00 within 30 min. For 60 min, the LRV was 1.11 ± 0.01 with BTEAC-PVA/PC ENMs, which was higher than that with PVA/PC ENMs (0.74 ± 0.01), and PC (0.63 ± 0.02). In summary, BTEAC-PVA/PC ENMs could remove greater amounts of all three of the bacteria (*S. aureus, E. coli,* and *K.pneumoniae*) than could PVA/PC ENMs and the PC membrane due to the presence of BTEAC. Gule et al. (2013) produced

furanone-containing poly (vinyl alcohol) (PVA/DMHF) nanofibers that were supported on a 0.22 μm filter; the antimicrobial activity was determined using a dead-end filtration system with the desired contact time. PVA/DMHF nanofibers decreased 3.5 log in a population of *P. aeruginosa* Xen 5, and *E. coli* Xen 14, and approximately 2.2 log in a population of *S. aureus* Xen 36, *S. typhimurium* Xen 26, and *K. pneumonia* Xen 39 after 30 min of contact followed by filtration. Du Plessis (2011) fabricated PVA nanofibers containing silver nanoparticles onto a 0.22 μm filter to determine the antimicrobial activity. After filtering 250 ml (10^6 cells/ml) filtering, the reduction of all three bacteria (*P. aeruginosa, E. coli,* and *K. pneumonia*) was 1.08-2.37.

The Gram-negative bacteria *E. coli,* and *K.pneumoniae* had a higher log removal value with short time (5~30 min) than did Gram-positive bacteria (*S. aureus),* whereas *S. aureus* had the highest log removal value after 60 min. *S. aureus* has a thicker peptidoglycan layer (15 – 80 nm) than that of *E. coli,* and *K.pneumoniae* (2 nm) (Lienkamp et al., 2008), which needed more time to inactivate with BTEAC because of its relatively short alkyl chains in the damaged cell. The antibacterial mechanism is mainly an electrostatic interaction between the positively charged ammonium ion in BTEAC and negatively charged bacteria on the cell membrane, causing damage and cell death. Endo et al. (1987) reported similar results in that polystyrene fibers were covalently bonded by tertiary amine (TAF), showing higher antimicrobial

activity to Gram-negative microorganisms (*E. coli, P. aeruginosa, K. pneumonia, S. typhimurium,* and *S. marcescens*) than to Gram-positive microorganisms (*S. aureus* and*, S. faecalis*) when shaken for 1 h. The arm of the tertiary amine was less than 0.1 nm, which is too short to enter the bacterial cell wall but, instead, could affect the cell membrane, specifically in Gram-negative bacteria. The outer membrane function and structure were damaged, causing bacterial cell death. In addition, the electrostatic interaction between TAF and bacteria surface is related to the antibacterial activity.

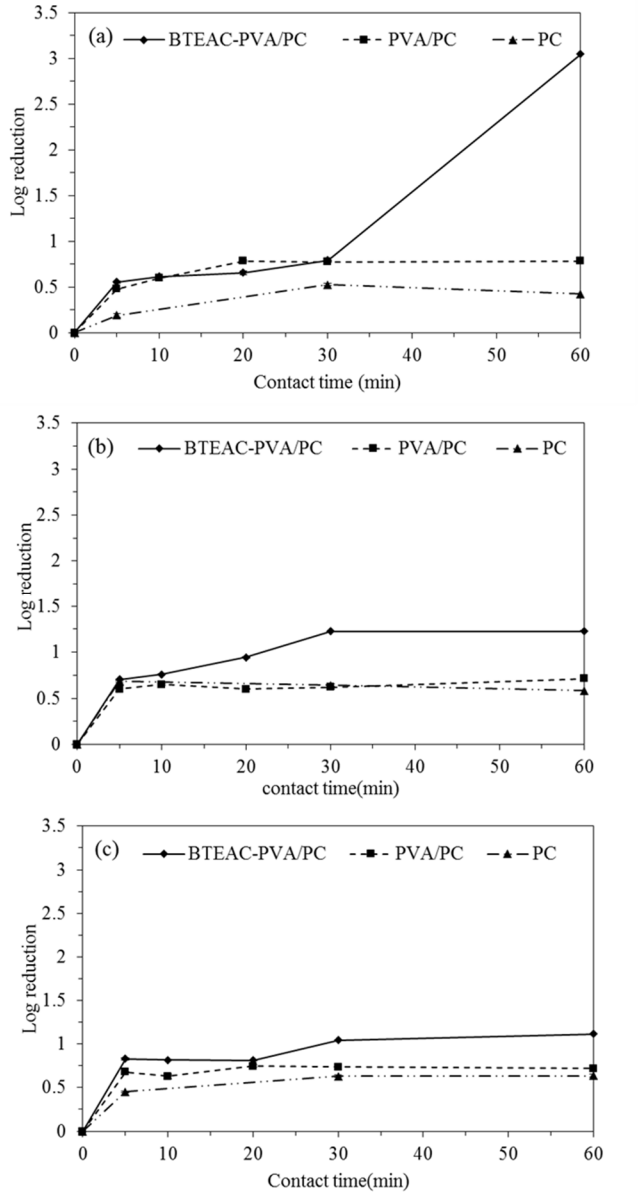

Figure 5.5 Log reduction of bacteria with BTEAC-PVA/PC ENMs, PVA/PC ENMs, and the PC membrane according to various contact times (0-60 min): (a) *S. aureus*; (b) *K. pneumonia*; (c) *E. coli*.

5.2.2.2 The effect of the number of bacteria for contact killing

Despite the increasing number of bacteria, BTEAC-PVA/PC ENMs decreased the bacterial population more than PVA/PC ENMs and the PC membrane (Table 5.3). The log reduction of *S. aureus* was slightly greater than that of PVA/PC ENMs and the PC membrane because of the short contact time (30 min) under all of the conditions (initial concentration = 7.13 - 7.83). For *K.pneumoniae*, the log reduction increased to 1.32 ± 0.00 with an initial log number of bacteria of 8.28 ± 0.03 (200 ml), and decreased to 0.81 ± 0.03 with an initial log number of bacteria of 8.68 ± 0.12 (500 ml). The reduction of *E. coli* steadily decreased with an increasing number of bacteria (100-500 ml), with log reductions of 1.05 ± 0.00, 1.01 ± 0.01, and 0.70 ± 0.00 at initial concentrations of 7.88 ± 0.08, 8.18 ± 0.08, and 8.57 ± 0.08, respectively.

As shown in Figure 5.6, the bacteria contact on BTEAC-PVA ENMs and PVA ENMs for 30 min was scanned to detect the green emission of live cells, and the red emission of damaged cells. Fluorescence microscopy images of all bacteria indicate that the population of red cells increased on BTEAC-PVA ENMs compared to that on PVA ENMs. Furthermore, *E. coli,* and *K.pneumoniae* lost their rod-shape structure because of membrane damage (Fig 5.6(d), 5.6(f)). Theoretically, Live/Dead BacLight staining divided live and damaged cells with cytoplasmic membrane permeability. Figure 5.6 confirmed

that BTEAC-PVA ENMs damaged membrane of *S. aureus, E. coli,* and *K.pnuemoniae*.

In addition, the outer membrane of bacteria would be damaged as observed by SEM images (Fig. 5.7). *S. aureus* cells appeared to be spherical and intact on PVA nanofibers, whereas these cells became pitted when in contact with BTEAC-PVA nanofibers. This damage of the outer membrane causes bacterial death. On the other hand, biofilm could be seen on PVA nanofibers with SEM images (Fig. 5.7), while some of the bacteria were entrapped between BTEAC-PVA nanofibers. Similarly, Gule et al. (2012b) showed in SEM images that *S. aureus* cells were damaged by PVA/AquaQure nanofibers, whereas these cells were intact on PVA nanofibers.

Table 5.3 The results of tests of various numbers of bacteria (contact time = 30 min)

	Concentration	BTEAC-PVA/PC			PVA/PC			PC		
	(Log CFU)	100 mL	200 mL	500 mL	100 mL	200 mL	500 mL	100 mL	200 mL	500 mL
S. aureus	Initial	7.13 ± 0.12	7.43 ± 0.12	7.83 ± 0.12	7.13 ± 0.12	7.43 ± 0.12	7.83 ± 0.12	7.13 ± 0.12	7.43 ± 0.12	7.83 ± 0.12
	Final	6.33 ± 0.03	6.68 ± 0.01	6.86 ± 0.04	6.36 ± 0.04	6.79 ± 0.03	6.94 ± 0.01	6.60 ± 0.05	6.96 ± 0.01	7.22 ± 0.00
	Reduction	0.79 ± 0.01	0.70 ± 0.00	0.97 ± 0.00	0.77 ± 0.01	0.64 ± 0.01	0.89 ± 0.00	0.53 ± 0.01	0.46 ± 0.00	0.61 ± 0.00
K. pneumoniae	Initial	7.98 ± 0.03	8.28 ± 0.03	8.68 ± 0.03	7.98 ± 0.03	8.28 ± 0.03	8.68 ± 0.03	7.98 ± 0.03	8.28 ± 0.03	8.68 ± 0.03
	Final	6.75 ± 0.02	6.96 ± 0.01	7.87 ± 0.01	7.36 ± 0.00	7.68 ± 0.02	8.07 ± 0.04	7.34 ± 0.03	7.75 ± 0.00	8.09 ± 0.02
	Reduction	1.22 ± 0.00	1.32 ± 0.00	0.81 ± 0.03	0.62 ± 0.00	0.60 ± 0.01	0.61 ± 0.02	0.64 ± 0.01	0.53 ± 0.00	0.59 ± 0.01
E. coli	Initial	7.88 ± 0.08	8.18 ± 0.08	8.57 ± 0.08	7.88 ± 0.08	8.18 ± 0.08	8.57 ± 0.08	7.88 ± 0.08	8.18 ± 0.08	8.57 ± 0.08
	Final	6.83 ± 0.01	7.17 ± 0.12	7.87 ± 0.01	7.14 ± 0.01	7.75 ± 0.04	8.07 ± 0.03	7.24 ± 0.04	8.02 ± 0.01	8.28 ± 0.03
	Reduction	1.05 ± 0.00	1.01 ± 0.01	0.71 ± 0.00	0.74 ± 0.00	0.42 ± 0.02	0.50 ± 0.01	0.63 ± 0.01	0.15 ± 0.01	0.30 ± 0.02

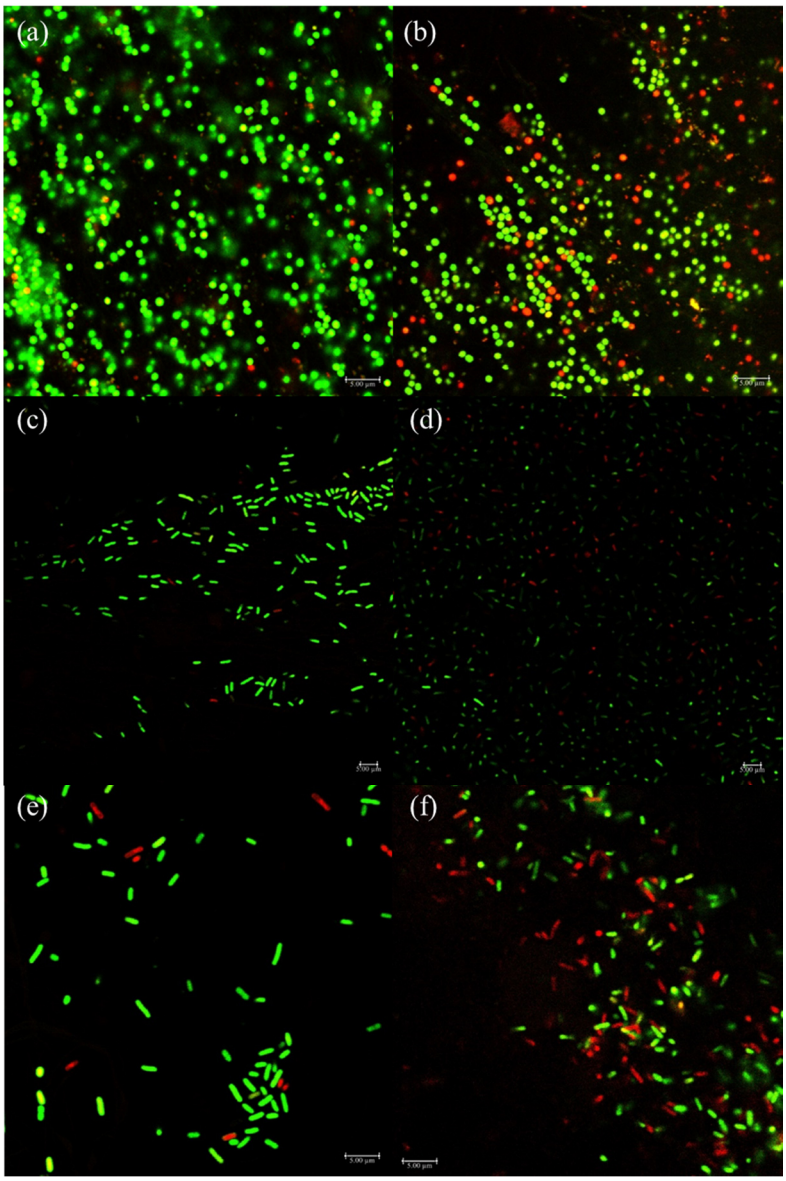

Figure 5.6 Fluorescent microscopy images showing the antibacterial activity of BTEAC-PVA ENMs and PVA ENMs with contact: (a) *S. aureus* – PVA ENMs; (b) *S. aureus* – BTEAC-PVA ENMs; (c) *K. pneumonia* – PVA ENMs; (d) *K. pneumonia* – BTEAC-PVA ENMs; (e) *E. coli* – PVA ENMs; (f) *E. coli* – BTEAC-PVA ENMs.

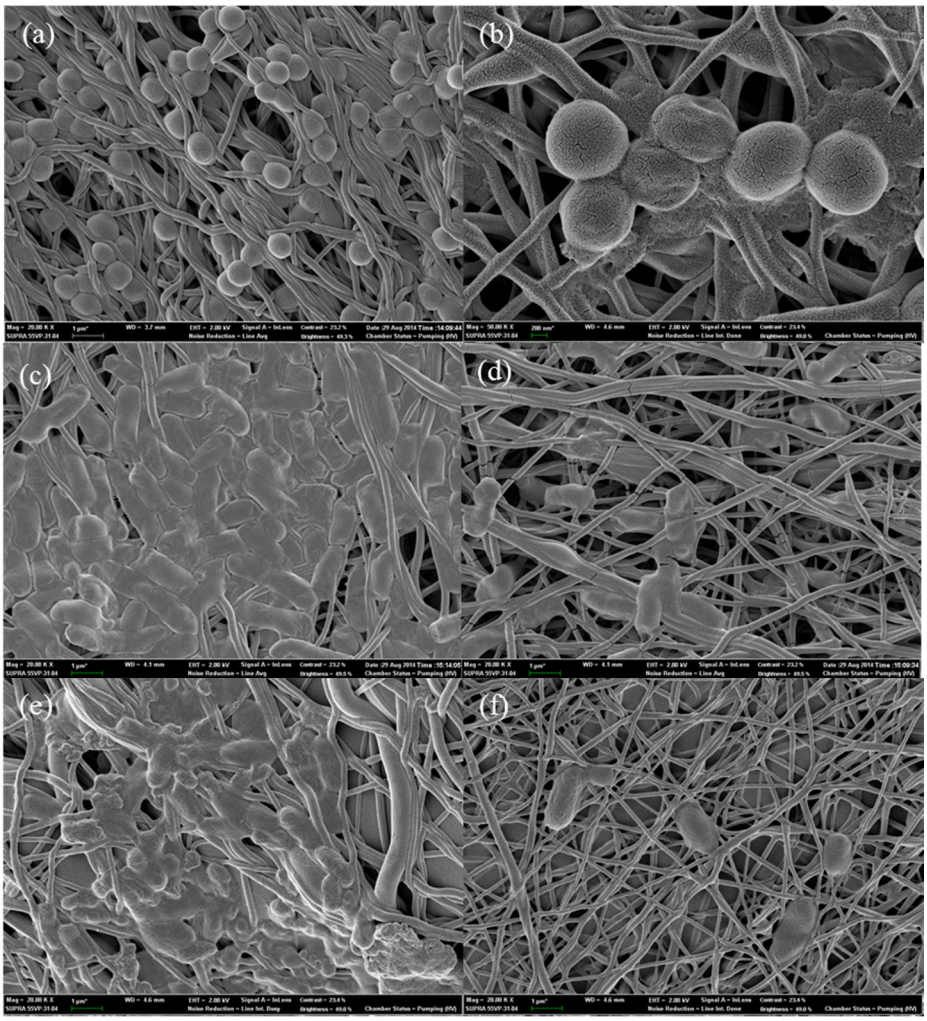

Figure 5.7 SEM images of bacterial contact on PVA and BTEAC-PVA ENMs (a) *S. aureus* – PVA ENMs; (b) *S. aureus*–BTEAC-PVA ENMs; (c) *K. pneumonia*– PVA ENMs; (d) *K. pneumonia*– BTEAC-PVA ENMs; (e) *E. coli*– PVA ENMs; (f) *E. coli* – BTEAC-PVA ENMs.

5.2.2.3 Regeneration studies for contact killing

BTEAC-PVA/PC ENMs generally showed retention of antimicrobial activity over 6 cycles (Fig. 5.8). The log reduction was not very different comparing cycles. BTEAC-PVA/PC ENMs had 1.43 ± 0.01 LRV of *K.pneumoniae*, 1.30 ± 0.00 LRV of *E. coli*, and 0.74 ± 0.08 LRV of *S. aureus* in the first cycle. The LRV of bacteria was estimated at 1.26 ± 0.05 (*K.pneumoniae*), 1.28 ± 0.12 (*E. coli*), and 0.63 ± 0.02 (*S. aureus*) in the last 6 cycles, respectively. Similarly, the LRV of mixed strains was 1.30 ± 0.05 at 1 cycle and was consistently greater than 1.30 over 6 cycles. These results indicate that BTEAC-PVA/PC ENMs showed antimicrobial activity not only with each strain but also with the mixed bacteria strains. Gule et al. (2013) conducted a regeneration test of PVA/DMHF nanofibers that steadily lost their antibacterial activity through 6 cycles from 2.8 to 1.5 LRV with a mixed strain culture. These results demonstrate that BTEAC-PVA/PC ENMs can be used several times to reduce bacteria without losing antimicrobial activity through surface contact. The leaching test also agreed well with these results. Moreover, BTEAC-PVA/PC ENMs were not integrated after 6 cycles. Therefore, BTEAC-PVA/PC ENMs maintain antimicrobial activity without disintegrating or leaching.

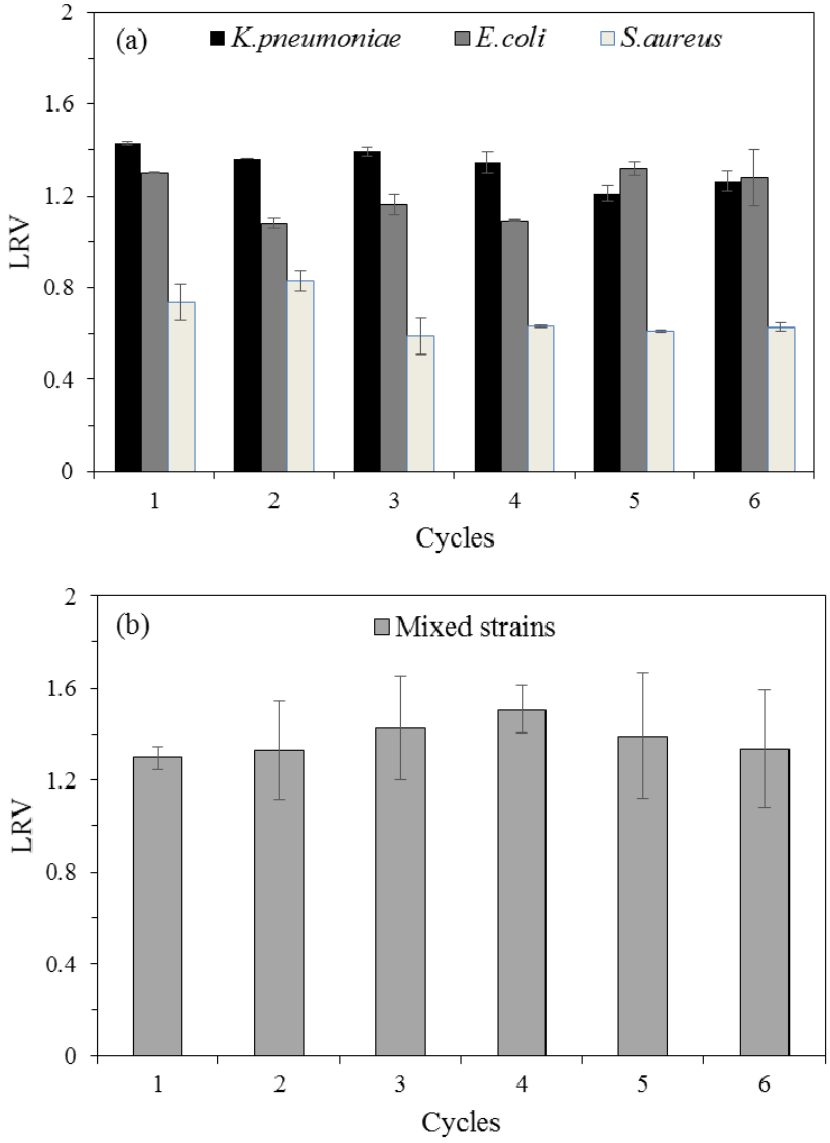

Figure 5.8 The results of regeneration testing over 6 cycles: (a) Bacteria (*S. aureus*, *K. pneumonia, E. coli)*; (b) Mixed bacteria species

5.2.2.4 Preventing biofilm formation

Sessile cells were reduced 1.78 log (*P. aeruginosa*) and 1.43 log (*S. aureus*) with BTEAC-PVA ENMS compared to PVA ENMs for 24 h (Table 5.4). Under all conditions, the number of sessile cells that were attached to BTEAC-PVA ENMs was lower that of PVA ENMs, while the number of planktonic cells was approximately similar during 72 h. As a result, an anti-biofouling effect was due to the contact-dependent killing of sessile cells rather than to a reduction in the number of planktonic cells because both cells were exposed to simultaneous conditions for biofilm growth.

Table 5.4 Growth of *P. aeruginosa* and *S. aureus* biofilm (sessile cells) and planktonic cells with BTEAC-PVA and PVA ENMs for 72 h.

ENMs	Bacteria	Incubation time		
		24 h	48 h	72 h
	P. aeruginosa			
w/o ENMs	Planktonic	8.99	8.46	8.65
PVA ENMs	Sessile	6.76	6.89	5.68
	Planktonic	8.94	8.93	8.73
BTEAC-PVA	Sessile	4.98	4.94	4.21
	Planktonic	8.90	8.41	8.40
	S. aureus			
w/o ENMs	Planktonic	8.19	8.03	8.15
PVA ENMs	Sessile	5.82	5.65	4.72
	Planktonic	8.09	8.18	8.25
BTEAC-PVA	Sessile	4.39	3.77	3.74
	Planktonic	8.16	8.19	8.04

Chapter 6

Immobilization of α-Chymotrypsin on Electrospun Poly(vinyl alcohol) /Poly(acrylic acid) Nanofibers for Anti-biofouling Activity

6.1 Materials and methods

6.1.1 Microtiter assay for biofilm removal and preventing biofilm formation using enzymes

Commercial enzymes such as Acylase I from porcine kidney (A3010), proteinase K (P6556), trypsin (T1426) and α-chymotrypsin from bovine pancreas (C4129), were purchased from Sigma Aldrich.

Single-species biofilms of *S. aureus* (ATCC 10537) and *P. aeruginosa* (ATCC 15442) were used in biofilm forming bacteria (Pitt et al., 2003; Zmantar et al., 2010). A microtiter assay was performed based on the growth and biofilm formation by bacteria in multiwell microtiter dishes (96 wells) (O'Toole et al., 1999).

The enzymes were tested in two ways. For the degradation biofilm, each overnight culture of *S. aureus* and *P. aeruginosa* was diluted 1:100 in sterile fresh media (NB and TSB); then, 200 μl of diluted solution was added to the wells of a polystyrene microtiter plate (JetBiofil, China), and incubated at 37 ℃ for 24 h. For *S. aureus*, 2% glucose was supplemented to maximize *ica* operon induction (Rachid et al., 2000). After incubation, the supernatant was discarded, and the plate was gently submerged in a small tub of water for washing out. This process was repeated three times to remove unattached cells and media. To evaluate the biofilm removal efficiency of the enzymatic treatment, 30 μg/ml

of acylase I and 3 types of proteases (proteinase K, trypsin, and α-chymotrypsin) were added to each well at 37 ℃ for 1 h. A well without enzymes was used as a control. The supernatant was discarded, washed again, and allowed to air dry for at least 1 h. Then, 200 μl of crystal violet solution (0.1%) was added to each well for 15 min. Microtiter plates were washed five times, adding 200 μl of glacier acetic acid (30%).

To examine the biofilm inhibition of enzymes, 30 μg/ml of each enzyme was added in sterile fresh media with a diluted overnight culture of bacteria, incubated at 37 ℃ for 24 h, stained with crystal violet and dissolved in glacier acetic acid in the same manner. Microtiter plates were read at 550 nm using an ELISA plate reader (Victor 3, US). All of the experiments were performed in 6 replicate wells for each treatment. The efficiency of the biofilm reduction ratio (%) was calculated by blank, control, and treated wells using Eq (1) (Pitts et al., 2003):

$$\text{Biofilm reduction ratio (\%)} = \left[\frac{(C-B)-(T-B)}{(C-B)}\right] \times 100\ \% \qquad (1)$$

where B is the average absorbance of blank wells (no biofilm, no treatment), C is the average absorbance of control wells (biofilm, no treatment), and T is the average absorbance of treated wells (biofilm, enzyme treatment).

6.1.2 Electrospinning of PVA/PAA nanofibers

A PVA solution (10 wt%) was prepared by dissolving PVA powder in deionized water (DW) at 80 ^{o}C for 16 h and then cooling the solution at room temperature. A PVA/PAA blend solution was mixed to a mass ratio 2:5:3 (PAA: PVA: DW) to achieve a total polymer concentration of 10 wt%, 5 wt% PAA and 5 wt% PVA, respectively. The mixed solution was stirred for 1 h before use to make the solution homogeneous. Electrospinning of the PVA/PAA nanofibers was performed at room temperature using an electrospinning system (ESP200/ESP100, NanoNC, Seoul, Korea). The as-prepared PVA/PAA solution was placed in a 25-mL syringe with a metal needle (inner diameter = 0.51 mm), which was connected to the positive terminal of a high-voltage power supply. The electrospun PVA nanofibers were collected on a rotating cylinder (diameter = 9 cm; speed = 1000 rpm) on a negative terminal that was wrapped with aluminum foil. To examine the effects of applied voltage on the synthesis of PVA/PAA nanofibers, the voltage was varied from 12.5 to 18 kV, whereas the flow rate of the spinning solution was fixed at 0.5 mL h^{-1} using a syringe pump (KDS 100, NanoNC, Seoul, Korea). Note that the tip-to-collector distance (TCD) was fixed at 15 cm during electrospinning. The PVA/PAA nanofibers were crosslinked by heat treatment at 145 ^{o}C for 30 min (Xiao et al., 2010).

6.1.3 Preparation of PVA/PAA-Cu(II) nanofibers

To determine the capacity of Cu(II) on PVA/PAA nanofibers, 0.05g of PVA/PAA nanofiber was added in a 50 mL solution with 500 mg/L Cu(II) in 50-mL conical tubes. The tubes were shaken at 30 °C and 150 rpm using a shaking incubator (Daihan Science, Korea). The PVA/PAA nanofiber were collected after 24 h. The initial and final Cu(II) were analyzed by Inductively Coupled Plasma Optical Emission Spectrometer (ICP-730 ES, Australia) to calculate the adsorption capacity of Cu(II) on PVA/PAA nanofibers. The Cu(II) capacity on PVA/PAA nanofibers was estimated by the following equation:

$$Q_e = \frac{(C_0 - C_e)V_0}{M} \quad (2)$$

where Q_e is the amount of Cu(II) on unit mass of PVA/PAA nanofibers (mg/g), C_0 is the initial concentration of Cu(II) (mg/L), C_e is the final concentration of Cu(II) (mg/L), V_0 is the volume of Cu(II) solution (ml), and M is the mass of the PVA/PAA nanofibers.

In addition, immersion test was conducted to measure leaching Cu(II) from PVA/PAA-Cu(II) nanofibers. The PVA/PAA-Cu(II) nanofibers (0.01 g) were immersed in 5 ml of water (28.5 °C) for various times (1, 2, 4, 8, and 24 h), and Cu(II) concentration in water was examined by inductively coupled plasma-atomic emission spectroscopy (ICP-AES) (Optima-4300, PerkinElmer, USA).

6.1.4 Immobilization of protease on PVA/PAA-Cu(II) nanofibers

The α-chymotrypsin from bovine pancreas was dissolved at a concentration of 1mg/ml in phosphate buffer solution (PBS). Then, 0.01 g of PVA/PAA-Cu(II) nanofibers was added in 3 ml of α-chymotrypsin solution (1 mg/ml). The tubes were shaken at 20 °C and 100 rpm for 2 h using a shaking incubator (Daihan Science, Korea). The α-chymotrypsin immobilization capacity was measured using the Bradford protein assay (Bio-Rad, US) (Bradford, 1976) and determined following equation (7) (Wang et al., 2007).

$$Q_{\alpha} = \frac{(C_0 - C_e)V_{\alpha} - C_r V_r}{M_c} \quad (3)$$

where Q_{α} is the amount of α-chymotrypsin on unit mass of PVA/PAA nanofibers (mg/g), C_r is the α-chymotrypsin concentration in the rinsing PBS (mg/L), V_{α} is the volume of treated α-chymotrypsin solution (ml), V_r is the volume of rinsing PBS (ml), and M_c is the mass of PVA/PAA-Cu(II) nanofibers.

6.1.5 Characterization of PVA-PAA nanofibers

The characteristics of the electrospun nanofibers were determined by various techniques. The morphology of the nanofibers was examined by a field

emission scanning electron microscope (FESEM, SUPRA 55VP, Carl Zeiss, Oberkochen, Germany). The average diameter of the nanofibers was determined by measuring fibers (n = 30) in each SEM image using ImageJ 1.43u software (National Institutes of Health, Bethesda, MD, USA). In addition, the element contents on the surface of PVA/PAA nanofibers were examined using an EDS analysis. Infrared spectra were obtained using a Nicolet 6700 (Thermo Scientific, Waltham, MA, USA) Fourier-transform infrared (FTIR) spectrometer at the range of 400–4000 cm^{-1}. The zeta potential values were measured from electrophoretic mobility using ELS-Z2 (Otsuka Electronics, Japan).

6.1.6 Degradation of biofilm EPS using PVA/PAA-Cu (II)-α nanofibers

EPS was extracted from *P. aeruginosa* following the modified method of Wingender et al. (2001). Simply, *P. aeruginosa* strains were cultivated as agar-grown biofilm at 37 ºC for 24 h. The bacterial lawn was scraped off the agar surface, suspended in a 0.14 M NaCl solution, and stirred for 30 min. The mixture was centrifuged at 40,000×g for 2 h at 4 ºC to remove bacterial cells. The supernatant was filtered through a cellulose acetate membrane (pore size = 0.22 μm) and then dialyzed against distilled water (4 ºC, 24 h).

A total of 0.05 g of PVA/PAA-Cu (II)-α nanofibers was added to 5 mL of biofilm EPS solution in 15-mL conical tubes. The tubes were incubated at 25 ^{o}C, and 100 rpm, and the samples were collected after various shaking times from 15 min to 3 h. The protein and carbohydrate concentrations of EPS were determined by the Bradford method (Bradford, 1976) and Anthrone method (Dreywood et al., 1946), respectively. Comparing the activity of free α-chymotrypsin powder, 1.28 mg (same dose of immobilized enzyme) of powders was added to 5 mL of biofilm EPS solution under the same conditions. Biofilm EPS solution was used as a control. In addition, regeneration test was conducted using 0.01 g of PVA/PAA-Cu(II)-α and PVA/PAA-Cu(II) nanofibers with 3 mL of EPS solutions in 15-mL conical tubes. The tubes were incubated for 1 h at 25 ^{o}C, and shaken at 100 rpm. This procedure was repeated 3 times for retaining activity of PVA/PAA-Cu(II)-α.

6.1.7 Anti-biofouling activity of adhesion-inhibition

Single-species biofilms of *P. aeruginosa* were used in biofilm-forming bacteria (Pitt et al., 2003). The method of biofilm formation on the membrane surface is described by Prijck et al. (2007) and Zodrow et al. (2009). Briefly, stationary-phase cultures of bacteria were diluted to 10^5 cell/ml in 5 mL of media and incubated at 37℃ for 24 h with 0.01 g of sterile PVA/PAA-Cu(II)-

α, PVA/PAA-Cu(II), and PVA-PAA nanofibers. Both the planktonic cells in the supernatant and the sessile cells in the biofilm were counted by the spread plate procedure. To enumerate the sessile cells, the nanofibers were removed from medium and rinsed gently in sterile DI water. Then, the nanofibers were soaked in 1 ml of NaCl (0.85 %) solution, vortexed (Vortex Genie 2, VWR Scientific, USA) on the highest setting for 30 s, and sonicated for 30 s. This procedure was performed twice to disrupt the biofilm (sessile cells) on the ENMs surface (Zodrow et al., 2009).

6.2 Results and discussion

6.2.1 Effect of enzyme treatment on formation and removal of biofilms

To investigate the effect of enzyme treatment on the reduction of biofouling, two types of experiments were performed. One method of reduction was adding enzyme at the beginning of the bacteria inoculum in microtiter plates to inhibit the formation of biofilm (Fig. 6.1). Another way was adding enzyme after the bacteria formed biofilms in microtiter plates during 24 h of incubation to degrade the biofilm (Fig. 6.2).

As observed in Fig. 6.1, the most efficient enzyme for inhibition of biofilms is acylase I (59.64%) for the biofilm of *P. aeruginosa* (Fig. 6.1(a)) and trypsin (45.14 %) for the biofilm of *S. aureus* (Fig. 6.1(b)), followed by α-chymotrypsin (*P. aeruginosa*: 53.50%, *S. aureus*: 35.52%) in both. For acylase I, the minimum biofilm inhibition rate was obtained with the Gram-positive bacterium *S. aureus,* whereas the highest biofilms inhibition rate (2.65%) was observed with the Gram-negative bacterium *P. aeruginosa* because acylase I is well known for quorum-quenching enzymes to degrade the N-acetyl homoserine lactone autoinducer of Gram-negative bacteria (Yeon et al., 2099). As observed in Fig. 6.2, α-chymotrypsin reduced most of the *P. aeruginosa* biofilms (58.72%), followed by trypsin (57.23%), proteinase K (55.72%), and acylase I (52.75%), while proteinase K reduced most of the *S. aureus* biofilms (46.51%), followed

by α-chymotrypsin (44.84%), trypsin (41.18%), and acylase I (10.91%). Thus, α-chymotrypsin was used as an immobilized enzyme because it prevents both biofilm formation and removal. Similarly, Leroy et al.(2008) evaluated the antifouling potential of commercial proteases, glucosidases and lipase and found that savinase, a protease, was the most effective enzyme in the prevention of bacterial adhesion and the removal of adhered bacteria. Molobela et al. (2010) determined the effect of commercial proteases (savinase, everlase, and polarzyme) and amylases (amyloglucosidase and bacterial amylase novo) on biofilms and extracted EPS formed by *P. fluorescens,* indicating that proteases, especially savinase and everlase, were the most effective enzymea for removing biofilms and degrading the EPS. Kim et al. (2013) investigated the reduction of biofouling on the RO membrane with enzymes (acylase I and proteinase K) by the incubation *P. aeruginosa* for 4 days. Acylase I (5 μg/ml), proteinase K (100 μg/ml), and a combination both enzymes removed 9.0, 56.6 and 33.7% of the bacteria on the RO membrane, respectively. Proteinase K decreased the EPS concentration, while acylase I decreased the number of bacteria but not the EPS concentration.

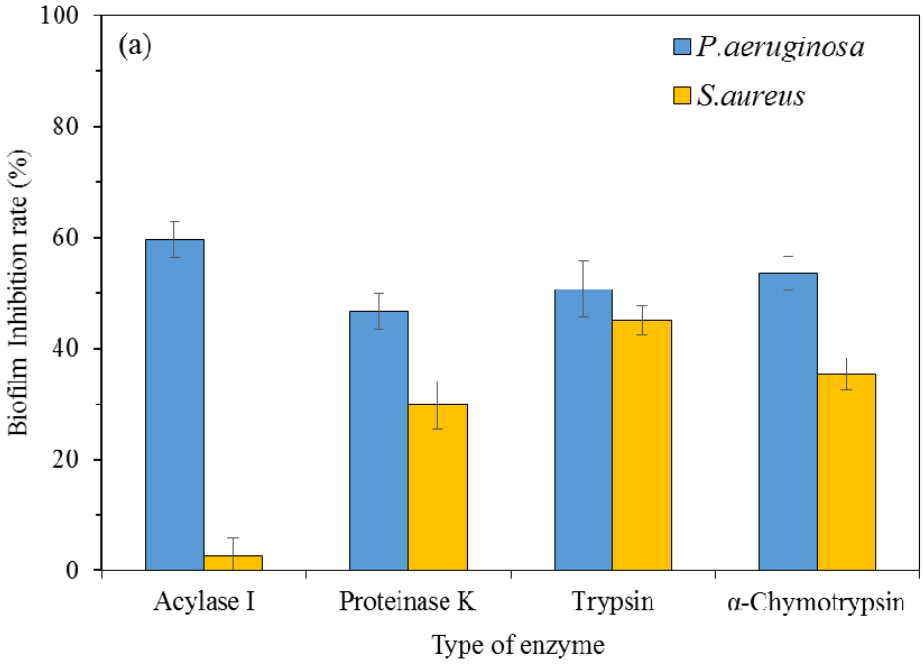

Figure. 6.1 Biofilm inhibition rate with enzyme treatment

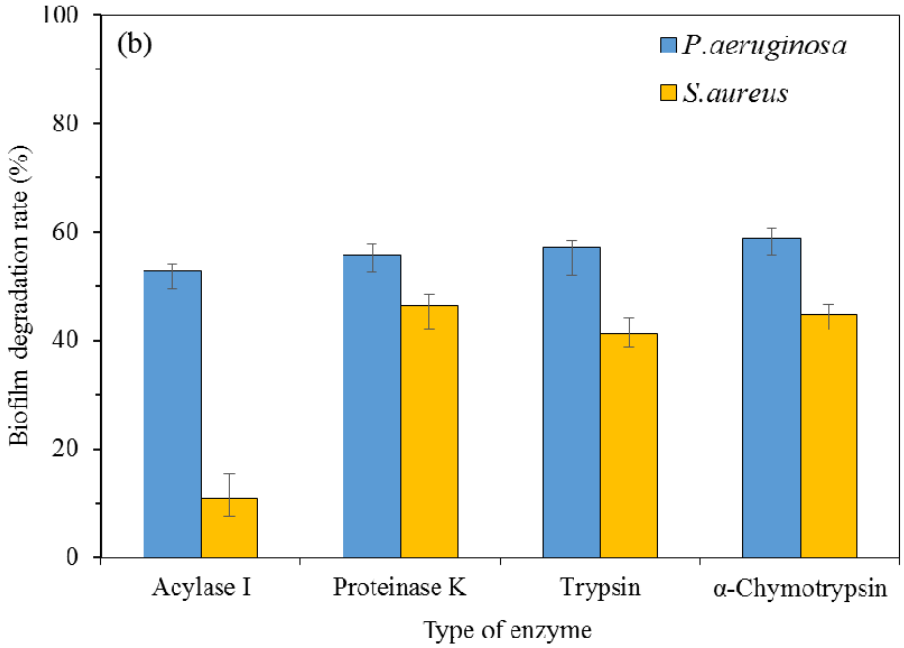

Figure. 6.2 Biofilm degradation ratio with enzyme treatment

6.2.2 Electrospun PVA/PAA nanofibers

FESEM images of PVA/PAA nanofibers that were prepared at various electrospinning voltages (12.5 -18 kV) are shown in Fig. 6.3. Generally, the average diameters of the nanofibers generally decreased with increasing applied voltage however, the average diameters at 17 kV were the smallest (333.42 ± 54.09 nm), and no beaded nanofibers were observed. Therefore, the optimal voltage was 17 kV in this study. The PVA/PAA nanofibers had diameters ranging from 263 to 475 nm, with the highest percent (46.67%) having a diameter of 300–350 nm (Fig. 6.4). Approximately 73.33% of the PVA nanofibers had diameters ranging between 250-350 nm. Strong crosslinking by ester linkage can form between the hydroxyl group of PVA and the carboxyl group of PAA after heat treatment (145 ℃, 30 min).

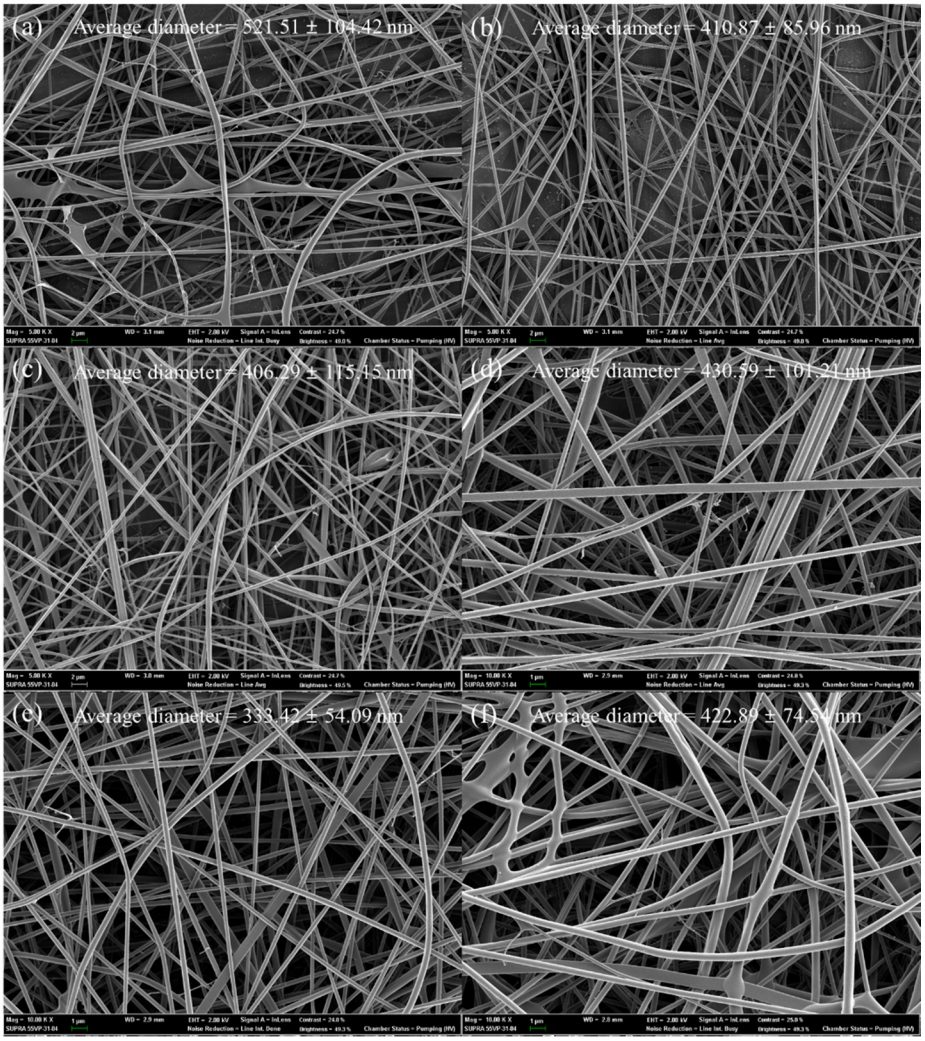

Figure. 6.3 FESEM images for PVA-PAA nanofibers prepared at various voltage conditions during electrospinning (flow rate (0.5 ml/h, TCD = 15cm) (a) 12.5 kV; (b) 13.5 kV; (c) 15 kV; (d) 16 kV; (e) 17 kV; (f) 18 kV.

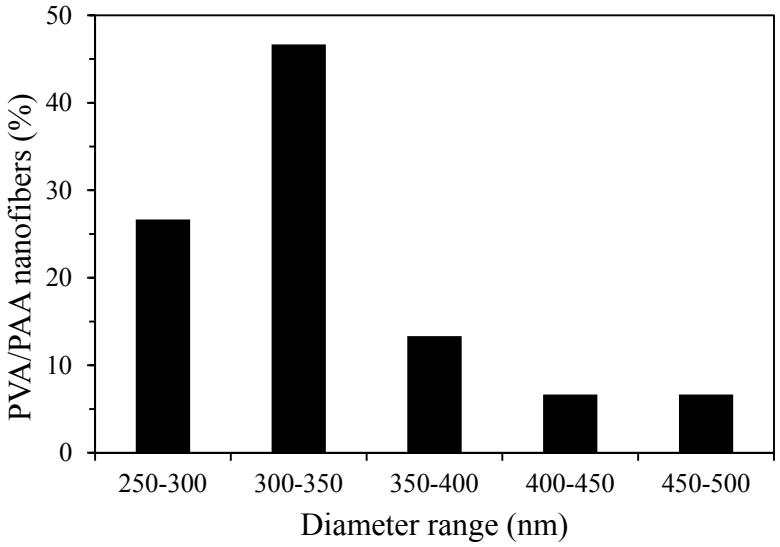

Figure. 6.4 The diameter distribution of PVA/PAA nanofibers (voltage = 17 kV, flow rate = 0.5 ml/h)

6.2.3 Preparation of PVA/PAA-Cu(II)-α nanofibers

The Cu(II) adsorption capacity of PVA/PAA nanofibers is 44.85 mg/g (initial Cu(II) concentration = 500 mg/L, reaction time = 24 h). The adsorption capability of PVA/PAA nanofibers is attributed to a strong interaction between soft acids and soft bases, leading to chelating/coordination bonds of the carboxyl group of PAA, and hydroxyl groups of PVA with Cu(II) ions (Rivas et al., 2004; Xiao et al., 2010, Feng et al., 2014). Xiao et al. (2010) removed Cu(II) ions using PVA/PAA nanofibers with an initial Cu(II) concentration of 50 mg/L with a removal capacity of 9 mg/g for 3 h of incubation. For immersing test, concentration of leaching Cu(II) ions was increasing from 0.015 μg to 0.358 μg with increasing immersing time from 1 h to 24 h. 0.358 μg of Cu(II) is about 0.08% of adsorbed Cu(II) ions on PVA/PAA-Cu(II) nanofibers that leaching is minimal. However, Cu(II) ions make intoxication of aquatic organism even in very low Cu(II) concentration ($EC_{50,48\,h}$ = 17.8 – 30 μg/L) that PVA/PAA-Cu(II) nanofibers need pre-washing to reduce leaching Cu(II) ions.

After Cu(II) adsorption onto PVA/PAA nanofibers, α-chymotrypsin was immobilized onto PVA/PAA-Cu(II) nanofibers because these Cu(II) ions form coordination bonds with amino groups on α-chymotrypsin (Fig 6.5). The immobilized amount of α-chymotrypsin on PVA/PAA-Cu(II) nanofibers is 25.56 ± 2.72 mg/g. The immobilized α-chymotrypsin on PVA/PAA-Cu(II)

nanofibers was observed in FESEM images (Fig. 6.6(a)). Some researchers have shown that Cu(II) provides a suitable binding force for immobilizing enzymes on the membrane (Chen et al., 2011; Feng et al., 2014). Chen et al. (2011) prepared a chemically treated cellulose membrane for chelating with Cu(II) ions and successfully immobilized penicillin G acylase. Feng et al. (2014) developed an electrospun PVA/PA6-Cu(II) nanofibrous membrane for the immobilization of catalase and found that the amount of immobilized catalase was 64 ± 4.6 mg/g. In addition, a antibacterial agent, epigallocatechin-3-gallate, chelated copper ions to increase stability and activity and was then electrospun into PVA nanofibers (Sun et al., 2011). In addition, Sun et al. (2011) immobilized Epigallocatechin-3-gallate (EGCG), an antimicrobial agent, in PVA nanofibers in the form of the EGCG-Cu(II) complex to increase stability.

FT-IR spectra were obtained in Fig. 6.6(b), with the broad band at approximately 3272 cm^{-1} corresponding to the stretching vibration of the O–H groups for the PVA/PAA. The peak at 2919 cm^{-1} was attributed to C–H stretching, whereas the bands at 1412 cm^{-1} corresponded to C–H bending (Gule et al., 2012; Abbasizadeh et al., 2013). In addition, the peaks at 822, 1091, and 1237 cm^{-1} were assigned to C–C–O, C–O, and C–C (stretching), respectively (Sui et al., 2005; Li et al., 2013; Siriwatcharapiboon et al., 2013). The 1704 cm^{-1} and 913 cm^{-1} bands were ascribed to carboxyl group (–CO–O–) a of the PAA and O–H groups out of plane motion of the carboxylic group, respectively (Kim

et al., 2005; Atymur & Uslu, 2014). PVA/PAA-Cu-α nanofibers have additional peaks at 1619 cm^{-1} and 1544 cm^{-1}, corresponding to amide groups (N–H) of α-chymotrypsin (Pallares et al., 2004; Hong et al., 2007).

The composition of PVA/PAA, PVA/PAA-Cu(II), and PVA/PAA-Cu(II)-α nanofibers was analyzed by EDS with SEM images (Fig. 6.7). PVA/PAA nanofibers were composed of carbon (65.07 wt%) and oxygen (34.93 wt%), and copper existed at 25.5 wt% in PVA/PAA-Cu(II). The color of nanofibers changed from white to dark green after the adsorption of Cu(II) ions. Xiao et al. (2010) also observed a color change after the adsorption of Cu(II) (50 mg/L). To composition of PVA/PAA-Cu(II)-α nanofibers varied due to the immobilization of α-chymotrypsin, nitrogen (3.03 wt%), chlorine (1.59 wt%), sodium (3.03 wt%), and copper (10.04 wt%).

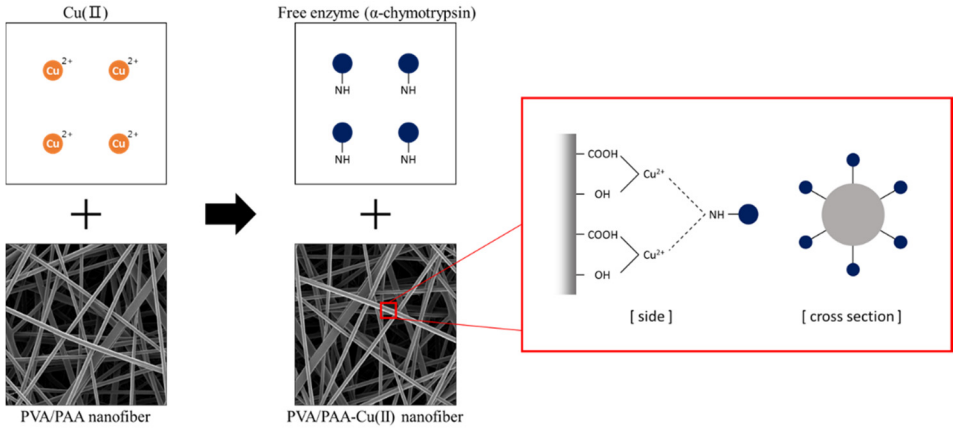

Figure 6.5 Schematic showing the immobilization of α-chymotrypsin on PVA/PAA-Cu(II) nanofibers.

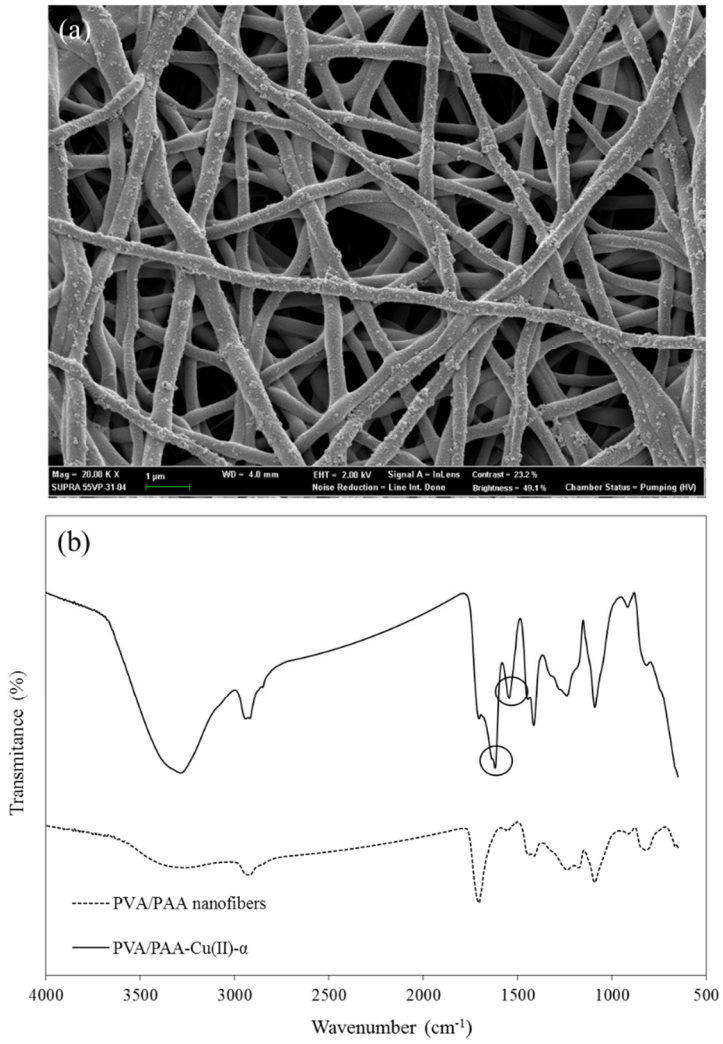

Figure 6.6 PVA/PAA-Cu(II)-α nanofibers: (a) FESEM image; (b) FT-IR spectra.

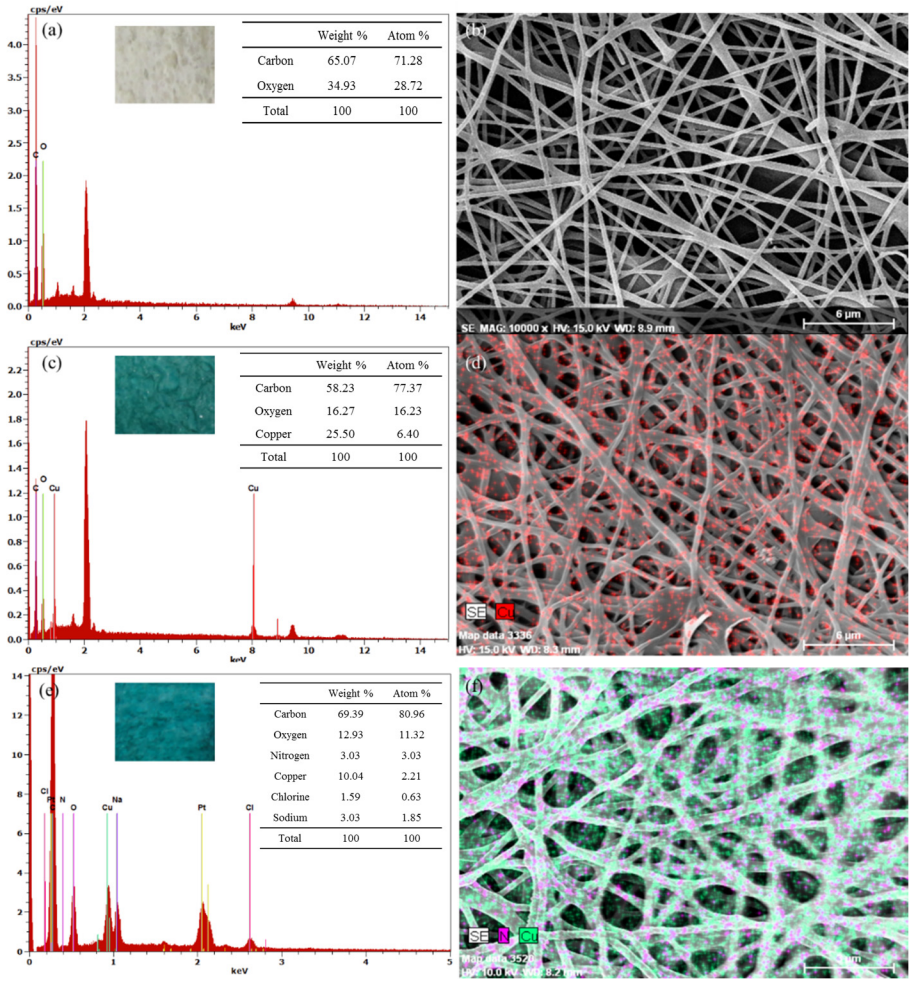

Figure. 6.7 FESEM and EDS analysis (a, b) PVA/PAA nanofibers; (c, d) PVA/PAA-Cu(II) nanofibers; (d, e) PVA/PAA-Cu(II)- α nanofibers.

6.2.4 Degradation of EPS from PVA/PAA-Cu(II)-α nanofibers

The initial concentrations of protein and carbohydrates from EPS of *P. aeruginosa* biofilm were 0.43 mg/mL and 0.32 mg/mL, respectively. The PVA/PAA-Cu(II)-α nanofibers degraded the protein concentration of the extracted EPS up to 0.26 mg/mL for 300 min (Fig 6.8(a)), whereas the control maintained a concentration of 0.41 mg/mL. Molobela et al. (2010) found that proteases (Savinase and Everlase) degraded the protein concentration of the extracted EPS from *P. fluorescens*. The same amount (1.28 mg) of free α-chymotrypsin powders was added to the EPS solution, indicating that the concentration of proteins steadily decreased (0.38-0.31 mg/mL) by increasing the incubation time (15-300 min). Considering PVA/PAA-Cu(II) nanofibers, the protein concentration slightly decreased because of the adsorption of protein on the surface of the nanofibers. In PVA/PAA-Cu(II)-α nanofibers, the protein concentration was lower than that of PVA/PAA-Cu(II) nanofibers due to activity of immobilized α-chymotrypsin, which retains the activity. Retaining the activity of the enzyme after immobilization on nanofibers is a positive observation for application in water filtration. Du Plessis et al. (2012) found that an immobilized enzyme (BAN) had a higher specific activity than did a free enzyme, while other enzymes, savinase and acalase, retained 83% and 90%, respectively, of their specific activity after immobilization. On the other hand, the concentration of carbohydrates remained at 0.28-0.30 mg/mL and 0.27-0.31

mg/mL for 5 h of incubation of PVA/PAA-Cu(II)-α nanofibers and free α-chymotrypsin, respectively, similar to the control concentration of 0.29-0.32 mg/mL, indicating that α-chymotrypsin did not affect the concentration of carbohydrates. Therefore, the anti-biofouling mechanism of α-chymotrypsin degrades protein from the EPS of *P. aeruginosa* biofilm.

Moreover, the PVA/PAA-Cu(II)-α nanofibers retained activity of degrading proteins over 3 cycles with simple washing after treatment (Figure. 6.9). Approximately, 24 % of proteins was degraded over 3 cycles using PVA/PAA-Cu(II)-α nanofibers (initial conc. = 0.55 mg/mL), whereas PVA/PAA-Cu(II) nanofibers adsorbed 7 – 14 % of proteins during incubation.

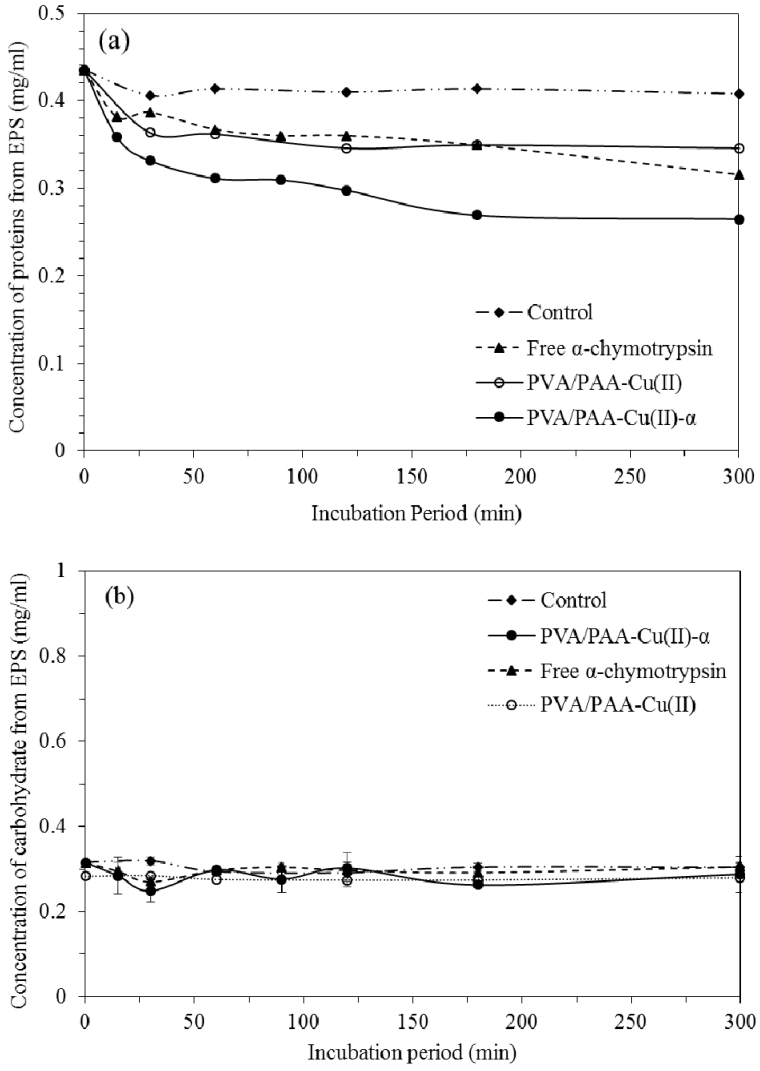

Figure. 6.8 Concentration of protein and carbohydrates from EPS produced by *P. aeruginosa* with PVA/PAA-Cu(II), free α-chymotrypsin, and PVA/PAA-Cu(II)-α nanofibers.

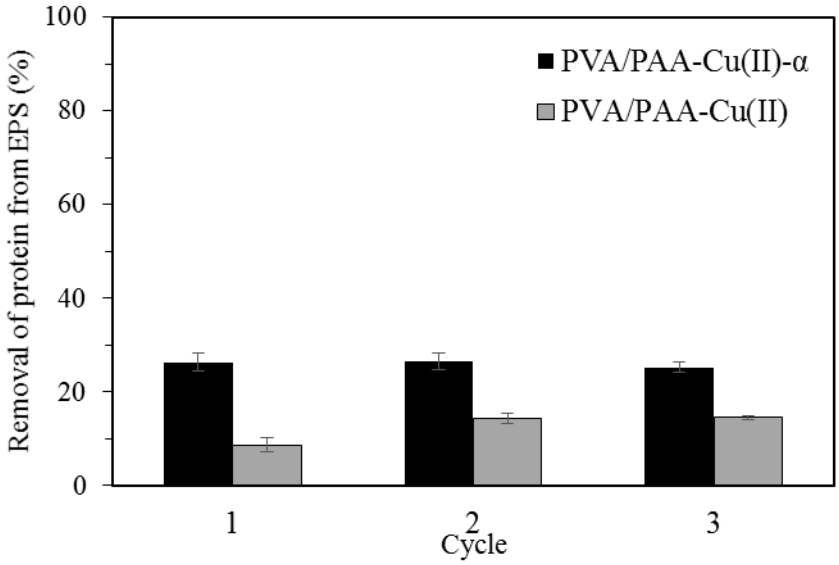

Figure. 6.9 The result of regeneration test of PVA/PAA-Cu(II)- α nanofibers.

6.2.5 Anti-biofouling activity of PVA/PAA-Cu(II)-α nanofibers

The number of planktonic cells was similar between the control (8.99 log) and PVA/PAA nanofibers (8.79 log), while, 0.9 log was reduced with PVA/PAA-Cu(II) nanofibers, indicating that Cu(II) ions have ability to kill bacteria (Table 6.1). Copper is one of the most toxic metals for the inactivation of bacteria and viruses in aquatic environments (Thurman & Gerba, 1989). In particular, bacterial cells exposed to copper surfaces experienced cell death caused by membrane damage (Santo et al., 2011).

Sessile cells were reduced 1.12 log with PVA/PAA-Cu(II) nanofibers compared to PVA/PAA nanofibers due to a reduction in the number of planktonic cells. The number of sessile cells that were attached to PVA/PAA-Cu(II)-α nanofibers was 0.81 log lower than those attached to PVA/PAA-Cu(II) nanofibers due to the anti-biofouling activity of α-chymotrypsin, whereas the number of planktonic cells was approximately similar. As a result, an anti-biofouling effect was due to a reduction of planktonic cells from Cu(II) ions, and the protein of the biofilm degraded with α-chymotrypsin. Du Plessis et al. (2013) immobilized commercial proteases (savinase and alcalase) and α-amylase (BAN) onto PAN nanofibers and then incubated them with bacteria (10^7 cells /ml) in a shaking incubator (25 rpm) at 37 ℃ for 20 h. Du Plessis et al. (2013) insisted that no biofilm growth was observed on enzyme immobilized PAN nanofibers using FESEM images.

Table 6.1 Growth of *P. aeruginosa* biofilm (sessile cells) and planktonic cells with PVA/PAA, PVA/PAA-Cu(II), and PVA/PAA-Cu(II)-α nanofibers.

Nanofibers	*P. aeruginosa*	
	Planktonic	Sessile
Control	8.99 ± 0.08	-
PVA/PAA	8.79 ± 0.04	6.71 ± 0.09
PVA/PAA-Cu(II)	7.89 ± 0.03	5.59 ± 0.10
PVA/PAA-Cu(II)- α	7.72 ± 0.05	4.78 ± 0.03

Chapter 7 General Conclusions and Recommendations

7.1 General Conclusions

This thesis was performed with two types of functionalized electrospun nanofibers for antimicrobial and anti-biofouling activity in water filtration systems. One was BTEAC-PVA nanofibers that have broad antimicrobial spectrum of contact killing bacteria and bacteriophages. BTEAC-PVA nanofibers possibly used for antimicrobial water filtration. Moreover, reduction of the number of sessile cells on the BTEAC-PVA nanofibers surface leading anti-biofouling activity. The other was PVA/PAA-Cu(II)-α nanofibers possessing anti-biofouling activity that degrade protein from EPS then destroy structure of biofilm.

1. In chapter 3, antimicrobial electrospun PVA nanofibers were prepared in this study using BTEAC as an antimicrobial agent. The BTEAC-PVA nanofibers were successfully fabricated by adding BTEAC into the PVA solution. The average diameter of the BTEAC-PVA nanofibers was closely related to the electrical conductivity, increasing with increasing electrical conductivity of the BTEAC-PVA solution. The antibacterial test with 2.6% BTEAC-PVA nanofibers demonstrated that the BTEAC-PVA nanofibers successfully inhibited the growth of S. aureus and K. pneumonia. In addition, the antiviral

test showed that the BTEAC-PVA nanofibers inactivated both MS2 and PhiX174. This study demonstrated that BTEAC-PVA electrospun nanofibers have antimicrobial potential against bacteria and viruses.

2. In chapter 4, BTEAC-PVA/GF ENMs were successfully adapted to antimicrobial water filtration system. BTEAC-PVA ENMs were cross-linked well and immobilized BTEAC on PVA nanofibers using heat and methanol treatment. BTEAC-PVA ENMs have a similar characteristics to microfiltration membrane, considering pore size and flux. The main mechanism of bacteria and bacteriophage reduction was electrostatic interaction between BTEAC and bacteria or bacteriophage at the beginning then inactivation. Therefore, BTEAC-PVA ENMs is a good candidate for both water purification membrane to remove microorganism.

3. Chapter 5, BTEAC-PVA ENMs were successfully adapted to water filtration system for anti-biofouling activity. BTEAC-PVA/PC ENMs retained flux even with high concentration of bacteria (~105 cfu/mL) and bacteriophage (~105 pfu/mL). The BTEAC-PVA/PC ENMs showed increasing antibacterial activity with increasing contact time,

and effected to Gram-negative (E. coli, K. pneumonia), Gram-positive bacteria (S. aureus), and mixed species in raw river water. Also, antimicrobial activity were maintained even after using six times. The main mechanism of anti-biofouling effect was contact-dependent killing bacteria. Simply, electrostatic interaction between BTEAC and bacteria at the beginning then inactivation. Therefore, BTEAC-PVA ENMs possessed antimicrobial and hydrophilic properties enhance the anti-biofouling effect.

4. Chapter 6, PVA/PAA-Cu(II)-α nanofibers were prepared by post electrospinning methods, and had anti-biofouling activity via protease, α-chymotrypsin. The α-chymotrypsin was chosen among quorum-quenching enzyme (acylase I), and proteases (proteinase K, trypsin, α-chymotrypsin) by microtiter assay. The α-chymotrypsin successfully degrade protein of EPS in *P. aeruginosa* biofilm in both free powder form and immobilized on PVA/PAA-Cu(II) nanofiber. Anti-biofouling effect was due to reduction of planktonic cells from Cu(II) ions, and protein of biofilm degraded with α-chymotrypsin.

The as-prepared PVA-based nanofibers, which are disk type filters, were evaluated filtration performance for application in water filtration system. The experiments in this dissertation were all small-scaled tests in laboratory, however the results of this dissertation provide the information about the synthetic method of nanofibers for pilot-scale test and module through mass production of company. It also helps to enhance the knowledge of applying QAC and enzyme on antimicrobial ENMs in water filtration especially for anti-biofouling. Water filtration with PVA based ENMs is cost-effective, eco-friendly, reducing requiring energy and labor, and no side effect. This could be useful for water treatment as a MF filter, and pre-filter for UF, RO membrane in water filtration system.

7.2 Recommendations

The following recommendations are made for the future researches on PVA-based ENMs for water filtration.

1. In this study, nanofibers were deposited on commercial rigid membrane to obtain mechanical strength. However, mechanical strength of PVA-based ENMs is still low that needs more study for increasing strength to apply in water filtration system. Further studies should be conducted about layering, and coating to increase strength. Moreover, polymer-additives and a few types of polymer (PAN, PA) can improve the strength of nanofibers that requires further studies.

2. Hydrophilic polymers are good material for water purification because they are inexpensive, non-toxic, and biodegradable. One challenge for use hydrophilic polymers is obtaining water stability via crosslinking. Only few methods have been introduced for crosslinking that needs more studies.

3. Co-electrospinning with various antimicrobial agent is another issue for future study. Many metal or metal nanoparticles have been studied for antimicrobial agent in ENMs, however, their release and toxicities in environment are controversial up to date. Also, nanoparticles need additional dispersion procedure for co-electrospinning. Further studies

are necessary for finding suitable antimicrobial agent to be incorporated with ENMs.

4. Biofouling is one of major problems to apply ENMs in water treatment leaded by biofilms. Although, there are few studies about using enzyme for anti-biofouling, enzyme is good biofilm control agents because of rapid degradability, commercially availability and nontoxic to environment. Intensive research for using enzymes for water filtration with ENMs is needed.

5. PVA-based antimicrobial ENMs can be used as point of use (POU) membrane for small water treatment plant in both purification and anti-biofouling aspect for rural areas. In Korea, water supply rate is very high in cities, whereas, the rate is only 62.2 % in rural areas in 2012. Many people in rural areas have used ground water and surface water without treatment leading exposure of microbial contamination. Therefore, studies for small water treatment plant is urgently needed to supply better quality of water that membrane system should be developed using ENMs.

REFERENCES

Abbasizadeh, S; Keshtkar, AR; Mousavian, MA. 2013. Preparation of a novel electrospun polyvinyl alcohol/titanium oxide nanofiber adsorbent modified with mercapto groups for uranium (VI) and thorium (IV) removal from aqueous solution. *Chemical Engineering Journal*, 220: 161-171.

Abbaszadegan, M; Monteiro, P; Ouwens, RN; Ryu, H; Alum, A. 2006. Removal and inactivation of cryptosporidium and microbial indicators by a quaternary ammonium chloride(QAC)-Treated zeolite in pilot filters. *Journal of Environmental Science and Health, Part A: Toxic/Hazardous Substances and Environmental Engineering*, 41: 1201-1210.

Adams, MH. 1959. Bacteriophages. *Interscience Publishers*, New York.

Adibzadeh, S; Bazgir, S. 2014. Fabrication and characterization of chitosan/poly(vinyl alcohol) electrospun nanofibrous membranes containing silver nanoparticles for antibacterial water filtration. *Iranian Polymer Journal*, 23: 645-654.

Alipour, SM; Nouri, M; Mokhtari, J; Bahrami, SH. 2009. Electrospinning of poly (vinyl alcohol)–water-soluble quaternized chitosan derivative blend. *Carbohydrate Research*, 344: 2496-2501.

American Association of Textile Colorists and Chemists. 2012. AATCC Test 100-2012, Antimicrobial Finishes on Textile Materials: Assessment of AATCC, Research Triangle Park, N.C. 27709, TM 100-1999.

An, J; Zhang, H; Zhang, JT; Zhao, YH; Yuan, XY. 2009. Preparation and antibacterial activity of electrospun chitosan/poly (ethylene oxide)

membranes containing silver nanoparticles. *Colloid and Polymer Science*, 287: 1425-1434.

Anitha, S; Brabu, B; Thiruvadigal, DJ; Gopalakrishnan, C; Natarajan, TS. 2012. Optical, bactericidal and water repellent properties of electrospun nano-composite membranes of cellulose acetate and ZnO. *Carbohydrate Polymers*, 87: 1065-1072.

Arumugam, GK; Khan, S; Heide, PA. 2009. Comparison of the effects of an ionic liquid and other salts on the properties of electrospun fibers, 2 – poly(vinyl alcohol). *Macromolecular Materials and Engineering*, 294: 45-53.

Atabey, E; Wei, SY; Zhang, X; Gu, HB; Yan, XR; Huang, YD; Shao, L; He, QL; Zhu, JH; Sun, LY; Kucknoor, AS; Wang, A; Guo, ZH. 2012. Fluorescent electrospun polyvinyl alcohol/CdSe@ZnS nanocomposite fibers. *Journal of Composite Materials*, 47: 3175-3185.

Atymur, A; Uslu, I. 2014. Promising materials for wound dressing: PVA/PAA/PVP electrospun nanofibers. *Polymer-Plastics technology and Engineering*, 56: 655-660.

Bai, B; Mi, X; Xiang, X; Heiden, PA; Heldt, CL. 2013. Non-enveloped virus reduction with quaternized chitosan nanofibers containing graphene. *Carbohydrate Research*, 380: 137-142.

Banerjee, I; Pangule, RC; Kane, RS. 2011. Antifouling coatings: recent developments in the design of surfaces that prevent fouling by proteins, bacteria, and marine organisms. *Advanced Materials*, 23: 690-718.

Bazargan, AM; Keyanpour-rad, M; Hesari, FA; Ganji, ME. 2011. A study on the microfiltration behavior of self-supporting electrospun nanofibrous

membrane in water using an optical particle counter. *Desalination*, 265: 148-152.

Bernardes, PC; De Andrade, NJ; Da Silva, LHM; De Carvalho, AF; Fernandes, PE; Araujo, EA; Lelis, CA; Mol PCG; De Sa, JPN. 2014. Modification of polysulfone membrane used in the water filtration process to reduce biofouling. *Journal of Nanoscience and Nanotechnology*, 14: 6355-6367.

Bhattarai, P; Thapa, KB; Basnet, RB; Sharma, S. 2014. Electrospinning: How to produce nanofibers using most inexpensive technique? An insight into the real challenges of electrospinning such nanofibers and its application areas. *International journal of biomedical and advance research*, 5: 401-405.

Bjorge, D; Daels, N; De Vrieze, S; Dejans, P; Van Camp, T; Audenaert, W; Hogie, J; Westbroek, P; De Clerck, K; Van Hulle, SWH. 2009. Performance assessment of electrospun nanofibers for filter applications. *Desalination*, 249: 942-948.

Bjorge, D; Daels, N; De Vrieze, S; Dejans, P; Van Camp, T; Audenaert, W; Westbroek, P; De Clerck, K; Boeckaert, C; Van Hulle, SWH. 2010. Initial testing of electrospun nanofiber filters in water filtration applications. *Water SA*, 36: 151-156.

Botes, M; Cloete, TE. 2010. The potential of nanofibers and nanobiocides in water purification. *Critical Reviews in Microbiology*, 36: 68-81.

Bradford, MM. 1976. A rapid and sensitive method for the quantitation of microgram quantities of protein utilizing the principle of protein-dye binding. *Analytical Biochemistry*, 72: 248-254.

Brady, D; Jordaan, J. 2009. Advances in enzyme immobilization. *Biotechnology Letters*, 31: 1639-1650.

Chen, CI; Ko, YM; Shieh, CJ; Liu, YC. 2011. Direct penicillin G acylase immobilization by using the self-prepared immobilized metal affinity membrane. *Journal of Membrane Science*, 380: 34-40.

Chen, L; Bromberg, L; Hatton, A; Rutledge, GC. 2008. Electrospun cellulose acetate fibres containing chlorhexidine as a bacteriocide. *Polymer*, 49: 1266-1275.

Cloete, TE; de Kwaadsteniet, M; Botes, M; Lopez-Romero, JM; Hierrezuelo-Leon, J; Cakmakci, M; Koyuncu, I; Garrido-Perez, E. 2010. Nanotechnology in water treatment applications. *Caister Academic Press*, Norfolk, UK.

Daels, N; De Vrieze, S; Sampers, I; Decostere, B; Westbroek, P; Dumoulin, A; Dejans, P. 2011. Potential of a functionalized nanofiber microfiltration membrane as an antibacterial water filter. *Desalination*, 275: 285-290.

De Britto, D; Goy, RC; Filho, SPC; Assis, OBG. 2011. Quaternary salts of chitosan: history, antimicrobial features, and prospects. *International Journal of Carbohydrate Chemistry*, 2011: 1-12.

De Prijck, K; Nelis, H; Coenye, T. 2007. Efficacy of silver-releasing rubber for the prevention of Pseudomonas aeruginosa biofilm formation in water. *Biofouling*, 23: 405-411.

De Vrieze, S; Daels, N; Lambert, K; Decostere, B; Hens, Z; Van Hulle, S; Clerck, KD. 2011. Filtration performance of electrospun polyamide nanofibers loaded with bactericides. *Textile Research*, 82: 37-44.

Ding, B; Yu, J. 2014. Electrospun Nanofibers for Energy and Environmental Applications. *Springer-Verlag*, Berlin, Heidelberg, Germany.

Dobrowsky, PH; Lombard, M; Cloete, WJ; Saayman, M; Cloete, TE; Carstens, M; Khan, S; Khan, W. 2015. Efficiency of microfiltration systems for the removal of bacterial and viral contaminants from surface and rainwater. *Water, Air, & Soil Pollution*, 226: 1-14.

Donlan, RM; Costerton, JW. 2002. Biofilms: survival mechanisms of clinically relevant microorganisms. *Clinical Microbiology Reviews*, 15: 167-193.

Dowd, SE; Pillai, SD; Wang, S; Corapcioglu, MY. 1998. Delineating the specific influence of virus adsorption and transport through sandy soils. *Applied and Environmental Microbiology*, 64: 405-410.

Dreywood, R. 1946. Qualitative test for carbohydrate material. *Industrial & Engineering Chemistry Analytical Edition*, 18: 499.

Du Plessis, DM. 2011. Fabrication and characterization of anti-microbial and biofouling resistant nanofibers with silver nanoparticles and immobilized enzymes for application in water filtration. Master's Thesis. Stellenbosch, South Africa.

Du Plessis, DM; Botes, M; Dicks, LMT; Cloete, TE. 2012. Immobilization of commercial hydrolytic enzymes on poly(acrylonitrile) nanofibers for anti-biofilm activity. *Journal of Chemical Technology and Biotechnology*, 88: 585-593.

El-Newehy, MH; Al-Deyab, SS; Kenawy, ER; Abdel-Megeed, A. 2012. Fabrication of electrospun antimicrobial nanofibers containing metronidazole using nanospider technology. *Fibers and Polymers*, 13: 709-717.

Endo, Y; Tani, T; Kodama, M. 1987. Antimicrobial activity of tertiary amine covalently bonded to a polystyrene fiber. *Applied and Environmental Microbiology*, 53: 2050-2055.

Feng, Q; Zhao, Y; Wei, AF; Li, CL; Wei, QF; Fong, H. 2014. Immobilization of catalase on electrospun PVA/PA6-Cu(II) nanofibrous membrane for the development of efficient and reusable enzyme membrane reactor. *Environmental Science & Technology*, 48: 10390-10397.

Fiksdal, L; Leiknes, T. 2006. The effect of coagulation with MF/UF membrane filtration for the removal of virus in drinking water. *Journal of Membrane Science*, 279: 364-371.

Finch, CA. 1992. Poly(vinyl alcohol) development. *Wiley*, England.

Gao, Y; Truong, YB; Zhu, Y; Kyratzis, IL. 2014. Electrospun antibacterial nanofibers: production, activity, and in vivo applications. *Journal of Applied Polymer Science*, 131: 1-13.

Geiger, DL; Call, DJ; Brooke, LT. 1984. Acute toxicities of organic chemicals to Fathead Minnows (Pimephales promelas). *Center for Lake Superior Environmental Studies*.

Gliścińska, E; Gutarowska, B; Brycki, B; Krucińska, I. 2012. Electrospun polyacrylonitrile nanofibers modified by quaternary ammonium salts. *Journal of Applied Polymer Science*, 128: 767-775.

Gopal, R; Kaur, S; Ma, Z; Chan, C; Ramakrishna, S; Mastuura, T. 2006. Electrospun nanofibrous filtration membrane. *Journal of Membrane Science*, 281: 581-586.

Gottenbos, B; Van der Mei, HC; Klatter, F; Nieuwenhuis, P; Busscher, HJ. 2002. In vitro and in vivo antimicrobial activity of covalently coupled quaternary ammonium silane coatings on silicone rubber. *Biomaterials*, 23: 1417-1423.

Greiner, A; Wendorff, JH. 2007. Electrospinning: A fascinating method for the preparation of ultrathin fibers. *Angewandte Chemie International Edition*, 46: 5670-5703.

Griffitt, RJ; Luo, J; Gao, J; Bonzongo, JC; Barber, DS. 2008. Effect of particle composition and species on toxicity of metallic nanomaterials in aquatic organisms. *Environment Toxicology and Chemistry*, 27: 1972-1978.

Gule, NP. 2011. Electrospun antimicrobial and antibiofouling nanofibers. Ph.D. thesis. Stellenbosch University.

Gule, NP; De Kwaadsteniet, M; Cloete, TE; Klumperman, B. 2012. Electrospun Poly (vinyl alcohol) nanofibres with biocidal additives for application in filter media, 1–properties affecting fibre morphology and characterisation. *Macromolecular Materials and Engineering*, 297: 609-617.

Gule, NP; De Kwaadsteniet, M; Cloete, TE; Klumperman, B. 2012. Electrospun poly (vinyl alcohol) nanofibres with biocidal additives for application in filter media, 2–antimicrobial activity, regeneration, leaching and water stability. *Macromolecular Materials and Engineering*, 297: 618-626.

Gule, NP; De Kwaadsteniet, M; Cloete, TE; Klumperman, B. 2013. Furanone-containing poly (vinyl alcohol) nanofibers for cell-adhesion inhibition. *Water Research*, 47: 1049-1059.

Hegstad, K; Langsrud, S; Lunestad, BT; Scheie, AA; Sunde, M; Yazdankhah, SP. 2010. Does the wide use of quaternary ammonium compounds enhance the selection and spread of antimicrobial resistance and thus threaten our health?. *Microbial Drug Resistance*, 16: 91-104.

Homaeigohar, S; Elbahri, M. 2014. Nanocomposite electrospun nanofiber membranes for environmental remediation. *Materials*, 7: 1017-1045.

Hong, BP; Jung, HM; Byun, HS. 2013. Preparation of polyvinylidene fluoride nanofiber membrane and its antibacterial characteristics with nanosilver or graphene oxide. *Journal of Nanoscience and Nanotechnology*, 13: 6269-6274.

Hong, J; Xu, DM; Gong, PJ; Sun, HW; Dong, L; Yao SD. 2007. Covalent binding of α-chymotrypsin on the magnetic nanogels covered by amino groups. *Journal of Molecular Catalysis B: Enzymatic*, 45: 84-90.

Hong, KH; Park, JL; Sul, IH; Youk, JH; Kang, TJ. 2006. Preparation of antimicrobial poly (vinyl alcohol) nanofibers containing silver nanoparticles. *Journal of Polymer Science Part B: Polymer Physics*, 44: 2468-2474.

Hu, SW; Brittain, WJ. 2005. Surface grafting on polymer surface using physisorbed free radical initiators. *Macromolecules*, 38: 6592-6597.

Huang, CC; Lin, CK; Lu, CT; Lou, CW; Chao, CY; Lin, JH. 2009. Evaluation of the electrospinning manufacturing process based on the preparation of PVA composite fibres. *Fibres & Textiles in Eastern Europe*, 17: 34-37.

Huang, ZM; Zhang, YZ; Kotaki, M; Ramakrishna, S. 2003. A review on polymer nanofibers by electrospinning and their applications in nanocomposites. *Composites Science & Technology*, 63: 2223-2253.

Ignatova, M; Starbova, K; Markova, N; Manolova, N; Rashkov, I. 2006. Electrospun nano-fibre mats with antibacterial properties from quaternised chitosan and poly (vinyl alcohol). *Carbohydrate Research*, 341: 2098-2107.

Isquith, AJ; Abbott, EA; Walters, PA. 1972. Surface-bonded antimicrobial activity of an organosilicon quaternary ammonium chloride. *Applied and Environmental Microbiology*, 24: 859-863.

Jacangelo, JG; Adham, SS; Laine, JM. 1995. Mechanism of cryptosporidium, Giardia, and MS2 virus removal by MF and UF. *Journal – American Water Works Association*, 87: 107-121.

Jang, WG; Jeon, KS; Byun, HS. 2013. The preparation of porous polyamide-imide nanofiber membrane by using electrospinning for MF application. *Desalination and Water Treatment*, 51: 5283-5288.

Kanazawa, A; Ikeda, T; Endo, T. 1993. Polymeric phosphonium salts as a novel class of cationic biocides. III. Immobilization of phosphonium salts by surface photografting and antibacterial activity of the surface-treated polymer films. *Journal of Polymer Science Part A: Polymer Chemistry*, 31: 1467-1472.

Kawabata, N; Nishiguchi, M. 1988. Antibacterial activity of soluble pyridinium-type polymers. *Applied and Environmental Microbiology*, 54: 2532-2535.

Kenawy, ER; Abdel-Fattah; YR. 2002. Antimicrobial properties of modified and electrospun poly (vinyl phenol). *Macromolecular Bioscience*, 2: 261-266.

Kenawy, ER; Mahmoud, YAG. 2003. Biologically active polymers, 6. *Macromolecular Bioscience*, 3: 107-116.

Kim, BS; Park, H; Lee, SH; Sigmund, WM. 2005. Poly (acrylic acid) nanofibers by electrospinning. *Materials Letters*, 59: 829-832.

Kim, DS; Park, HB; Rhim, JW; Lee, YM. 2005. Proton conductivity and methanol transport behavior of cross-linked PVA/PAA/silica hybrid membranes. *Solid State Ionics*, 176: 117-126.

Kim, JH; Choi, DC; Yeon, KM; Kim, SR; Lee, CH. 2011. Enzyme-immobilized nanofiltration membrane to mitigate biofouling based on quorum quenching. *Environmental Science & Technology*, 45: 1601-1607.

Kim, LH; Kim, SJ; Kim, CM; Shin, MS; Kook, SH; Kim, IS. 2013. Effects of enzymatic treatment on the reduction of extracellular polymeric substances(EPS) from biofouled membranes. *Desalination and Water Treatment*, 51: 6355-6361.

Kim, SJ; Nam, YS; Rhee, DM; Park, HS; Park, WH. 2007. Preparation and characterization of antimicrobial polycarbonate nanofibrous membrane. *European Polymer Journal*, 43: 3146-3152.

Kong, HY; Jang, JS. 2008. Antibacterial properties of novel poly (methyl methacrylate) nanofiber containing silver nanoparticles. *Langmuir*, 24: 2051-2056.

Kong, Y; Hay, JN. 2002. The measurement of the crystallinity of polymers by DSC. *Polymer*, 43: 3873-3878.

Kristensen, JB; Meyer, RL; Laursen, BS; Shipovskov, S; Besenbacher, F; Poulsen, CH. 2008. Antifouling enzymes and the biochemistry of marine settlement. *Biotechnology Advances*, 26: 471-481.

Kurihara, S; Skamaki, S; Mogi, S; Ogata, T; Nonaka. 1996. Crosslinking of poly(vinyl alcohol)-graft-N-isopropylacrylamide copolymer membranes

with glutaraldehyde and permeation of solutes through the membrane. *Polymer*, 37: 1123-1128.

Langlet, J; Ogorzaly, L; Schrotter, JC; Machinal, C; Gaboriaud, F; Duval, JFL; Gantzer, C. 2009. Efficiency of MS2 phage and Qβ phage removal by membrane filtration in water treatment: Applicability of real-time RT-PCR method. *Journal of Membrane Science*, 326: 111-116.

Larkin, PJ. 2011. Infrared and Raman spectroscopy; principles and spectral interpretation, first ed. *Elsevier*, Massachusetts.

Leclerc, H; Edberg, S; Pierzo, V; Dellattre, JM. 2000. Bacteriophages as indicators of enteric viruses and public health risk in groundwaters. *Journal of Applied Microbiology*, 88: 5-21.

Lee, JS; Choi, KH; Ghim, HD; Kim, SS; Chun, DH; Kim, HY; Lyoo, WS. 2004. Role of molecular weight of atactic poly (vinyl alcohol)(PVA) in the structure and properties of PVA nanofabric prepared by electrospinning. *Journal of Applied Polymer Science*, 93: 1638-1646.

Leroy, C; Delbarre, C; Ghillebaert, F; Compere, C; Combes, D. 2008. Effects of commercial enzymes on the adhesion of a marine biofilm-forming bacterium. *Biofouling*, 24: 11-22.

Lev, J; Holba, M; Kalhotka, L; Mikula, P; Kimmer, D. 2012. Improvements in the structure of electrospun polyurethane nanofibrous materials used for bacterial removal from wastewater. *International Journal of Theoretical and Applied Nanotechnology*, 1: 16-20.

Li, L; Hsieh, YL. 2005. Ultra-fine polyelectrolyte fibers from electrospinning of poly (acrylic acid). *Polymer*, 46: 5133-5139.

Li, NN; Xiao, CF; An, SL; Hu, XY. 2010. Preparation and properties of PVDF/PVA hollow fiber membranes. *Desalination*, 250: 530-537.

Li, W; Li, XY; Chen, Y; Li, XX; Deng, HB; Wang, T; Huang, R; Fan, G. 2013. Poly (vinyl alcohol)/sodium alginate/layered silicate based nanofibrous mats for bacterial inhibition. *Carbohydrate Polymers*, 92: 2232-2238.

Li, Y; Su, Y; Zhao, X; Zhang, R; Zhao, J; Fan, X; Jiang, Z. 2014. Surface fluorination of polyamide nanofiltration membrane for enhanced anti fouling property. *Journal of Membrane Science*, 455: 15-23.

Li, Z; Lee, DY; Sheng, XX; Cohen, RE; Rubner, MF. 2006. Two-level antibacterial coating with both release-killing and contact-killing capabilities. *Langmuir*, 22: 9820-9823.

Lienkamp, K; Madkour, AE; Musante, A; Nelson, CF; Nusslein, K; Tew, GN. 2008. Antimicrobial polymers prepared by ROMP with unprecedented selectivity: a molecular construction kit approach. *Journal of American Chemical Society*, 130: 9836-9843.

Linh, NTB; Min, YK; Song, HY; Lee, BT. 2010. Fabrication of polyvinyl alcohol/gelatin nanofiber composites and evaluation of their material properties. *Journal of Biomedical Materials Research Part B: Applied Biomaterials*, 95: 184-191.

Liu, CX; Zhang, DR; He, Y; Zhao, XS; Bai, RB. 2010. Modification of membrane surface for anti-biofouling performance: effect of anti-adhesion and anti-bacteria approaches. *Journal of Membrane Science*, 346: 121-130.

Liu, F; Nishikawa, T; Shimizu, W; Sato, T; Usami, H; Amiya, S; Ni, QQ; Murakami, Y. 2012. Preparation of fully hydrolyzed polyvinyl alcohol

electrospun nanofibers with diameters of sub-200 nm by viscosity control. *Textile Research Journal*, 82: 1635-1644.

Lopez-Gallego, F; Bentancor, L; Mateo, C; Hidalgo, A; Alonso-Morales, N; Della-Ortiz, G. 2005. Enzyme stabilization by glutaraldehyde crosslinking of adsorbed proteins on aminated supports. *Journal of Biotechnology*, 119

Lu, W; Liu, X; Zhao, S; Na, H; Zhao, Y; Yuan, X. 2012. *Polymer Engineering & Science*, 52: 1661- 1671.

Lundin, JG; Coneski, PN; Fulmer, PA; Wynne, JH. 2014. Relationship between surface concentration of amphiphilic quaternary ammonium biocides in electrospun polymer fibers and biocidal activity. *Reactive and Functional Polymers*, 77: 39-46.

Ma, H; Burger, C; Hsiao, BS; Chu, B. 2011. Ultra-fine cellulose nanofibers: new nano-scale materials for water purification. *Journal of Materials Chemistry*, 21: 7507-7510.

Ma, H; Burger, C; Hsiao, BS; Chu, B. 2012. Nanofibrous microfiltration membrane based on cellulose nanowhiskers. *Biomacromolecules*, 13: 180-186.

Ma, H; Hsiao, BS; Chu, B. 2014. Functionalized electrospun nanofibrous microfiltration membranes for removal of bacteria and viruses. *Journal of Membrane Science*, 452: 446-452.

Ma, ZW; Kotaki, M; Ramakrishna. 2006. Surface modified nonwoven polysulphone (PSU) fiber mesh by electrospinning: A novel affinity membrane. *Journal of Membrane Science*, 272: 179-187.

Ma, ZW; Kotaki, M; Yong, T; He, W; Ramakrishna, S. 2005. Surface engineering of electrospun polyethylene terephthalate (PET) nanofibers

towards development of a new material for blood vessel engineering, *Biomaterials*, 26: 2527-2536.

Madigan, MT; Martinko, JM; Dunlap, PV; Clark, DP. 2009. Brock biology of microorganisms, twelfth ed. *Pearson Benjamin Cummings*, California.

Mahapatra, A; Garg, N; Nayak, BP; Mishra, BG; Hota, G. 2012. Studies on the synthesis of electrospun PAN-Ag composite nanofibers for antibacterial application. *Journal of Applied Polymer Science*, 124: 1178-1185.

Majumdar, P; Lee, E; Patel, N; Stafslen, SJ; Daniels, J; Chisholm, BJ. 2008. Development of environmentally friendly, antifouling coatings based on tethered quaternary ammonium salts in a crosslinked polydimethylsiloxane matrix. *Journal of Coatings Technology and Research*, 5: 405-417.

McDonnell, G; Russell, AD. 1999. Antiseptics and disinfectants: activity, action, and resistance. *Clinical Microbiology Reviews*, 12: 147-179.

McKenna, R; Xia, D; Willingmann, P; Ilag, LL; Krishnaswamy, S; Rossmann, MG; Olson, NH; Baker, TS; Incardona, NL. 1992. Atomic structure of single-stranded DNA bacteriophage ΦX174 and its functional implications. *Nature*, 355: 137-142.

Mei, Y; Yao, C; Fan, K; Li, X. 2012. Surface modification of polyacrylonitrile nanofibrous membranes with superior antibacterial and easy-cleaning properties through hydrophilic flexible spacers. *Journal of Membrane Science*, 417-418: 20-27.

Mei, Y; Yao, C; Li, X. 2014. A simple approach to constructing antibacterial and anti-biofouling nanofibrous membranes. *Biofouling*, 30: 313-322.

Mi, X; Saagar, KS; Heldt, CL. 2014. Virus adsorption of water-stable quaternized chitosan nanofibers. *Carbohydrate Research*, 387: 24-29.

Mi, X; Vijayaragaven, S; Heldt, CL. 2014. Virus adsorption of water-stable quaternized chitosan nanofibers. *Carbohydrate Research*, 387: 24-29.

Molobela, P; Cloete, TE; Beukes, M. 2010. Protease and amylase enzymes for biofilm removal and degradation of extracellular polymeric substances(EPS) produced by Pseudomonas fluorescens bacteria. *African Journal of Microbiology Research*, 4: 1515-1524.

Momba, MNB; Kfir, R; Venter, SN; Cloete, TE. 2000. An overview of biofilm formation in distribution systems and its impact on the deterioration of water quality. *Water SA*, 26: 59-66.

Mulder, M. 1996. Basic Principles of membrane technology. *Springer Science & Business Media*, New York, USA.

Na, L; Zhongzhou, L; Shuguang, X. 2000. Dynamically formed poly(vinyl alcohol) ultrafiltration membranes with good anti-fouling characteristics. *Journal of Membrane Science*, 169: 17-28.

Naebe, M; Lin, T; Staiger, MP; Dai, L; Wang, X. 2008. Electrospun single-walled carbon nanotube/polyvinyl alcohol composite nanofibers: structure-property relationships. *Nanotechnology*, 19: 1-8.

Nasreen, SAAN; Sundarrajan, S; Nizar, SAS; Balamurugan, R; Ramakrishna, S. 2014. In situ polymerization of PVDF-HEMA polymers: electrospun membranes with improved flux and antifouling properties for water filtration. *Polymer Journal*, 46: 167-174.

Nirmala, R; Kalpana, D; Jeong, JW; Oh, HJ; Lee, JH, Navamathavan, R; Lee, YS; Kim, HY. 2011. Multifunctional baicalein blended poly (vinyl alcohol) composite nanofibers via electrospinning. *Colloids and Surfaces A: Physicochemical and Engineering Aspects*, 384: 605-611.

Nisola, GM; Park, JS; Beltran, AB; Chung, WJ. 2012. Silver nanoparticles in a polyether-block-polyamide copolymer towards antimicrobial and antifouling membranes. *RSC Advances*, 2: 2439-2448.

Oh, BS; Yang, HY; Jung, YJ; Kang, JW. 2007. Microfiltration of MS2 bacteriophage: effect of ozone on membrane fouling. *Journal of Membrane Science*, 306: 244-252.

Oh, SJ; Kim, N; Lee, YT. 2009. Preparation and characterization of PVDF/TiO_2 organic-inorganic composite membranes for fouling resistance improvement. *Journal of Membrane Science*, 345: 13-20.

Olsen, SM; Pedersen, LT; Laursen, MH; Kill, S; Dam-Johansen, K. 2007. Enzyme-based antifouling coatings: a review. *Biofouling*, 23: 369-383.

O'Toole, GA; Pratt, LA; Watnick, PI; Newman, DK; Weaver, VB; Kolter, R. 1999. Genetic approaches to study of biofilms. *Academic Press*, San Diego, CA.

Pallares, I; Vendrell, J; Aviles, FX; Ventura, S. 2004. Amyloid fibril formation by a partially structured intermediate state of α-chymotrypsin. *Journal of Molecular Biology*, 342: 321-331.

Pant, HR; Bajgai, MP; Nam, KT; Seo, YA; Pandeya, DR; Hong, ST; Kim, HY. 2011. Electrospun nylon-6 spider-net like nanofiber mat containing TiO2 nanoparticles: a multifunctional nanocomposite textile material. *Journal of Hazardous Materials*, 185: 124-130.

Park, D; Larson, AM; Klibanov, AM; Wang, Y. 2013. Antiviral and Antibacterial Polyurethanes of Various Modalities. *Applied Biochemistry and Biotechnology*, 169: 1134-1146.

Park, JC; Ito, T; Kim, KO; Kim, KW; Kim, BS; Khil, MS; Kim, HY; Kim, IS. 2010. Electrospun poly(vinyl alcohol) nanofibers : effect of degree of hydrolysis and enhanced water stability. *Polymer Journal*, 42: 273-276.

Park, SJ; Kim, SB; Kim, KW. 2010. Analysis of bacterial cell properties and transport in porous media. *Journal of Environmental Science and Health, Part A: Toxic/Hazardous Substances and Environmental Engineering*, 45: 682-691.

Peng, Q; Lu, S; Chen, D; Wu, X; Fan, P; Zhong, R; Xu, Y. 2007. Poly(vinylidene fluoride)-graft-poly(N-vinyl-2-pyrrolidone) copolymers prepared via a RAFT-Mediated process and their use in antifouling and antibacterial membranes. *Macromolecular Bioscience*, 7: 1149-1159.

Peppas, NA; Merrill, EW. 1976. Poly(vinyl alcohol) hydrogels : Reinforcement of radiation-crosslinked networks by crystallization. *Journal of Polymer Science: Polymer Chemistry Edition*, 14: 441-457.

Petrinca, AR; Donia, D; Cicchetti, R; Valentini, F; Argentin, G; Carbone, M; Pietroiusti, A; Magrini, A; Palleschi, G; Divizia, M. 2010. Interaction between single wall carbon nanotubes and a human enteric virus. *Journal of Virological Methods*, 168: 1-5.

Pitt, B; Hamilton, MA; Zelver, N; Stewart, PS. 2003. A microtiter-plate screening method for biofilm disinfection and removal. *Journal of Microbiological Methods*, 54: 269-276.

Qi, YY; Tai, ZX; Sun, DF; Chen, JT; Ma, HB; Yan, XB; Liu, B; Xue, QJ. 2013. Fabrication and characterization of poly (vinyl alcohol)/graphene oxide nanofibrous biocomposite scaffolds. *Journal of Applied Polymer Science*, 127: 1885-1894.

Qin, Q; Liu, Y; Chen, SC; Zhai, FY; Jing, XK; Wang, YZ. 2012. Electrospinning fabrication and characterization of poly(vinyl alcohol)/layered double hydroxides composite fibers. *Journal of Applied Polymer Science*, 126: 1556-1563.

Rachid, S; Ohlsen, K; Wallner, U; Hacker, J; Hecker, M; Ziebuhr, W. 2000. Alternative transcription Factor σ^B is involved in regulation of biofilm expression in a staphylococcus aureus mucosal isolate. *Journal of Bacteriology*, 182: 6824-6826.

Ramakrishana, S; Fujihara, K; Teo, WE; Lim, TC; Ma, Z. 2005. An Introduction to Electrospinning and Nanofibers. *World Scientific Publishing*, Singapore.

Ramakrishana, S; Jose, R; Archana, PS; Nair, AS; Balamurugan R, Venugopal, J; Teo, WE. 2010. Science and engineering of electrospun nanofibers for advances in clean energy, water filtration, and regenerative medicine. *Journal of Material and Science*, 45: 6283-6312.

Reisner, DE; Pradeep, T. 2014. Aquananotechnology. *CRC Press*, New York, USA.

Ren, XH; Akdag, A; Zhu, CY; Kou, L; Worley, SD; Huang, TS. 2009. Electrospun polyacrylonitrile nanofibrous biomaterials. *Journal of Biomedical Materials Research Part A*, 91: 385-390.

Rivas, BL; Schiappacasse, LN; Pereira, UE; Moreno-Villoslada, I. 2004. Interactions of polyelectrolytes bearing carboxylate and/or sulfonate groups with Cu(II) and Ni(II). *Polymer*, 45: 1771-1775.

Roy, D; Knapp, JS; Guthrie, JT; Perrier, S. 2007. Antibacterial cellulose fiber via RAFT surface graft polymerization. *Biomacromolecules*, 9: 91-99.

Rujitanaroj, P; Pimpha, N; Supaphol, P. 2010. Preparation, characterization, and antibacterial properties of electrospun polyacrylonitrile fibrous membranes containing silver nanoparticles. *Journal of Applied Polymer Science*, 116: 1967-1976.

Rwei, SP; Huang, CC. 2012. Electrospinning PVA solution-rheology and morphology analyses. *Fibers and Polymers*, 13: 44-50.

Sajeev, US; Anand, KA; Menon, D; Nair, S. 2008. Control of nanostructures in PVA, PVA/chitosan blends and PCL through electrospinning. *Bulletin of Materials Science*, 31: 343-351.

Santo, CE; Lam, EW; Elowsky, CG; Quaranta, D; Domaille, DW; Chang, CJ; Grass, G. 2011. Bacterial killing by dry metallic copper surfaces. *Applied and Environmental Microbiology*, 77: 794-802.

Schöller, K; Baumann, L; Hegemann, D; De Courten, D; Wolf, M; Rossi, RM; Scherer, LJ. 2014. Preparation of light-responsive membranes by a combined surface grafting and postmodification process. *Journal of Visualized Experiments*, 85: e51680-e51680.

Seo, JM; Arumugam, GK; Khan, S; Heiden, PA. 2009. Comparison of the effects of an ionic liquid and triethylbenzylammonium chloride on the properties of electrospun fibers, 1 – poly(lactic acid). *Macromolecular Materials and Engineering*, 294: 35-44.

Sheldon, RA. 2007. Enzyme immobilization: The quest for optimum performance. *Advanced Synthesis & Catalysis*, 349: 1289-1307.

Siriwatcharapiboon, W; Tinnarat, N; Supaphol, P. 2013. Preparation and characterization of electrospun poly (vinyl alcohol) nanofibers containing

platinum or platinum-ruthenium nanoparticles. *Journal of Polymer Research*, 20: 1-8.

Sondi, I; Salopek-sondi, B. 2004. Silver nanoparticles as antimicrobial agent: a case study on E. coli as a model for Gram negative bacteria. *Journal of Membrane Science*, 153: 71-82.

Srisitthiratkul, C; Pongsorrarith, V; Intasanta, N. 2011. The potential use of nanosilver-decorated titanium dioxide nanofibers for toxin decomposition with antimicrobial and self-cleaning properties. *Applied Surface Science*, 257: 8850-8856.

Stewart, PS; McFeters, GA; Huang, CT. 2000. Biofilm control by antimicrobial agents. In Biofilms II: Process Analysis and Applications. *Bryers, J.F., eds*, Newyork.

Su, YJ; Zhang, CL; Wang, Y; Li, P. 2012. Antibacterial property and mechanism of a novel Pu-erh tea nanofibrous membrane. *Applied Microbiology and Biotechnology*, 93: 1663-1671.

Sui, XM; Shao, CL; Liu, YC. 2005. White-light emission of polyvinyl alcohol/ZnO hybrid nanofibers prepared by electrospinning. *Applied Physics Letters*, 87: 113-115.

Sun, FQ; Li, XS; Xu, JK; Cao, PT. 2010. Improving hydrophilicity and protein antifouling of electrospun poly(vinylidenefluoride-hexafluoropropylene) nanofiber membranes. *Chinese Journal of Polymer Science*, 28: 705-713.

Sun, LM; Zhang, CL; Li, P. 2011. Characterization, antimicrobial activity, and mechanism of a high-performance (-)-epigallocatechin-3-gallate(EGCG)-Cu^{II}/polyvinyl alcohol(PVA) nanofibrous membrane. *Journal of Agricultural and Food Chemistry*, 59: 5087-5092.

Sun, Y; Sun, G. 2002. Durable and regenerable antimicrobial textile materials prepared by a continuous grafting process. *Journal of Applied Polymer Science*, 84: 1592-1599.

Supaphol, P; Chuangchote, S. 2008. On the electrospinning of poly (vinyl alcohol) nanofiber mats: a revisit. *Journal of Applied Polymer Science*, 108: 969-978.

Suslu, A; Albayrak, AZ; Urkmez, AS; Bayir, E; Cocen, U. 2014. Effect of surfactant types on the biocompatibility of electrospun HAp/PHBV composite nanofibers. *Journal of Materials in Medicine*, 25: 2677-2689.

Tan, KT; Obendorf, SK. 2007. Fabrication and evaluation of electrospun nanofibrous antimicrobial nylon 6 membranes. *Journal of Membrane Science*, 305: 287-298.

Tan, SH; Inai, R; Kotaki, M; Ramakrishna, S. 2005. Systematic parameter study for ultra-fine fiber fabrication via electrospinning process. *Polymer*, 46: 6128-6134.

Thurman, RB; Gerba, CP; Bitton, G. 1989. The molecular mechanisms of copper and silver ion disinfection of bacteria and viruses. *Critical Reviews in Environmental Control*, 18: 295-315.

Tong, HW; Wang, M. 2010. Electrospinning of fibrous polymer scaffolds using positive voltage or negative voltage: a comparative study. *Biomedical Materials*, 5: 054110.

Tong, HW; Wang, M. 2011. Electrospinning of Poly(Hydroxybutyrate-co-hydroxyvalerate) fibrous scaffolds for tissue engineering applications: Effects of electrospinning parameters and solution properties. *Journal of Macromolecular Science, Part B: Physics,* 50: 1535-1558.

Tsao, IF; Wang, HY; Shipman, Jr. 1989. Interaction of infectious viral particles with a quaternary ammonium chloride (QAC) surface. *Biotechnology and Bioengineering*, 34: 639-646.

USEPA. 2006. National primary drinking water regulations: Long term 1 enhanced surface water treatment rule. Final rule. United States Environmental Protection Agency, Washington, D.C..

USEPA. 2012. 2012 edition of the drinking water standards and health advisories. United States Environmental Protection Agency, Washington, D.C..

USEPA. 2013. Pesticide ecotoxicity database. United States Environmental Protection Agency, Washington, D.C..

Valegard, K; Liljas, L; Fridborg, K; Unge, T. 1990. The three-dimensional structure of the bacterial virus MS2. *Nature* 345, 36-41.

Voigt, WV. 2009. Water stable, antimicrobial active nanofibers generated by electrospinning from aqueous spinning solutions. Ph.D. Thesis. RWTH Aachen University, Aachen, Germany.

Wang, R; Liu, Y; Li, B; Hsiao, BS; Chu, B. 2012. Electrospun nanofibrous membranes for high flux microfiltration. *Journal of Membrane Science*, 392-393: 167-174.

Wang, XF; Chen, XM; Yoon, KH; Fang, DF; Hsiao, BS; Chu, B. 2005. High flux filtration medium based on nanofibrous substrate with hydrophilic nanocomposite coating. *Environmental Science & Technology*, 39: 7684-7691.

Wang, XF; Fang, DF; Yoon, KH; Hsiao, BS; Chu, B. 2006. High performance ultrafiltration composite membranes based on poly(vinyl alcohol) hydrogel

coating on crosslinked nanofibrous poly(vinyl alcohol) scaffold. *Journal of Membrane Science*, 278: 261-268.

Wang, XF; Zhang, K; Yang, Y; Wang, LL; Zhou, Z; Zhu, MF; Hsiao, BS; Chu, B. 2010. Development of hydrophilic barrier on nanofibrous substrate as composite membrane via a facile route. *Journal of Membrane Science*, 356: 110-116.

Wang, XF; Zhang, K; Zhu, MF; Yu, H; Zhou, Z; Chen, YM; Hsiao, BS. 2008. Continuous polymer nanofiber yarns prepared by self-bundling electrospinning method. *Polymer*, 49: 2755-2761.

Wang, ZG; Ke, BB; Xu, ZK. 2007. Covalent immobilization of redox enzyme on electrospun nonwoven poly(acrylonitrile-co-acrylic acid) nanofiber mesh filled with carbon nanotubes: a comprehensive study. *Biotechnology and Bioengineering*, 97: 708-720.

Wang, ZG; Wan, LS; Liu, ZM; Huang, XJ; Xu, ZK. 2009. Enzyme immobilization on electrospun polymer nanofibers: An overview. *Journal of Molecular Catalysis B: Enzymatic*, 56: 189-195.

Wingender, J; Strathmann, M; Rode, A; Leis, A; Flemming, HC. 2001. Isolation and biochemical characterization of extracellular polymeric substances from Pseudomonas aerugionosa. *Methods in Enzymology*, 336: 302-314.

Xavier, JB; Picioreanu, C; Rani, SA; van Loosdrecht, MCM; Stewart, PS. 2005. Biofilm control strategies based on enzymatic disruption of the extracellular polymeric substance matrix- a modeling study. *Microbiology*, 51: 3817-3832.

Xiao, SL; Shen, MW; Ma, Hui, M; Guo, R; Zhu, MF; Wang, SY; Shi, XY. 2010. Fabrication of water-stable electrospun polyacrylic acid-based nanofibrous mats for removal of copper (II) ions in aqueous solution. *Journal of Applied Polymer Science*, 116: 2409-2417.

Yao, L; Haas, TW; Guiseppi-Elie, A; Bowlin, GL; Simpson, DG; Wnek, GE. 2003. Electrospinning and stabilization of fully hydrolyzed poly(vinyl alcohol) fibers. *Chemistry of Materials*, 15: 1860-1864.

Yeon, KM; Lee, CH; Kim, JB. 2009. Magnetic enzyme carrier for effective biofouling control in the membrane bioreactor based on enzymatic quorum quenching. *Environmental Science & Technology*, 43: 7403-7409.

You, H; Li, X; Yang, Y; Wang, BY; Li, ZX; Wang, XF; Zhu, MF; Hsiao, BS. 2013. High flux low pressure thin film nanocomposite ultrafiltration membranes based on nanofibrous substrates. *Separation and Purification Technology*, 108: 143-151.

You, Y; Lee, SJ; Min, BM; Park, WH. 2006. Effect of solution properties on nanofibrous structure of electrospun poly (lactic-co-glycolic acid). *Journal of Applied Polymer Science*, 99: 1214-1221.

Yousef, A; Barakat, NAM; Al-Deyab, SS; Nirmala, R; Pant, B; Kim, HY. 2012. Encapsulation of CdO/ZnO NPs in PU electrospun nanofibers as novel strategy for effective immobilization of the photocatalysts. *Colloids and Surfaces A: Physicochemical and Engineering Aspects*, 401: 8-16.

Zhang, CX; Yuan, XY; Wu, LL; Han, Y; Sheng, J. 2005. Study on morphology of electrospun poly (vinyl alcohol) mats. *European Polymer Journal*, 41: 423-432.

Zhang, LF; Luo, J; Menkhaus, TJ; Varadaraju, H; Sun, YY; Fong, H. 2011. Antimicrobial nano-fibrous membranes developed from electrospun polyacrylonitrile nanofibers. *Journal of Membrane Science*, 369: 499-505.

Zhang, W; Chen, M; Diao, GW. 2011. Electrospi8nning β -cyclodextrin/poly(vinyl alcohol) nanofibrous membrane for molecular capture. *Carbohydrate Polymers*, 86: 1410-1416.

Zmantar, T; Kouidhi, B; Miladi, H; Mahdouani, K; Bakhrouf, A. 2010. A Microtiter plate assay for Staphylococcus aureus biofilm quantification at various pH levels and hydrogen peroxide supplementation. *New Microbiologica*, 33: 137-145.

Zodrow, K; Brunet, L; Mahendra, S; Li, D; Zhang, A; Li, QL; Alvarez, PJJ. 2009. Polysulfone ultrafiltration membranes impregnated with silver nanoparticles show improved biofouling resistance and virus removal. *Water Research*, 43: 715-723.

국문 초록

본 논문에서는 전기방사를 통해서 폴리비닐 알코올계 (PVA) 나노섬유를 제조하고, 4 차 암모늄 화합물이나 프로테아제를 첨가하여 기능성을 부여함으로, 수처리 여과 과정에서 항균 및 항바이오파울링 효과를 평가해보고자 하였다. 본 연구에서 제조한 전기방사 나노섬유는 4 차 암모늄 화합물 중 하나인 벤질 트리에틸암모늄 클로라이드 (BTEAC)를 함유한 PVA 나노섬유와 프로테아제인 알파-카이모트립신 (α-chymotrypsin)을 함유한 PVA/PAA 나노섬유이다. BTEAC-PVA 나노섬유는 공동 전기방사법으로, PVA/PAA-Cu(II)-α 나노섬유는 전기방사 후 담금처리를 통해 제조하였다. 제조된 나노섬유들은 주사전자현미경 (SEM), 에너지 분산형 X-선 분광기 (EDS), 시차주사 열량 측정법 (DSC), 열 중량 측정기 (TGA), 푸리에 변환 적외선 분광기 (FTIR), 그리고 모세관류 포로미터 (CFP)와 같은 다양한 분석기술을 통해 분석해 보았다.

BTEAC-PVA 나노섬유는 2.6 %의 BTEAC 를 첨가하여 제조한 것으로 항박테리아와 항바이러스 효과를 지닌다. 박테리아 저감은 접촉시간이 증가함에 따라 증가되며, 박테리아의 성장을 제한한다. 항바이러스 실험은 박테리오파지 MS2 와 PhiX174 를 이용하여

진행되었으며, 두 박테리오파지 모두 비활성화되는 것을 발견하였다. BTEAC-PVA/GF ENMs 를 제조하여, 물에 대한 안정성, 플럭스, 기공 크기, 유출, 물벼룩을 이용한 독성 평가를 수행한 결과 정밀여과 필터로 이용될 수 있는 친환경 필터임을 확인할 수 있었다. 항균기능 평가로는 *E.coli* 의 경우 10 mL 전량 여과시에 4.88 LRV 가 제거되었으며, *S.aureus* 의 경우 5.75 LRV 가 제거되었다. 500 mL 용액을 전량 여과한 경우 각각 2.26 LRV, 3.29 LRV 까지 제거되었다. 강물을 이용한 여과실험 결과 총 대장균군은 초기농도 67 CFU/mL 에서 500 mL 전량여과시 모두 불검출되었다. 항바이오파울링 실험 결과 BTEAC-PVA/PC ENMs 는 PC 멤브레인보다 바이오파울링에 대한 저항성이 있어 플럭스를 유지하는 것이 관찰되었으며, 이는 부착된 미생물이 BTEAC-PVA 나노섬유 표면에 접촉하여 박테리아 멤브레인의 손상에 따른 것으로 형광 현미경과 주사현미경을 통해 확인하였다. 재이용 실험을 통해 BTEAC-PVA/PC ENMs 의 항균기능이 6 반복시 꾸준히 유지되는 것을 확인할 수 있었으며, 강물을 이용한 다양한 미생물 군 실험에서도 항균기능이 유지되는 것을 관찰하였다.

PVA/PAA 나노섬유의 경우 Cu(II)이온을 배위결합을 통해 흡착시킨 후 α-chymotrypsin 을 고정시킨다. α-chymotrypsin 은 프로테아제

중 하나로, *P. aeruginosa* 의 경우 53.5 %, *S.aureus* 의 경우 35.53 %의 바이오필름 형성을 방지하는 것을 확인하였다. 또한 기 형성된 바이오필름의 경우에도 *P. aeruginosa* 의 경우 58.2 %, *S.aureus* 의 경우 43.5 %를 감소시켰다. Cu(II)이온은 PVA/PAA 나노섬유의 단위 g 질량당 44.85 mg 흡착되었으며 (초기 Cu(II)이온농도 = 500 mg/L, 반응시간 = 24 h), α-chymotrypsin 은 25.56 mg 이 고정되었다. PVA/PAA-Cu(II)-α 나노섬유는 EPS 의 단백질을 분해함으로써 항바이오파울링 효과가 있음을 확인하였다.

기능성 PVA 나노섬유는 수처리 필터로서 적용이 가능하며, 다양한 실험들을 통해 항균기능과 항바이오파울링 효과를 나타내었다. 또한, 본 연구 결과는 4 차 암모늄 화합물과 프로테아제를 함유한 PVA 전기방사 나노섬유를 친환경적으로 제조하기 위한 과학적 기초 자료를 제공하고, 개발된 나노섬유가 수처리 막여과 시스템에 적용될 수 있는 가능성을 확인하였다.

주요어: 전기방사 나노섬유, 폴리비닐 알코올, 항미생물, 4 차 암모늄 화합물, 프로테아제, 수처리 여과

학 번: 2011-30344